SUSTAINABILITY OF NATURAL RESOURCES' EFFICIENCY

EDITOR
Serkan GÜLDAL

AUTHORS
Aysun ŞENGÜL
Ayşe Elif ÖZSOY ÖZBAY
Ayşen HAKSEVER
Çağrı ÜN
Hasan Üstün BAŞARAN
Işıl SANRI KARAPINAR
Muhammed Enes UMCU
Sinan ERCAN
Soner ÇELEN
Yağmur UYSAL.
Yusuf FEDAİ
Yusuf URAS

İKSAD
Publishing House

SUSTAINABILITY OF NATURAL RESOURCES' EFFICIENCY

EDITOR

Serkan GÜLDAL

AUTHORS

Aysun ŞENGÜL

Ayşe Elif ÖZSOY ÖZBAY

Ayşen HAKSEVER

Çağrı ÜN

Hasan Üstün BAŞARAN

Işıl SANRI KARAPINAR

Muhammed Enes UMCU

Sinan ERCAN

Soner ÇELEN

Yağmur UYSAL.

Yusuf FEDAİ

Yusuf URAS

İKSAD Publishing House

(The Licence Number of Publicator: 2014/31220)
TURKEY TR: +90 342 606 06 75
USA: +1 631 685 0 853
E mail: iksadyayinevi@gmail.com
www.iksadyayinevi.com

ISBN: 978-625-8213-08-9
Cover Design: İbrahim KAYA
September / 2022
Ankara / Turkey
Size = 16x24 cm

CONTENTS

PREFACE

Efficient use of natural resources is one of the best solutions for sustainability. Thus, researchers introduce numerous methods for efficiency. In this book, many chapters are collected about the studies which subject from the quality of resources to efficiency methods. The experts in the related fields provide analysis and propose solutions. The book language avoids technical terminology to provide an enjoyable reading experience regardless of expertise.

The six chapters cover many disciplines from unique perspectives. In the first chapter, the properties of high quality water are explained by scientifically accepted metrics. The properties are solidified by a specific example, and the chapter is titled as *"Hydrogeochemistry of the Drinking Water Sources of the Tombak Region (Kahramanmaraş, Turkey) and Their Effects on Human Health"* In the second chapter, efficient methods are proposed to reduce energy consumption for car engines. It is titled *"Late Fuel Injection Combined with Retarded Intake Valve Closure for Improved Exhaust System Warm-Up in Diesel Automotive Vehicles."* In this chapter, it is shown that a slight change in the available technology can have a high impact to reduce energy waste. The proposed method is evaluated by a simulator in realistic manners. Similarly, in the third chapter, researchers answered what is necessary to build energy efficient buildings. The chapter provides hints to the reader in plain language, and it is titled *"Reviewing of Parameters Affecting Energy Consumption in Buildings."* In chapter four, an analysis of concrete building structures is given in terms of seismic vulnerability. The comparative study is presented with the title *"A Comparative Assessment of the Seismic Vulnerability Evaluation Methodologies for Reinforced Concrete Buildings."* In chapter five, the results of global warming are discussed. The results of greenhouse gas emissions because of transportation are given with the data recorded over decades. Additionally, the statistical results are extrapolated to the nearby future if transportation systems deplete natural resources as in previous years. The chapter is titled *"Investigation and Mitigation Studies of Transportation Based Greenhouse Gas Emissions in Adana City."* In chapter six, efficient use of sand silica is given with the title *"Theoretical and Experimental Comparison of Minimum Fluidization Speed."* The processing of sand silica is given in experimental and theoretical investigation with an extensive literature review. For the chapters, all responsibilities for the provided content belong to the authors.

We are appreciated of authors' contribution to this book and IKSAD publishing house. We hope this book informs and opens new doors to the reader as intended in Sustainability by efficiency.

Assist. Prof. Serkan GÜLDAL
August 2022

CHAPTER 1

HYDROGEOCHEMISTRY OF THE DRINKING WATER SOURCES OF THE TOMBAK REGION (KAHRAMANMARAŞ, TURKEY) AND THEIR EFFECTS ON HUMAN HEALTH

Assoc. Prof. Dr. Yusuf URAS[1*], MSc. Sinan ERCAN[2] and Prof. Dr. Yağmur UYSAL[3]

[1] Kahramanmaras Sutcu Imam University, Geological Engineering Department, Kahramanmaras, Turkey. uras74@gmail.com; ORCID: 0000-0001-5561-3275
[2] Kahramanmaras Sutcu Imam University, Geological Engineering Department, Kahramanmaras, Turkey. sinanercan1989@gmail.com; ORCID: 0000-0002-4476-9095
[3] Mersin University, Environmental Engineering Department, 33343, Mersin-Turkey. yuysal@mersin.edu.tr; ORCID: 0000-0002-7217-8217
***Corresponding Author**

INTRODUCTION

Water is one of the most basic needs of human life. Today, more than half of the world's population uses groundwater resources to survive. These water resources are used as drinking water for domestic needs and for the continuation of vital activities, as well as for industrial and agricultural activities (Delgado et al. 2010). Therefore, it is very important to determine the quality of groundwater with such a wide range of uses and to ensure that these resources meet the criteria specified in the standards. Geochemical processes and reactions with aquifer minerals in ground and surface waters have a significant impact on water quality. These geochemical processes are responsible for temporal and spatial changes in groundwater and surface water chemistry and quality (Missi et al. 2020).

Groundwater is water containing high mineral concentration. As the groundwater passes through the soil layers, it dissolves the minerals contained in the soil. Therefore, groundwater contains more ions and minerals than surface waters. Some of these minerals are required for human health to be present in the waters. Examples include fluorine, calcium, and iodine. However, the presence of large amounts of ions in the water also increases the risk of containing ions harmful to human health.

One of the ions determined by geochemical analysis of drinking water is iodine. Iodine is an important micronutrient for human health. Adequate iodine intake is required for the production of thyroid hormones, which play a vital role in the regulation of metabolism, continuity of growth, and normal development of many organs (Azzakhninia et al. 2019). 30-40 mg/kg dose of iodine intake is lethal. Acute oral toxicity causes gastrointestinal irritation, dehydration, and shock. Hypersensitization reactions are also observed while iodism may occur due to chronic iodine intake. Many functional and developmental abnormalities occur in iodine intake deficiency. These anomalies are defined by Hetzel as "Iodine Deficiency Disorders (IDDs)" (Hetzel 1983). Iodine deficiency is associated with adverse pregnancy outcomes including fetal loss, profound intellectual disability (cretinism), and goiter. The most common disease that occurs due to

iodine intake deficiency is goiter. In order to prevent insufficient iodine intake, World Health Organization (WHO) states that daily iodine intake is necessary for adults and this value should not exceed 150 µg/d (WHO 2007). This value was determined as 50 µg/d in 0-6 months' babies, 90 µg/d in children aged 6 months to 6 years, 120 µg/d in the 7-10 age group, and 200–300 µg/d during pregnancy and lactation (Delange, 2001). Although iodine deficiency has negative effects on people of all age groups, insufficient iodine intake at a concentration of <150 µg/d, especially for young and adults, can cause various diseases such as mental retardation, hypothyroidism and goiter.

The human body receives the iodine that it needs through mostly foods and drinking water. The amount of iodine in drinking water enables us to obtain information about the iodine status of the area where drinking water is supplied. Although iodine intake through food is more effective in determining iodine deficiency, the lack or excess of iodine concentrations in the drinking water consumed by people is an important guide in determining the health problems that may be seen depending on the iodine concentration in that region.

In this study, all geochemical parameters of the drinking water sources of Tombak region, which is located approximately 130 km northwest of Kahramanmaraş city center, were determined and the possible effects of water on the health of the local people were investigated. For this purpose, Cangı spring (CG-1), Yareli spring (YR-2) and Taşpınar fountain (TP-3), which are the three main drinking water resources of the region, were selected as the drinking water resources for sampling. In addition, the general geology, isotope geology, hydrogeochemistry and medical geology of the area where drinking water resources are located have been investigated. The results of the analyzes showed that the drinking water sources meet the standard values, only that they do not contain any iodine. For this reason, the effects of these water resources on health were evaluated in terms of iodine deficiency.

1. SAMPLING AND ANALYTICAL METHODS

In order to evaluate the drinking water resources of Tombak region in terms of geology and water quality, water samples were collected in different months over a 1-year period (Figure 1). The 1 L sample containers that were washed with distilled water in the laboratory were rinsed again with the water to be sampled in the field to prevent possible contamination. Various water parameters, such as pH, dissolved oxygen (DO), electrical conductivity (EC), and temperature, were determined in situ during sampling. The samples brought to the laboratory for analysis were kept in a refrigerator (+4 ^{o}C). Heavy metal and anion–cation analyses of these samples were performed at the ACME Analytical Laboratories (Vancouver, BC, Canada) using ion chromatography (IC), inductively coupled plasma mass spectrometry (ICP-MS), and ICP optical emission spectrometry (ICP-OES) techniques. Oxygen-18 (^{18}O), deuterium (^{2}H), and tritium (^{3}H) isotopic analyses were also carried out in the isotope laboratories of the Technical Research and Quality Control Department (TRQC) of the General Directorate of State Hydraulic Works in Ankara, Turkey. Following the analyses of the drinking water sources of Tombak region, the water samples were classified initially, and the analytical results were compared against each other to establish a correlation between the samples and with other factors. The main purpose of this chemical classification is to determine the origin of the waters, to compare the dominant and total dissolved ion concentrations, and to evaluate whether the water from the difference sources is suitable for human health. Therefore, we tried to evaluate the anion-cation and heavy metal composition of groundwater samples and rationalize the abnormalities in the measured parameters. One of the major factors affecting the quality of water resources for Tombak Region is the lithological properties of the rock units through which these waters flow. Therefore, it is important to determine the hydrogeochemical

characteristics of the water sources and to identify the lithological units that are in contact with these water sources.

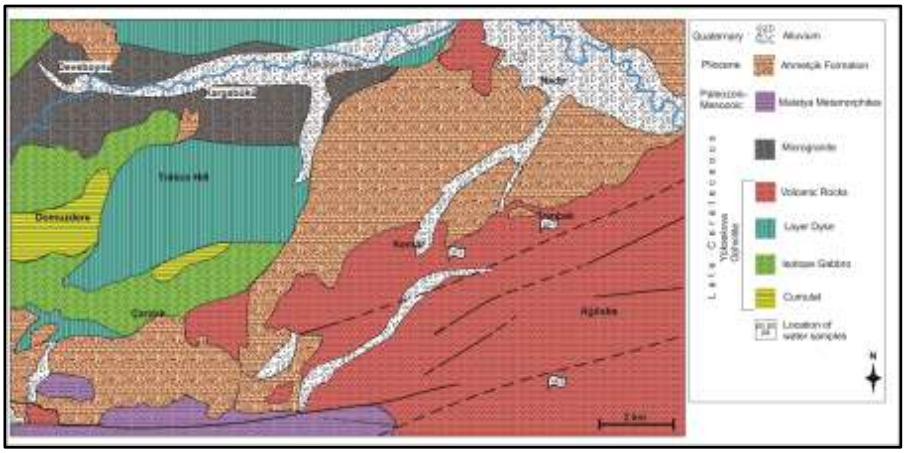

Figure 1 Geological location map and cross section of the Tombak region and its surrounding area

1.1. Geological Setting Of The Study Area

The study area is located approximately 130 km northwest of Kahramanmaraş city center and is within the borders of the Kahramanmaraş L37-c3 map in the 1 / 25.000 scaled topographic map. The lithological units from the oldest to the youngest in the study area and its surroundings consist of Yüksekova ophiolite, Esence granitoid, Malatya metamorphics, Ahmetçik formation and the youngest unit, alluvium at the bottom. The Late Cretaceous Yüksekova Ophiolites are composed of ultramafic cumulates, isotropic gabbro, stratified dyke complex and volcanic sedimentary rocks (Perinçek and Kozlu 1984). The unit land is gray, grayish green and brown tones. The Yüksekova ophiolite is cut by the units belonging to the Esence granitoid and overlies the Pliocene aged Ahmetçik formation with an angular unconformity. The granitoids are located along the Göksun stream valley in an east-west direction and around Deveboynu region, Kargabükü region and Esence town (Figure 1). The unit mainly consists of aplitic dykes cutting granodiorite and microgranodiorite.

The Esence granitoid cuts the volcanic rocks around Tombak region and the plate dyke complex around Tülüce hill and Büyükboz hill (Figure 2). The Ahmetçik formation crops out in the central part of the study area, around Polatyolu ridge, east of Esence town, west of Nadirköy and Soğucak regions, east of Yeni Mahalle and north of Deveboynu region. The unit is observed as alternation of conglomerate, limestone, sandstone and marl. It comes with angular mismatch in all subunits. Quaternary alluvium is the youngest unit in the study area (Figure 3). Alluvium containing igneous, metamorphic and sedimentary rock fragments in the size of blocks, gravel, sand, silt, clay and mud is observed especially along the Göksun Stream and other small streams in and around the study area (Rızaoğlu 2000).

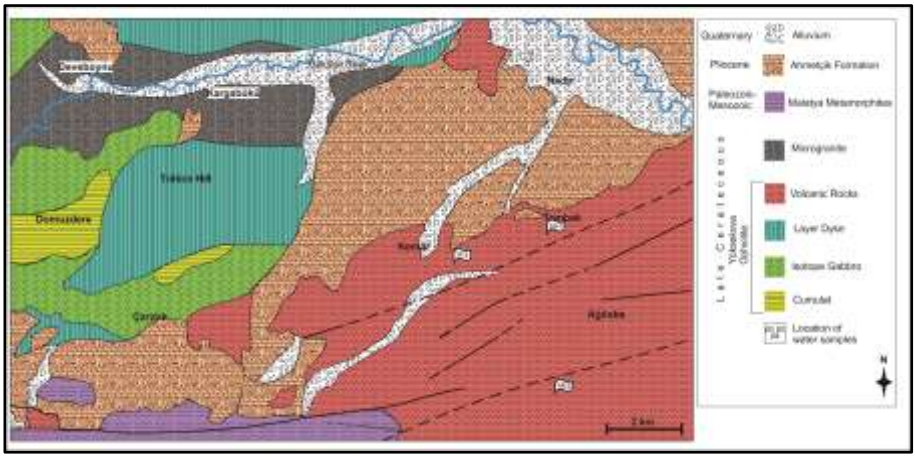

Figure 2. The view of the volcanic rocks

Figure 3. Photographs Showing the Water Sources of the Tombak Region (Cangı Spring (CG-1), Yareli Spring (YR-2) and Taşpınar Fountain (TP-3)

1.2. Hydrogeology of the Study Area

Kahramanmaraş Province is located in a region where three different geographical regions of Turkey (Mediterranean, Eastern Anatolia and Southeastern Anatolia regions) are closest to each other; thus resulting in three different climatic conditions in this area. While the northern parts of Kahramanmaraş Province are considered to have a continental climate due to the increasing altitude, the southern parts of the province experience climatic conditions similar to the "Degenerate Mediterranean Climate". As a result, in the study area, summer periods are hot and dry, and winter periods are rainy and mild.

The long-term (1930–2020) monthly precipitation records of Kahramanmaraş province show that it decreased from 120 mm to 2.2 mm in the January-August period, and this value increased again from 11 mm to 130.6 mm in the September-December period (Turkish State Meteorological Service, 2021) (Figure 4). Due to the mild and wet climate conditions mentioned above, the study area is rich in surface waters. In the study area, which has a rich location in terms of surface

waters due to its rainy and temperate climate characteristics, a very jointed and fractured structure is formed due to the Ahmetçik formation and Yüksekova ophiolites and intense tectonic effects. With this structural feature, the Ahmetçik formation and Yüksekova ophiolites in the Tombak-Göksun region acquire a permeable character to allow surface waters to go deeper and form a suitable aquifer environment where the deeper waters can be collected underground.

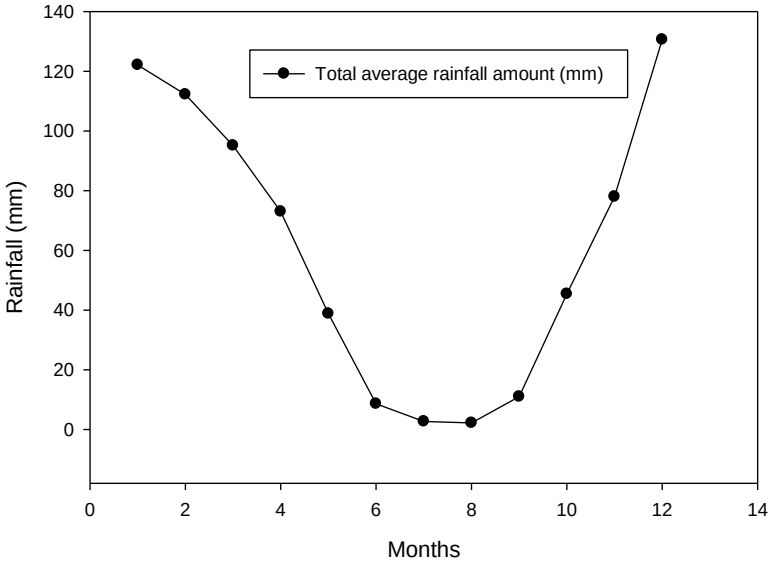

Figure 4. Changes in the total monthly precipitation values for Kahramanmaraş city including Tombak region (1930-2020 period) (DMI, 2021)

2. RESULTS AND DISCUSSIONS

2.1. Hydrogeochemistry of the Study Area

The quality of the spring waters collected at certain depths of the earth acquire different physical and chemical properties depending on the chemical properties of the rocks they pass through and interact with, and the source from which they are obtained and the environmental conditions. Chemical analyzes were carried out by taking samples from three main water springs in Tombak Region at certain periods throughout the year. Temperature, pH, EC, alkalinity,

trace element concentrations, anion-cation composition and metal concentration measurements were made to determine the quality of water resources (Table 1).

Table 1 Geochemistry of the drinking water sources of the Tombak region

	Water Sources[a]		
Geochemical parameters	CG-1	YR-2	TP-3
Temperature (°C)	7.00-14.00	7.40-14.80	8.00-10.70
pH	7.40-8.10	8.10-8.60	7.60-9.00
EC (µS/cm)	397-532	211-397	323-656
DO (%)	12.0-4.0	15.30-38.14	15.6-42.20
Na^{+} (ppm)	6.38-7.92	0.34-1.51	7.2-10.0
K^{+} (ppm)	0.00-0.36	0.29-0.58	0.00-0.43
Ca^{+2} (ppm)	62.98-75.22	23.65-38.64	39.40-78.32
Mg^{+2} (ppm)	17.25-19.65	5.40-7.50	18.83-26.93
Cl^{-} (ppm)	5.08-10.49	2.35-5.03	7.2-12.09
HCO_3^{-} (ppm)	231.00-252.00	106.20-136.90	194.60-293.70
CO_3^{-2} (ppm)	*NA*	*NA*	*NA*
SO_4^{-2} (ppm)	35.7-41.65	9.10-12.80	18.97-68.78
Fe^{+2} (ppm)	8.00-10.00	8.00-10.00	8.00-10.00
NO_3^{-} (ppm)	17.12-18.87	3.21-4.91	7.83-37.01
NH_4^{+} (ppm)	**NA*	**NA*	**NA*
NO_2^{-} (ppm)	**NA*	**NA*	**NA*
PO_4^{-3} (ppm)	**NA*	**NA*	**NA*
F^{-} (ppm)	0.11-0.18	0-0.2	0-0.18
I^{-} (ppm)	**NA*	**NA*	**NA*
S^{-2} (ppm)	4.00-8.00	9.00-12.00	19.00-22.00
TDS (ppm)	262.02-351.12	139.26-262.02	213.18-432.96
Al	2.00	5.00	2.00
Au	0.06	0.20	0.05
As	0.50	0.50	0.50
Ag	0.05	0.05	0.05
Ba	12.13	3.32	1.15
Cr	9.00	3.80	11.30

Cu	0.80	0.30	1.60
Hg	0.10	0.10	0.10
Mn	0.05	0.09	0.05
Ni	0.20	0.20	0.20
Sn	0.05	0.13	0.05
Pb	0.30	0.20	0.20
Pt	0.01	0.01	0.01
Ru	0.05	0.05	0.05
Zr	0.02	0.02	0.02

**NA: This parameter was not assigned*

The possible effects of these drinking waters on human health were evaluated according to the results obtained from the samples. USA salinity (EC_{25}-SAR Richards, 1954) and Wilcox (EC_{25}-% Na; Wilcox 1955) diagrams were used to determine the usability of water as irrigation water, and water classes were determined using Piper (1953) and Schoeller (1967) diagrams. In addition, the analysis results of water samples were evaluated by taking into account the Turkish Standards Water Regulation for Human Consumption (TSI-266 2015), WHO criteria and the Water Pollution Control Regulation (WPCR 2004).

Drinking water resources in the Tombak region are classified as cold waters because their temperatures vary between 7-14.8 °C annually. The pH results varied between 7.4-9.0 revealing that these spring waters had slightly alkaline properties, and in the range determined by TSI 266, WHO and EPA for drinking water.

Electrical conductivity is an index of dissolved solids in water and depends on temperature, concentration and type of ions (Hem, 1985). High EC values can be explained by high dissolution of minerals in the soil and/or longer stay of groundwater in the aquifer (Oinam et al., 2011). Irrigation water quality is categorized into 5 different classes in terms of EC parameter (Richards, 1954). EC <250 µs/cm (excellent), 250-750 µs/cm (good), 750-2000 µs/cm (permissible), 2000-3000 µs/cm (doubtful), >3000 µs/cm (not

applicable). Since the EC values of all samples in this study were determined in the range of 211-656 µs/cm, it is suitable for irrigation water. The EC values of spring waters varying in the range of 211-656 µS/cm also showed that the minerals that cause salinity in the water were present in very low concentrations in these springs. The slightly alkaline pH of the spring waters in the study area is another reason for the low EC. Because, in acidic conditions with low pH values, groundwater dissolves aquifer rocks, causing mineral salts to mix with groundwater and therefore cause high EC values.

While the dissolved oxygen saturation (%) of the two water sources of YR-2 and TP-3 was similar, the oxygen saturation of the CG-1 source was found to be very low. The low DO (%) content of a water source indicates that this water comes from deeper layers of the earth. Na^+ concentrations in all water sources ranged from 0.34-10.0 ppm, much lower than the allowable limit of 200 mg/L (WHO 2017). The low Na^+ ions in water resources also reveal why the electrical conductivity of water resources is low.

Total dissolved solids (TDS) in groundwater are mainly related to inorganic salts (especially CO_3^{-2}, HCO_3^-, Ca^{+2}, Mg^{+2}, K^+, Na^+, SO_4^{-2}, Cl^-) and dissolved organic matter. Salts can be of geogenic origin (decomposition of rocks) or anthropogenic origin (domestic/industrial wastewater discharge, pipe material feature in the water transport line) (Raju et al., 2015). Groundwater was categorized into 4 different classes by Davis and De Wiest (1966). Type I (TDS<500 mg/L) preferred as drinking water; Type II (TDS: 500-1000 mg/L) permitted, Type III (TDS<3000 mg/L) suitable for irrigation, Type IV (TDS>3000 mg/L) not suitable as drinking water and irrigation water. In this study, the TDS concentrations of water sources measured in the range of (139.26-432.96 ppm) showed that these spring waters are suitable for drinking water and considerably lower than the limit values reported by WHO (1000 ppm) and EPA (500 mg/L).

Sulfate (SO_4^{-2}) is one of the most common anions found in natural waters after bicarbonate and chloride, and its concentration varies from a few mg to a few thousand mg per liter. Sulfates are formed by the dissolution of heavy metal sulfides in nature, partially oxidized under the influence of atmospheric events. The main sources of sulfate in groundwater are gypsum and anhydrite, and it can be also formed by oxidation of sulfur, sulfites and thiosulfates. Sulfate is generally found in low concentrations in groundwater due to reducing conditions that inhibit sulfur oxidation in the aquifer (Alam et al. 2016). In this study, the SO_4^{-2} concentrations of spring waters were measured in the range of 9.10-68.78 ppm. These values are considerably lower than the limit value of 250 mg/L ppm declared by TSI 266, WHO and EPA.

Chloride (Cl^-), is an anion commonly found in all drinking waters, and is known as the halogen, which is the most abundant in nature. It can be mixed into the waters from rocks and underground formations or as a result of fresh water-salt water interference. It is found in water in the form of NaCl, as well as in compounds as $CaCl_2$ and $MgCl_2$. In general, the amount of chloride in groundwater is low in rainy regions and high in arid regions. Chloride is taken into account as a factor in determining the quality of natural waters to be suitable for drinking water supply. Waters with high chloride concentrations also generally have high mineral (salt) content. The chloride content of these spring waters was determined as 2.35-12.09 ppm. These results are supported by the low EC values. The chloride concentration limit was 250 ppm in the standards of EPA, TSI 266 and WHO. This low concentration range demonstrated the suitability of these waters for use as drinking water.

Nitrate (NO_3^-) is a very easily soluble form of nitrogen and can quickly dissolve into groundwater from the soil. If a high NO_3^- concentration is found in groundwater, the probable causes of this are wastewater, fertilizers and animal wastes. In particular, the excessive

use of fertilizers with a high nitrogen content in agriculture is one of the main reasons for the high NO_3^- concentration in groundwater. In most of the studies conducted in groundwater in Turkey, NO_3^-concentration was found to be above the limit values. It has been determined that the NO_3^- contents of the spring waters we analyzed in our study vary between 3.21-37.01 ppm, and that these values will not cause any problems for public health in terms of NO_3^- and that they are below the maximum allowable value (50 ppm in the standards of WHO, EPA and TSI 266) in drinking water.

Carbonate (CO_3^{-2}), bicarbonate (HCO_3^-) ions and carbon dioxide (CO_2) are the main form of carbonate compounds in freshwater. The content of HCO_3^- and CO_3^{-2} ions could indicate the local geochemical environment, so the determination of their content is very important (Nan et al. 2016). Possible sources of bicarbonate are carbon dioxide released as a result of the oxidation of organic materials in the aquifer (Khashogji and El Maghraby 2013). The fossil carbon content of calcite and dolomite in the aquifer also contributes to the presence of bicarbonates in the environment. Calcium, magnesium and bicarbonate concentrations increase in groundwater as a result of the time dissolution of carbonaceous substances, namely organics, and bicarbonate ions may also result from the decomposition of silicate minerals (Gastmans et al. 2010).

Heavy metal composition of the groundwater samples was measured to determine any possible abnormalities in the contents of the spring waters. According to the results, it can be said that the heavy metal concentrations of water sources were not high concentrations when they were compared to the standards to use them drinking water. Therefore, it was concluded that it would not be correct to associate any abnormality on the health of people living in this area with the heavy metal content of the waters. At the same time, all these values mean that there is no obstacle to the use of water for any purpose.

While the water resources of Tombak region are classified as "very good" according to the Wilcox diagram (Figure 5), they are located in the C_1-S_1 area in the US Salinity Laboratory diagram (Figure 6). S_1 is an indicator that they are "low sodium water", so all water resources are classified as Class I waters (<20%; very good) according to their Na% content. Since water resources are in the very good water class in Wilcox classification, there is no problem in using them as irrigation water.

The anion-cation concentrations measured in the samples taken from the water sources of Tombak region were evaluated using Piper and Schoeller diagrams (Figure 7 and 8). With these diagrams, interpretations were made regarding the origin of the waters examined and the lithology with which they were in contact. According to the Piper diagram, CG-1, YR-2, TP-3 spring waters belong to the fifth zone and are in the class of waters with carbonate hardness is more than 50%. As is known, the chemical composition of groundwater changes depending on the chemistry of the rocks it is in contact with. It is possible to predict the aquifer lithology in the groundwater system to which a water sample belongs with the Schoeller Diagram (Figure 8). In other words, the lithology with which groundwater comes into contact can be determined. Lines combining concentration (mg/L) values of water samples taken from springs follow a parallel path to each other. This situation is an indication that all spring waters are fed from the same aquifer.

Considering the cation and anion concentrations in CG-1, YR-2, TP-3 sources according to the Schoeller diagram, it was seen that the order of these ions was $Ca^{+2}>Mg^{+2}>Na^{+}+K^{+}$, and $HCO_3^{-}>SO_4^{-2}>Cl^{-}$. These drinking water sources are also classified as "normal chlorinated water" according to chloride concentration, "normal sulphated water" according to sulphate concentration and "normal carbonated water" according to bicarbonate concentrations in the Schoeller diagram.

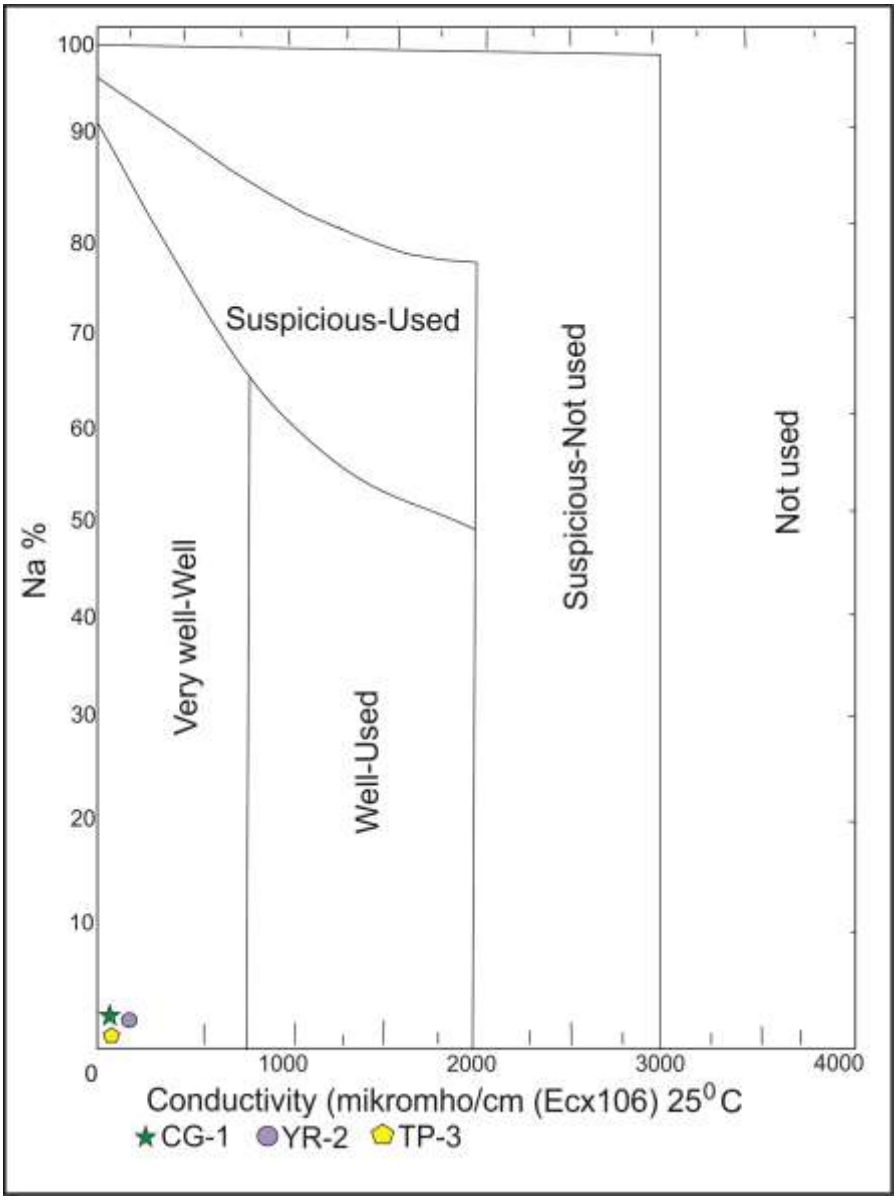

Figure 5. The Wilcox diagram of the drinking water sources of Tombak region

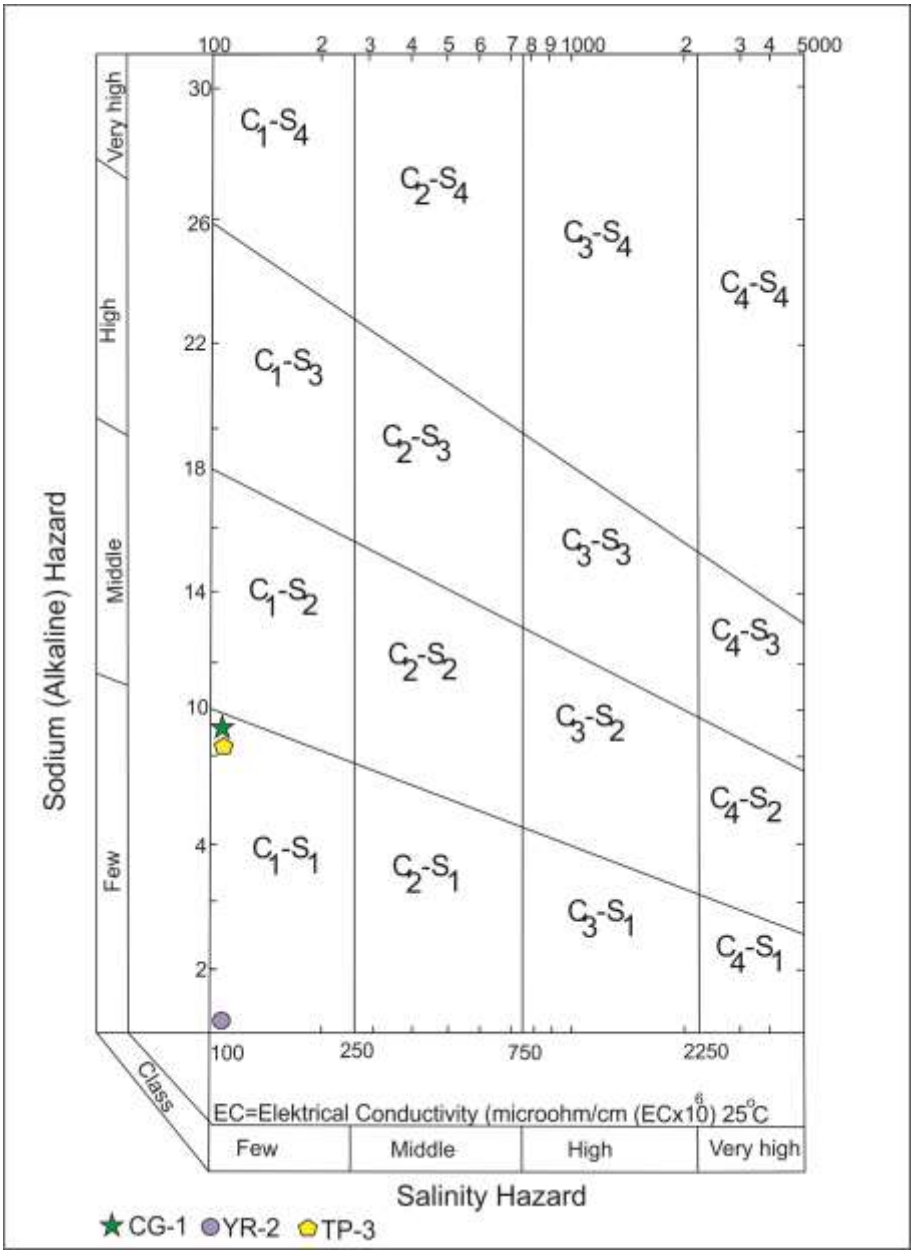

Figure 6. The U.S. Salinity Laboratory diagram of the drinking water sources of the Tombak region

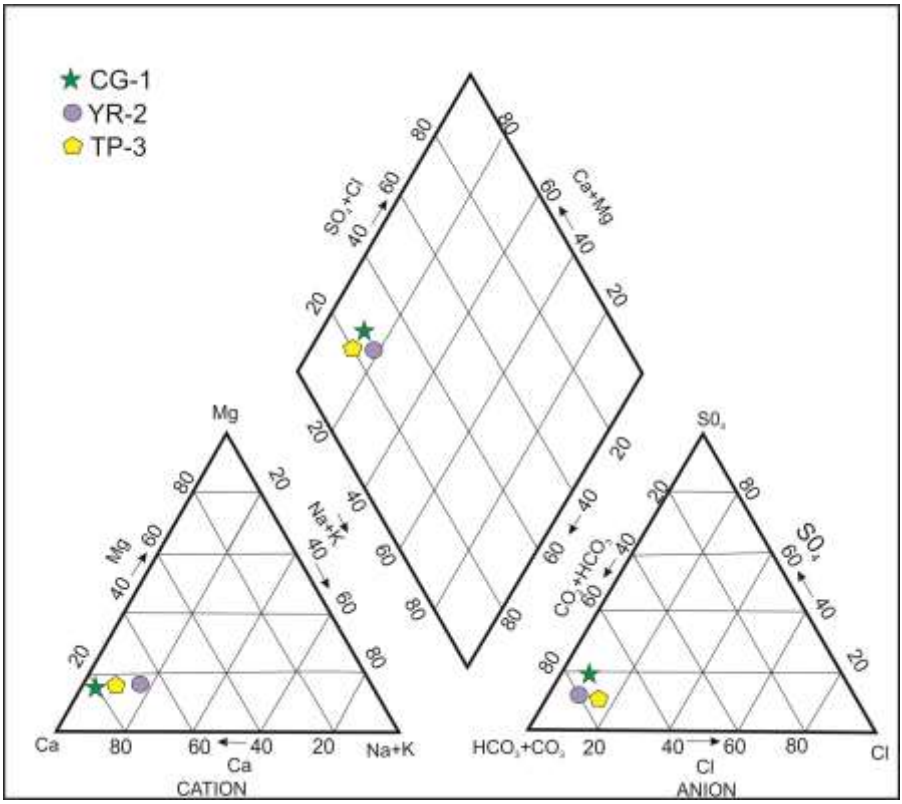

Figure 7. Piper diagram of the drinking water sources of the Tombak region

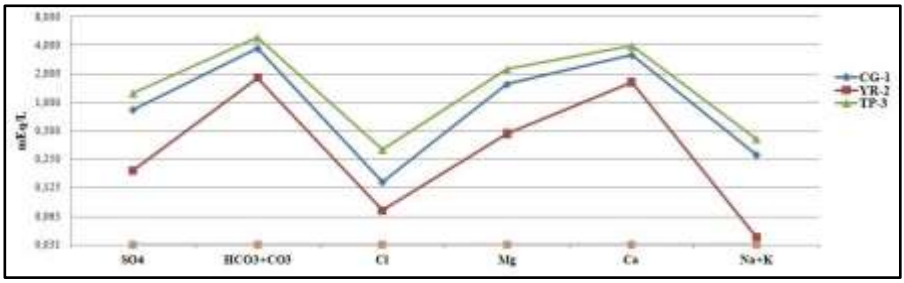

Figure 8. Schoeller diagram of the drinking water sources of the Tombak region

2.2. Environmental Isotopes in Springs

Stable isotopes of hydrogen and oxygen that make up water are sources of information about the origin of water, and its physical and chemical processes that take place during the hydrological cycle. The

age of groundwater, its interaction with various waters, determination of feeding areas, determination of residence time in the aquifer, and its renewal can be evaluated by isotope studies. In this study, environmental isotope studies were carried out to determine the aquifer source, recharge area, and water–rock interaction times of the drinking water sources in the Tombak region. In these studies, tritium (^{3}H) radioisotopes and stable isotopes of oxygen ($\delta^{18}O$) and deuterium ($\delta^{2}H$) were used. Recharge elevation estimates were calculated using $\delta^{18}O$ and d $\delta^{2}H$ values (Table 2), and variations between these values were compared to the Global Meteoric Water Line (GMWL, expressed as $D=8x\delta^{18}O+10$; Craig 1961) and Mediterranean Water Line (MWL, $\delta D=8*(\delta^{18}O)+15$) (Gat and Garmi 1970). In meteoric waters, these values vary depending on the annual precipitation and temperature. The isotope ratio in the waters increases with the decrease in temperature while $\delta^{18}O$ and $\delta^{2}H$ values decrease with an increase of altitude and latitude of the region. The values of $\delta^{18}O$ and $\delta^{2}H$ in the drinking water sources of Tombak region varied between -9.08 and -10.69 %, and between -59.32 and -63.88 %, respectively (Table 2). The results show that the data corresponding to the recharge elevation estimates of the drinking water sources of Tombak region are plotted on both the GMWL and the MWL, and that the aquifers recharging the water resources are fed by meteoric water without evaporation, that is, by surface precipitation (rain and snow) (Figure 9a).

Table 2 Results of ^{18}O, ^{2}H, and ^{3}H analyzes

Water sources	$\delta^{18}O$ (‰)	$\delta^{2}H$ (‰)	d-excess (‰)	^{3}H (TU)
CG-1	-9.81	-61.66	16.82	3.10
YR-2	-10.69	-63.88	21.64	3.52
TP-3	-9.08	-59.32	13.32	4.40

Considering the location of the sources with the MWL, it is seen that the waters of CG-1 spring are in an aquifer that is fed less by precipitation, and relatively closer to the effect of evaporation compared to other sources. Deuterium excess values (d-excess) vary depending on the effects of the rainfall regime. Waters affected by the same precipitation regime have similar values. The high deuterium excess values obtained are indicative of a dominantly marine precipitation, whereas continental precipitation predominates on the points with low deuterium excess (Kehinde, 1993). Mean values are related to feeding by precipitation of both origins. The excess values of deuterium were calculated from the $\delta^{18}O$ and $\delta^{2}H$ values of the water sources by using the formula of $d = \delta^{2}H\text{-}8x\ \delta^{18}O$ (Dansgaard, 1964). Table 2 shows that the d values for the water sources of Tombak region range between 13.32 (%o) (TP-3 source) and 21.64 (%o) (YR-2 source). Based on these d-excess values, the water sources of Tombak region can be regarded as marine precipitation. Spring samples show higher $\delta^{18}O$ values than well water samples and are isotopically depleted according to v-SMOW (Lermi and Ertan 2019). The isotopes of $\delta^{18}O$, $\delta^{2}H$ and ^{3}H are the parameters that enable us to comment on the length of time the waters stay in the aquifer and their feeding heights, and they can be utilized to trace water transport during different stages of the hydrologic cycle. High values of $\delta^{18}O$ and ^{3}H indicated that the waters were fed from low elevations, and the transition period was short, respectively (Figure 9b). Both the high ^{3}H values contents of the drinking water sources together with their low EC values indicated shorter residence times in the aquifer, since longer flow times resulted in higher radioactive decay of tritium. These water sources were found to have ^{3}H values of between 3.10 and 5.53 (TU). TP-3 source is the source with the highest TU value of 5.53 (TU), and the shortest circulation among the all water resources.

The Cl^{-}-^{3}H relationship is used in the interpretation of the underground circulation times of meteoric origin waters. Deep

circulation waters have high Cl^- and low δ^3H values. The ^3H isotope, which has a radioactive structure, decays depending on the contact time of groundwater with the aquifer. ^3H bearing waters are defined as young waters with transit times of 5–10 years (Clark and Fritz 1997). When the ^3H content of the precipitation that feeds groundwater is known, comments can be made about the age of groundwater and its relationship with other waters. The decrease in the ^3H value indicates the increase in the circulation time of the water underground. According to the Cl^-–^3H graph, the water sources of Tombak region had high ^3H and low Cl^- contents, and their aquifers were recharged by young groundwater with short transit times. The spring waters in the study area can be interpreted as shallow-fed or mixed waters. It is possible to say that the source with the deepest circulation among water resources was CG-1(Figure 9c). The δ^2H-^3H graph confirmed the $\delta^{18}O$-^3H and Cl^--^3H graphs. In terms of deuterium-tritium values, the source with the shortest contact time with the aquifer was TP-3, and the source with the longest contact time was CG-1 (Figure 9d).

The dissolved substance content and EC of the waters in contact with the aquifer increase with time. The high tritium values indicate that sea water has entered the aquifer. It can be said that the interaction of water with low EC value and high tritium value with rocks is shorter. This situation can be interpreted as the geological structure and units in the region do not significantly affect the groundwater. EC values change during dry and rainy periods. Factors such as decreased precipitation and increased evaporation can be shown as the cause of the increase in the EC value during the dry period.

High ^3H concentrations and low EC values imply short period and insignificant levels of water–rock interactions for the regional groundwater, and they are indicative of residence times of <50 years (Carreira et al. 2013) (Figure 9e). According to isotope analysis results, it was observed that there was a harmony between the Yuksekova Ophiolites of Tombak area, and the lithological features of the

conglomerate-limestone-sandstone and marl intercalated unit belonging to the Ahmetçik formation. Accordingly, it can be said that in the area where the water resources of Tombak region are located, there is a water cycle that reaches the aquifer in the Yüksekova ophiolites, stays there for a short time and reaches the surface in the form of springs.

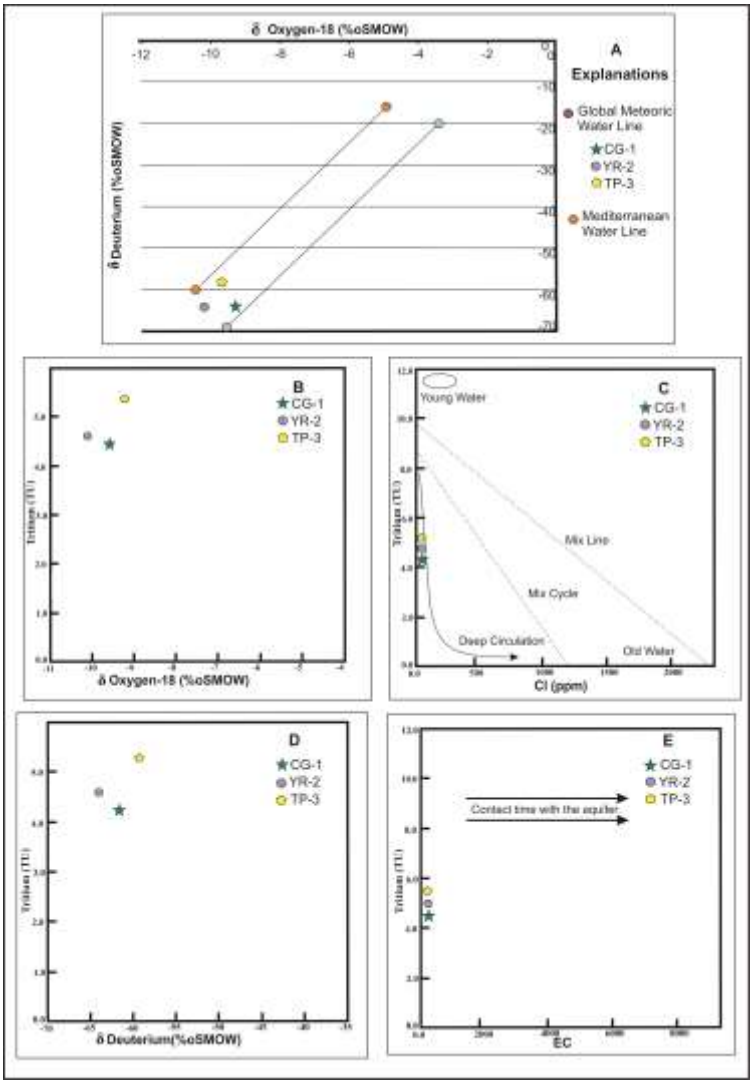

Figure 9. a) The relationship between the drinking water sources of Tombak region and the Global Meteoric Water Line, the Mediterranean Water Line, and $\delta^{18}O$ b) $\delta^{18}O$-^{3}H relationship of water sources, c) Cl^{-3}-H relationship of water sources, d) $\delta^{2}H$–TU relationship of water sources, e) EC–TU relationship of water sources

2.3. Effects of Water Sources on Human Health

Iodine is an essential component of thyroid hormones and is essential for human life. Due to insufficient iodine concentration in drinking water, deficient iodine intake causes serious problems in humans. Goiter disease is one of them. When iodine deficiency occurs in the human body, the thyroid gland works harder to produce the thyroxine hormone necessary for metabolism, and thus the thyroid gland enlarges and causes goiter. When the incidence of this disease exceeds 5% in people living in the same region, the disease is declared as "endemic goiter" (WHO, 2007). Goiter disease can adversely affect the health of people of all age groups. It is known to cause situations such as miscarriage in pregnant women, growth and mental retardation in babies and children, hereditary diseases such as deafness and dwarfism; lack of concentration, understanding retardation, learning difficulties in children and adolescents, and diseases such as laziness and hypothyroidism in adults.

Iodine intake does not depend solely on the use of iodized salt. The iodine amount of the water source used in a region is also the determining factor in the amount of iodine directly entering the human body. The limit value of iodine in water determined by the World Health Organization (WHO) is 10 mg/L (WHO, 2017). When anion-cation measurements were made to determine the characterization of the waters, it was determined that the drinking water sources of Tombak region do not contain any iodine. In this study, it is estimated that iodine deficiency of spring waters of Tombak region may cause endemic goiter. In a study conducted in the Tombak region in 1999, it was stated that the iodine content of the water samples taken from the same sources was lower than 1 mg/L and the incidence of goiter in the people living in the region was quite high, such as 71.1% (Kılınç, 2001). Based on this curiosity, it was determined that goiter disease was seen at a high rate in the local people in the interviews we made with the local people during our study. Based on the results of our study, it is thought that the low iodine content of the water resources in the region may be among the causes of this health problem.

CONCLUSIONS

In this study, drinking water samples were taken from Cangı spring (CG-1), Yareli spring (YR-2) and Taşpınar fountain (TP-3) in Tombak-Göksun (Kahramanmaraş) region in different months during a year and their physical and chemical analyzes were completed. When the results of the analyzes were examined, it was determined that the chemical parameters of the spring waters in all regions were suitable for drinking and utility water criteria, but all three sources were insufficient in terms of iodine content. It is thought that this iodine deficiency seen in drinking water sources increases the incidence of hypothyroidism-related goiter in the majority of the local people. This conclusion was reached as a result of face-to-face interviews with the people of the region. According to these results, it was concluded that in order to reduce or eliminate the health problems caused by iodine deficiency in water resources, it would be appropriate to inform the local people about the use of iodized salt to increase their daily iodine intake and to consume more iodine-containing foods.

The water resources of the Tombak-Göksun (Kahramanmaraş) region present a permeable structure due to the fractured structure found in the Late Cretaceous Yüksekova ophiolites. Surface waters pass through the Yüksekova ophiolites and reach the aquifer, stay there for a short time and emerge as a source in different areas. The water resources are in the "C1-S1" class according to the US salinity classification in terms of irrigation water quality, and it indicates that it is S1, that is, "low sodium water". According to Wilcox diagram, % Na values show us that all three water sources are Class I (<20%; very good) waters. According to these values, it is understood that there is no harm in using water resources for irrigation purposes. Anion-cation concentrations were evaluated using Piper and Schoeller diagrams and, it was determined that CG-1, YR-2, TP-3 spring waters correspond to the fifth area (waters with more than 50% carbonate hardness) according to the Piper diagram. Based on the results of the chemical analyzes of the drinking water samples collected for 1 year and during the four seasons and the interpretations made using the Schoeller diagram, it has been shown that the drinking water resources used by

the inhabitants of the Tombak region were obtained from similar sources and the same aquifer lithology. These waters are classified as "normal chloride waters" according to chloride concentration, "normal sulfate waters" according to sulfate concentration, and "normal carbonated waters" according to carbonate + bicarbonate concentration.

When evaluated in terms of isotope hydrogeology; according to the reference curves in the $\delta^{18}O$ and $\delta^{2}H$ graphs, it is possible to say that the waters in the region are meteoric waters away from the effects of evaporation. According to the deuterium excess values, it is thought that the waters are fed from marine precipitation. In terms of Cl^-- δ^3H relationship, it is also possible to say that CG-1 has the deepest circulation among water resources. According to the δ^2H-^3H graph, it is seen that the source with the shortest contact time with the aquifer is TP-3 and the source with the longest contact time with the aquifer is CG-1. In the assessment of $\delta^{18}O$ and ^3H, it can be said that the retention time of the waters in the aquifer is less than 50 years for all water resources.

Acknowledgements

This study was funded and supported by the Unit of Research Project (BAP) (Project No: 2017/1-30 YLS) of Kahramanmaraş Sutcu Imam University. The authors are grateful to KSU-BAP for the financial support provided for the pursuit of this project.

REFERENCES

Alam, M.O., Shaikh, W.A., Chakraborty, S., Avishek, K., Bhattacharya, T. (2016). Groundwater arsenic contamination and potential health risk assessment of gangetic plains of Jharkhand, India. Expo. Health, 8: 125–142. https://doi.org/10.1007/s12403-015-0188-0

Azzakhninia, I., Abdelouasb, A., Talbi, E.H. (2019). Iodine content in groundwater of North Eastern Morocco and its relation with the incidence of goiter. Materials Today, 13(3),1151-60. https://doi.org/10.1016/j.matpr.2019.04.083

Carreira, P.M., Marques, J.M., Nunes, D., Santos, F.A.M., Goncalves, R., Pina, A., Gomes, A.M. (2013). Isotopic and geochemical tracers in the evaluation of ground water residence time and salinization problems at Santiago Island, Cape Verde. Earth and Planetary Science, 7:113–117. https://doi.org/10.1016/j.proeps.2013.03.063

Craig, H. (1961). Isotopic variations in meteoric water. Science, 133:1702–1703. https://doi.org/10.1126/science.133.3465.1702

Clark, I., Fritz, P. (1997). Environmental isotopes in hydrogeology. CRC Press/Lewis Publishers, Baton Rouge.

Dansgaard, W. (1964). Stable isotopes in precipitation. Tellus, 16:(4), 436–468. https://doi.org/10.1111/j.2153-3490.1964.tb00181.x

Davis, S.N., De Wiest, R.J.M. (1966). Hydrogeology, vol. 463. Wiley, New York.

Delange, F., De Benoist, B., Pretell, B., Dunn, J.T. (2001). Iodine deficiency in the world: where do we stand at the turn of the century? Thyroid 11:437–447. https://doi.org/10.1089/105072501300176390

Delgado, C., Pacheco, J., Cabrera, A., Batllori, E, Orellana R, & Bautısta, F. (2010). Quality of groundwater for irrigation in tropical karst environment: the case of Yucatan, Mexico. Agricultural Water Management, 97:(10), 1423–1433. https://doi.org/10.1016/j.agwat.2010.04.006

Gastmans, D., Chang, H.K., Hutcheon, I. (2010). Groundwater

geochemical evolution in the northern portion of the guarani aquifer system (Brazil) and its relationship to diagenetic features. Appl Geochem 25:16–33,

Gat, J.R., Garmi, L., (1970). Evolution of the isotopic composition of atmospheric waters in the Mediterranian Sea area. Journal of Geophysical Research, 75:(15), 3039-3048. https://doi.org/10.1029/JC075i015p03039

Hem, J.D. (1985). Study and interpretation of the chemical characteristics of natural waters, 3rd ed. USGS Water Supply Paper. 2254, pp 117–120.

Hetzel, B.S. (1983). Iodine deficiency disorders (IDD) and their eradication. Lancet, 2:1126–1129. https://doi.org/10.1016/s0140-6736(83)90636-0

Khashogji, M.S., El Maghraby, M.M.S. (2013). Evaluation of groundwater resources for drinking and agricultural purposes, Abar Al Mashi area, south Al Madinah Al Munawarah City, Saudi Arabia. Arab J Geosci 6(10):3929–3942. https://doi.org/10.1007/s12517-012-0649-8

Kehinde, M.O. (1993). Preliminary isotopic studies in the Bida basin, central Nigeria. Environmental Geology, 22: 212–217. https://doi.org/10.1007/BF00767406

Kılınç, M., Yüregir, G., Ezberci, F., Ekerbiçer, H., Büyükbefle, M.A. (2001). Evaluation of thyroid hormones and goiter in a rural community in a region of Anatolia. Turkish Journal of Medical Sciences, 31:(6), 547-552.

Lermi, A., Ertan, G. (2019). Hydrochemical and isotopic studies to understand quality problems in groundwater of the Niğde Province, Central Turkey. Environmental Earth Sciences 78: 365. https://doi.org/10.1007/s12665-019-8365-2

Missi, C., Atekwana, E. (2020). Physical, chemical and isotopic characteristics of groundwater and surface water in the Lake Chilwa Basin, Malawi. Journal of African Earth Sciences, 162: 103737. https://doi.org/10.1016/j.jafrearsci.2019.103737

Nan Z., Yi H., Zhu R., Xue-Liang Z. (2016). Fast Detection of Carbonate and Bicarbonate in Groundwater and Lake Water by

Coupled Ion Selective Electrode, Chinese Journal of Analytical Chemistry, 44(3):355-360. https://doi.org/10.1016/S1872-2040(16)60913-1.

Oinam, J.D., Ramanathan, A., Linda A., Singh, G. (2011). A study of arsenic, ironand other dissolved ion variations in the groundwater of Bishnupur District. Manipur India Environ. Earth Sci. 62(6):1183–1195.

Perinçek, D., Kozlu, H. (1984). Stratigraphy and structural relations of the units in the Afşin-Elbistan-Doğanşehir region (Eastern Taurus). Bulletin of The Mineral Research and Exploration, 181-198.

Piper, A.M. (1944). A graphic procedure in the geochemical interpretation of water analyses. Eos, Transactions American Geophysical Union, 25: 914-928. http://dx.doi.org/10.1029/TR025i006p00914

Raju, N.J., Patel, P., Gurung, D., Ramb, P., Gossel, W., Wycisk, P. (2015). Geochemical assessment of groundwater quality in the Dun valley of central Nepal using chemometric method and geochemical modelling. Groundw. Sustain. Dev. 1(1-2):135–145.

Richards, L.A. (1954). Diagnosis and improvement of saline and alkali soils. Soil Science 78:154-155.

Rızaoğlu, T., Parlak, O., İşler, F. (2005). Esence granitoyidinin (Göksun-Kahramanmaraş) jeokimyası. Yerbilimleri (Earth Sciences). 26(1):1-13. https://dergipark.org.tr/tr/pub/yerbilimleri/issue/13627/165109.

Schoeller, H. (1967). Geochemistry of groundwater. An international guide for research and practice. UNESCO, 1967, chap 15, pp 1-18.

TSI 266, Turkish Standards Institute (2015). Water-Water Intended for Human Consumption

Turkish State Meteorological Service (2021). Available at: www.dmi.gov.tr.

Wilcox, L.V. (1955). Classification and use of irrigation water. US Department of Agriculture, Circular 969, Washington DC.

World Health Organization (2007). United Nations Children's Fund & International Council for the Control of Iodine Deficiency Disorders. Assessment of iodine deficiency disorders and monitoring their elimination. 3rd ed. Geneva, Switzerland.

World Health Organization (2017). Guidelines for Drinking-Water Quality: Fourth Edition Incorporating the First Addendum. Geneva. https://www.ncbi.nlm.nih.gov/books/NBK442373

WPCR, (2004). Water Pollution and Control Regulations. Official Gazette 31.12.2004, No:25687.

CHAPTER 2

LATE FUEL INJECTION COMBINED WITH RETARDED INTAKE VALVE CLOSURE FOR IMPROVED EXHAUST SYSTEM WARM-UP IN DIESEL AUTOMOTIVE VEHICLES

Assist. Prof. Hasan Üstün BAŞARAN[1]

[1] Izmir Katip Celebi University, Faculty of Naval Architecture and Maritime, Naval Architecture and Marine Engineering Department, Izmir, TURKEY.
hustun.basaran@ikcu.edu.tr, 0000-0002-1491-0465.
*A prior version of this work is presented in the ISPEC 10th International Conference on Engineering and Natural Sciences on May 16-18, 2021 / Siirt, Turkey.

INTRODUCTION

Currently, diesel engines are widely preferred in automotive vehicles and marine vessels due to their reliable and fuel-saving performance. Although electric vehicles gain popularity every year, particularly for on-road transportation, diesel engines are still expected to be used in the future [Leach et al. (2020)]. The most significant obstacle on diesel engine usage for today and in the near future seems to be the strict norms on tailpipe emission rates. Both light-duty and heavy-duty diesel vehicles are required to operate with highly reduced nitrogen oxide (NOx) and particulate matter (PM) emission rates in the EU and US [Dieselnet, standards (2022), EPA (2022)]. As Figure 1 below is examined, it is seen that since 1992 the allowable limit for NOx and PM in the EU for heavy-duty (HD) diesel engines is reduced up to 95 % and 97 %, respectively [Jurchiş et al. (2018)]. It can be estimated that Euro 7 will probably demand stricter NOx and PM limits and pose even a greater threat for future diesel engine utilization.

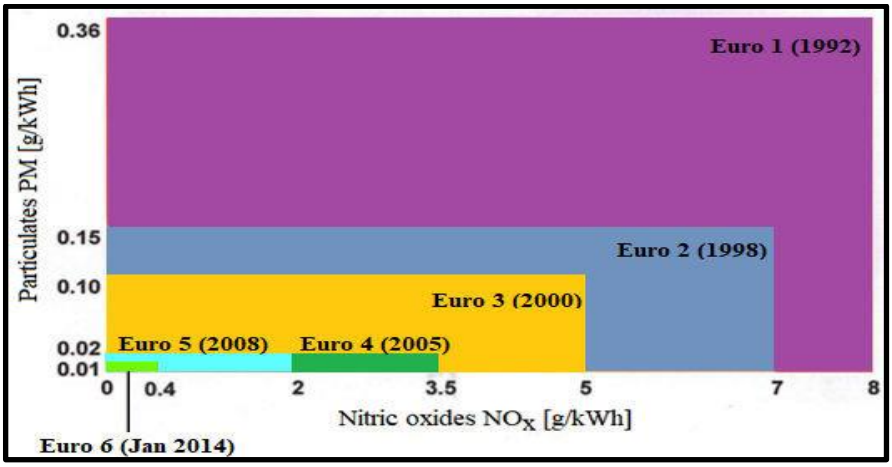

Figure 1: Euro 1-6 emission standards for HD diesel engines [Jurchiş et al. (2018)]

Due to the ever-decreasing trend of emission regulations stated on Figure 1, researchers are constantly studying on diesel engines to lower the NOx and PM emission rates [Joshi (2022)]. One popular technique is to use exhaust gas recirculation (EGR) through directing some percentage of engine-out gas back into the cylinders [Zheng et al. (2004)]. EGR is found to be highly effective at decreasing NOx

emission rates as it can reduce the in-cylinder temperature and oxygen availability [Hountalas et al. (2008)]. However, EGR also causes a rise in PM rates [Yao et al. (2010)]. Therefore, it should be applied in a controlled manner. Another popular technique is to utilize alternative fuels instead of diesel fuel on diesel engines [Othman et al. (2017)]. Hydrogen, ammonia, methanol and liquefied natural gas (LNG) are some of the proposed alternative fuels for marine diesel engines [Mallouppas & Yfantis (2021)]. There is a growing trend towards the use of alternative fuels in highway vehicles as well [Chen et al. (2021), Ardebili et al. (2021), Valera & Agarwal (2019)]. In addition to alternative fuels, some researchers try to develop advanced combustion methods to reduce emission rates [Epping et al. (2002), Reitz & Duraisamy (2015), Chaichan (2014)]. Electric vehicles depending on batteries and hydrogen fuel cells are also examined as alternatives to diesel vehicles [Cunacan et al. (2021)]. Although these technologies have a high potential to limit emission rates, they are generally cost-ineffective, have limited performance and also compared to diesel vehicles, the infrastructure for battery-based or fuel cell-based transportation is not yet completed.

Those aforementioned methods are effective to decrease harmful emission rates. However, they cannot adequately curb the NOx and PM rates at all operating points. Thus, engine systems for on-road vehicles and marine vessels are usually equipped with exhaust after-treatment (EAT) systems [Martinovic et al. (2021), Selleri et al. (2021)]. These systems are mostly placed at the downstream of turbine on exhaust systems. Exhaust gas is cleaned at those systems before getting released into the environment. Currently, commercial vehicles mostly prefer to use three-way catalytic converter (TWC) as the typical EAT system at their exhaust units. A schematic of a TWC is shown below in Figure 2 [Shaver et al. (2022)].

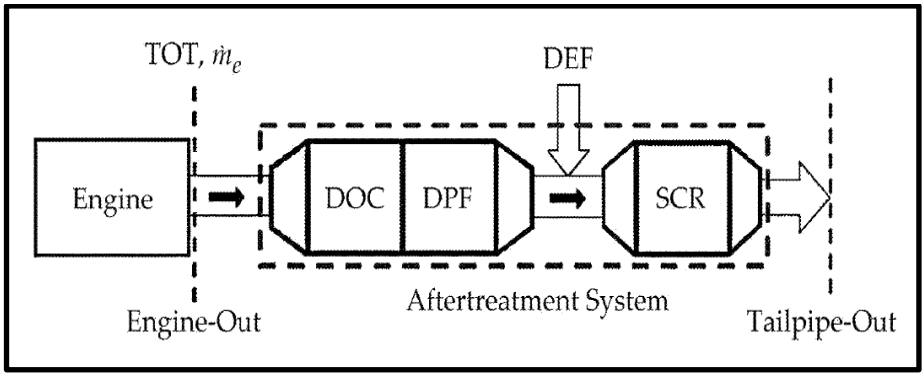

Figure 2: A typical TWC system [Shaver et al. 2022]

The engine-out gas shown on Figure 2 flows through the diesel oxidation catalyst (DOC) at first. At this point, unburned hydrocarbons (UHCs) and carbon monoxide (CO) are decreased in the exhaust flow. At the downstream of DOC, diesel particulate filter (DPF) is placed. DPF traps the PM in the exhaust flow and burns it through either passive or active regeneration after a certain amount of PM is collected in the filters [Guan et al. (2015)]. After DPF, engine-out gas finally flows through the Selective Catalytic Reduction (SCR), the third and the last element of the TWC system. Generally, diesel exhaust fluid (DEF) is injected on the DPF-out pipeline before the gas enters the SCR system. DEF is mostly composed of urea and deionized water and after the injection, the heat on DPF-out exhaust flow decomposes DEF to ammonia. Inside the SCR system, ammonia is utilized to reduce the harmful NOx through catalysts. At the downstream of SCR, there are only water and nitrogen which can be released safely into the atmosphere [Guan et al. (2014)].

TWC systems have a considerable potential to limit NOx, PM and CO emission rates. However, they also own a significant drawback. Unfortunately, the catalysts inside those systems generally need to cross a threshold temperature (mostly ~ 250^{o}C) in order to keep emission conversion efficiency at high levels. Thus, EAT systems are not expected to perform in an effective manner, particularly below 250^{o}C [Koebel et al. (2000), Girard et al. (2009), Kim et al. (2020)]. Unless some external heating device such as an electrical heating

equipment or an afterburner or a heat storage unit is particularly placed on an engine system [Kessels et al. (2010), Gao et al. (2019), Paule et al. (2011), Gaiser & Seethaler (2007)], the only way to heat the EAT system is to use the exhaust heat energy [Gosala et al. (2018), Basaran (2020), Sun et al. (2021)]. At high speeds, both exhaust temperature (represented as turbine-out temperature (TOT) in Figure 2) and exhaust flow rate ($\dot{m}_e$) are generally high which simplifies the EAT thermal management. However, at cold-start, idling and low-loaded operations of on-road and marine vessels, exhaust temperature generally remains much below 250^{o}C and exhaust flow rate is relatively low compared to that achieved at high loads. Those low engine performance characteristics are unable to sustain an effective TWC in diesel vehicles [Stanton (2013)]. Therefore, there is a requirement to elevate exhaust temperatures at these aforementioned conditions to obtain improved TWC and thus, reduced NOx and PM emission rates [Munnannur et al. (2022)].

This study focuses on the enhancement of EAT heat-up through co-application of late fuel injection (LFI) and retarded intake valve closure (RIVC). While LFI is found to be effective at keeping exhaust flow rates at high levels, RIVC is seen to be highly effective at increasing the temperature at after-treatment inlet. LFI-alone cannot increase the engine-out temperature above 250^{o}C and results in high fuel consumption penalty. RIVC-alone is fuel-saving and can elevate the temperature above 250^{o}C. However, aggressive use of RIVC causes a noticeable reduction in exhaust flow rate which highly degrades the EAT warm up time. It is seen that combining those two aforementioned techniques can not only keep fuel penalty at a relatively low level but also improve the EAT warm up effectiveness through high exhaust temperature and slightly reduced exhaust flow rates.

1. METHODOLOGY

This work aims to rise the engine-out temperature of a heavy-duty diesel engine through internal measures. LFI and RIVC are the two main engine-base modifications applied in the system to enhance the temperature and mass flow rate parameters at EAT inlet. At the

beginning, the layout of the engine model is demonstrated and explained explicitly. The specifications for the main engine elements are stated and the exhaust-out parameters to be examined in the model are particularly emphasized. Then, LFI and RIVC methods are explained, respectively. The combined application of those two strategies is the main motivation to yield improved performance parameters at EAT inlet in this study.

1.1. Diesel Engine Properties and Engine Simulation

Highway vehicles such as trucks, vans and inner-city buses and vessels such as fishing boats, tugboats and yachts are mostly equipped with heavy-duty (HD) diesel engines for their operation. Those vehicles do not always work at high speeds and high loads. At urban transport, vehicles are mostly required to operate at light loads due to traffic congestion. At marine transport, vessels generally need to operate at idling or low loads during loading or unloading of goods or passengers at ports. At those conditions, engine systems do not consume that much fuel oil or marine diesel oil compared to high-loaded operations, which mostly yields increased air-to-fuel ratio (AFR) and decreased temperature inside the cylinders. This low in-cylinder environment generally does not allow exhaust-out temperature to exceed 250^{o}C and thus, deteriorates the catalytic converter effectiveness. Considering the inflexible emission norms in diesel vehicles and the significant role of EAT systems to meet those norms, after-treatment thermal management is a timely and serious problem to be addressed by engine researchers and producers.

The specifications of the HD automotive engine utilized in this research are stated in Table 1. It is a four-stroke, turbocharged compression-ignition engine and its compression ratio is given as 17.3. A relatively low-loaded operating condition, engine speed of 1200 RPM and engine load of 2.5 bar BMEP, is selected where turbine-out temperature (TOT) is not adequately warm (TOT < 250^{o}C) for efficient TWC operation.

Table 1: Diesel Engine Properties.

Model	Four-stroke heavy-duty diesel engine
Air intake	Turbocharged
Bore (mm)	107
Stroke (mm)	124
Compression ratio	17.3:0
Exhaust valve opening	20°CA BBDC
Exhaust valve closure	20°CA ATDC
Intake valve opening	20°CA BTDC
Intake valve closure	25°CA ABDC
Cylinder firing order	1-5-3-6-2-4
Calorific value of the fuel (kJ/kg)	42700
Operating speed and load	1200 RPM and 2.5 bar BMEP

Figure 3 illustrates the simulation of the diesel engine used for the analysis of the exhaust unit thermal management [Lotus Engineering (2022), Lotus Engineering Software (2020)]. The model is built through use of the specifications stated in Table 1. As given on the firing order, the system owns six cylinders. Each cylinder works with 4 valves to complete a cycle during the operation. Those 4 valves are controlled in the system considering the opening and closing timings stated explicitly in Table 1. As engine design parameters are altered to yield higher engine-out temperature, fuel injection quantity is modified to keep the system load fixed at a brake mean effective pressure (BMEP) of 2.5 bar. The theory for the calculations in the simulation is explained explicitly in former studies [Basaran & Ozsoysal (2017), Basaran (2019)]. Those references can be examined for the calculation of engine performance parameters with this model.

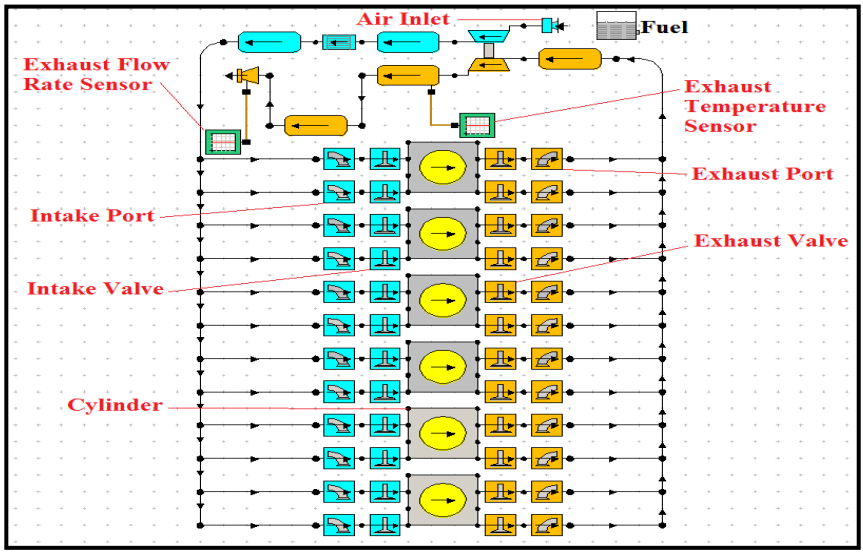

Figure 3: Diesel engine simulation

As mentioned in the Introduction section, catalytic converters are noticeably temperature-dependent. In a simulation without any external supporting device, there is only exhaust gas heat for rapid EAT warm up. Reasonable control of exhaust temperature is a must to achieve this purpose. Therefore, as shown in the upper part of Figure 3, a temperature sensor (with unit ^{o}C) is set to measure the temperature at the downstream of the turbine. A particular TWC system is not placed on the simulation. On a typical HD diesel engine system, turbine-out gas instantly goes towards the catalytic converter without losing considerable temperature. Therefore, the temperature at the turbine exit can be assumed to be the temperature at the catalytic converter inlet. As EAT is directly proportional to the temperature, the exhaust temperature sensor checks the primary parameter for EAT warm up. The second important parameter to be considered is the exhaust mass flow rate (kg/min). In Figure 3, a different sensor (flow rate sensor) is put on the upper left part of the model. Heat transfer from the exhaust gas to the catalytic converter relies not only on exhaust temperature but also on exhaust flow rate. Thus, this second sensor aims to measure the change in flow rate streaming towards the catalytic converter in the simulation. Considering high exhaust flow rate is beneficial for fast

EAT warm up, two different engine-base methods are combined to keep flow rate at relatively high levels without causing a significant fuel consumption penalty.

1.2. LFI Technique

As shown in Figure 3, there is not an external element (such as an electrical heating device) to heat up the exhaust unit. The model attempts to achieve sufficient warm up through internal measures, which depend only on engine design parameters. The first parametric change is achieved through the modulation of the injection timing of the fuel. As seen in Figure 4, while the nominal fuel injection timing – early fuel injection – occurs close to the end of the compression stroke and before the top dead center, LFI occurs a little bit further than the top dead center when the piston moves downward at the power stroke. In the study, fuel injection timing (FIT) is changed between -1°CA and 13°CA after top dead center (ATDC) which is stated explicitly in Table 2. FIT is retarded 14°CA from the nominal position through 7 steps.

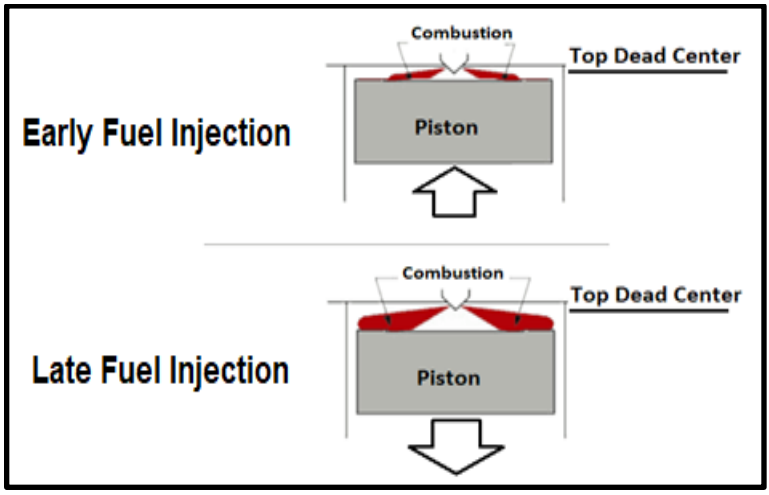

Figure 4: Early and late fuel injection processes inside the cylinder [adapted from Dieselnet, technology guide (2022)]

Table 2: Change of engine parameters at different steps.

Method	Engine Parameter	STEPS							
		Nominal	1st	2nd	3rd	4th	5th	6th	7th
LFI	FIT (ºCA ATDC)	-1	1	3	5	7	9	11	13
RIVC	IVC (ºCA ABDC)	25	35	45	55	65	75	85	95
RIVC + LFI	IVC + FIT	(25) + (-1)	(35) + (1)	(45) + (3)	(55) + (5)	(65) + (7)	(75) + (9)	(85) + (11)	(95) + (13)

1.3. RIVC Technique

The second parametric change is on the closure timing of all intake valves in the system. As given previously in Table 1, intake valves are shut off completely at 25ºCA after bottom dead center (ABDC). This base timing is delayed with 10ºCA increments as stated specifically in Table 2 in order to apply RIVC technique. The method can be better understood by examining Figure 5 [Basaran (2021)]. In late intake valve closure (LIVC) mode, intake valve is closed at retarded timings until it is equal to 95ºCA ABDC, the final timing given in Table 2. RIVC method enhances fuel consumption and engine-out temperature. However, extreme use of RIVC is found to decelerate EAT warm up due to high airflow reduction in many previous analyzes [Basaran (2021), Garg et al. (2016)]. Therefore, as given in Table 2, this work considers the retardation of both FIT and IVC (IVC+FIT) – referred to as the combined RIVC+LFI technique in the next section – to avoid extreme RIVC and thus, accelerate EAT heat up in diesel vehicles.

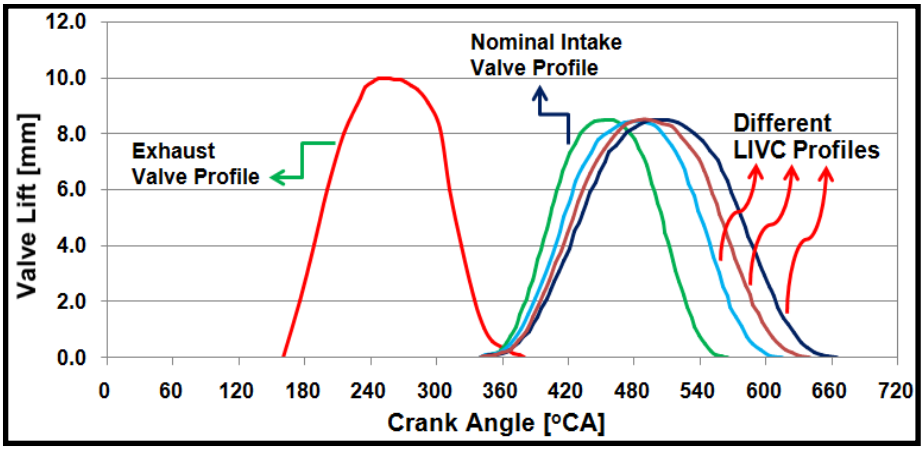

Figure 5: Retarded intake valve closure process [Basaran (2021)]

2. RESULTS AND DISCUSSION

Using the methods defined explicitly in the Methodology section, the effects of LFI, RIVC and combined RIVC+LFI strategies on the diesel engine system are demonstrated in this section. It is intended to determine the potential of each method for exhaust heat management.

2.1. Effect of Fuel Injection Timing on Engine System

The first method examined in the study is the delayed fuel injection timing. The impact of LFI on engine-out temperature and AFR is demonstrated in Figure 6 below. Fuel injection timing is modulated between -1°CA and 13°CA after top dead center (ATDC). Starting from the nominal timing (-1°CA ATDC), injection timing is delayed 2°CA degrees in every step. It is shown that the temperature at the exhaust unit rises steadily in the system as injection timing is postponed further from its starting position. This steady temperature rise stems partially from the steady decrease of AFR as shown in Figure 6. AFR is a significant parameter to determine the in-cylinder and exhaust temperatures. Many previous works show that it needs to be reduced in order to elevate exhaust temperatures [Basaran & Ozsoysal (2017), Garg et al. (2016), Gosala et al. (2018)]. Similar to those works, LFI leads to a reduction of AFR as well. However, an

aggressive reduction is not seen in Figure 6. AFR approaches close to 55 at the most retarded injection timing.

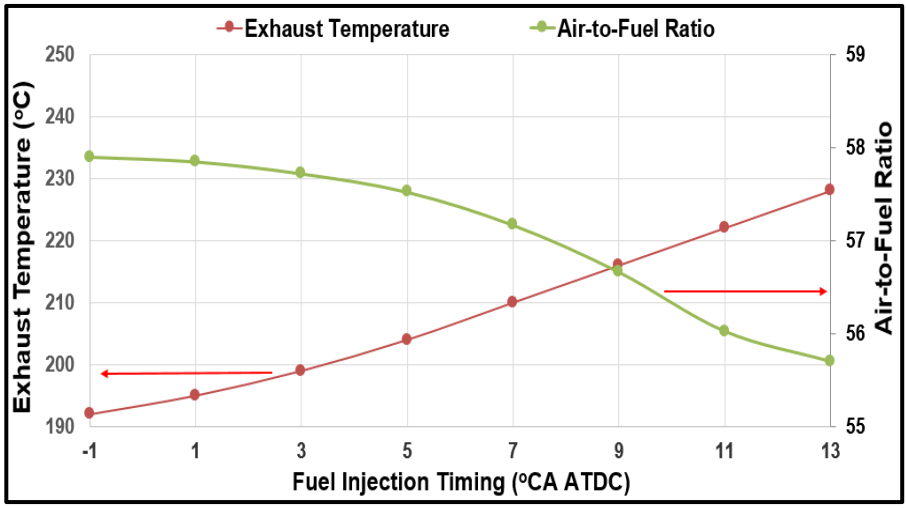

Figure 6: Impact of LFI on exhaust-out temperature and AFR

Figure 7 demonstrates why AFR does not go through a dramatic change in LFI mode. Volumetric efficiency remains more or less the same in this mode. This is because, unlike aforementioned previous works, only fuel injection rate is modulated in this technique and there is no interruption to airflow into the cylinders. As seen in Figure 7, in every step of the LFI mode, the system needs extra fuel injection to maintain engine BMEP constant. It can be relatively easier to boost exhaust temperature via decreasing the airflow. Since the system deals with relatively lower mass to be heated in this mode. However, without decreasing the in-cylinder charge (similar to the case in LFI mode in Figure 7), the system has to warm up higher mass and thus, needs much higher fuel to achieve this heat up. That high in-cylinder mass is the reason why it is difficult to yield a high temperature rise through using LFI in diesel engine systems (only up to 30°C even with a 14°CA fuel injection delay in Figure 6).

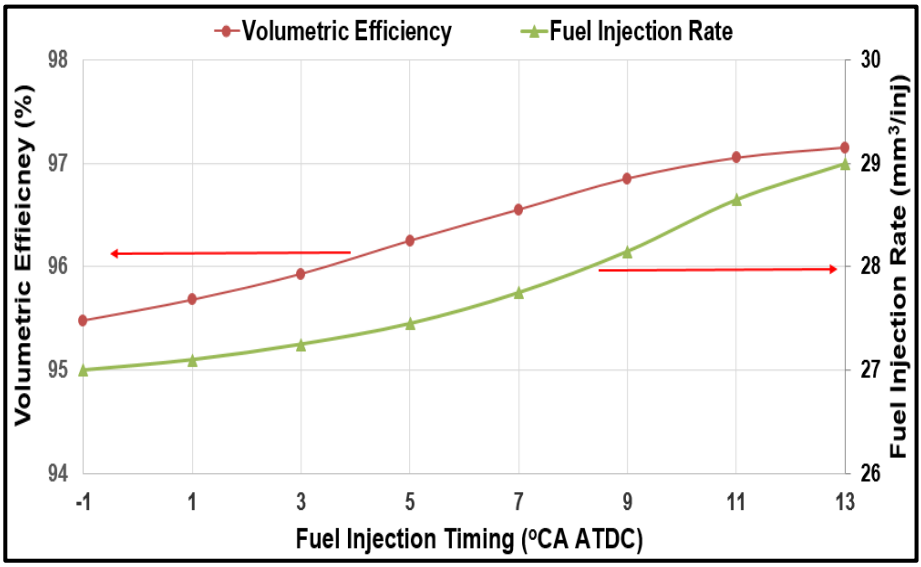

Figure 7: Impact of LFI on fuel injection rate and volumetric efficiency

As the system requires more fuel to be consumed for the same engine load, brake thermal efficiency (BTE) decreases from almost 29% to lower than 27% in Figure 8. This is predicted since $IMEP_{power}$ – measure of power generating potential of the engine – constantly decreases in Figure 8, which explains the need to utilize larger quantities of fuel in Figure 7. It is seen from Figure 7 & Figure 8 that the temperature rise via LFI leads to fuel-inefficient operation in the system. In addition to the low-efficient operation, exhaust temperature barely reaches 230ºC and cannot exceed 250ºC in Figure 6. This is the downside of using LFI to consider. However, LFI does not allow any airflow reduction, as indicated in Figure 7 and thus, it has the potential to maintain high exhaust flow rate. This is the upside of utilizing LFI, a possible improvement in EAT warm-up via high exhaust rates.

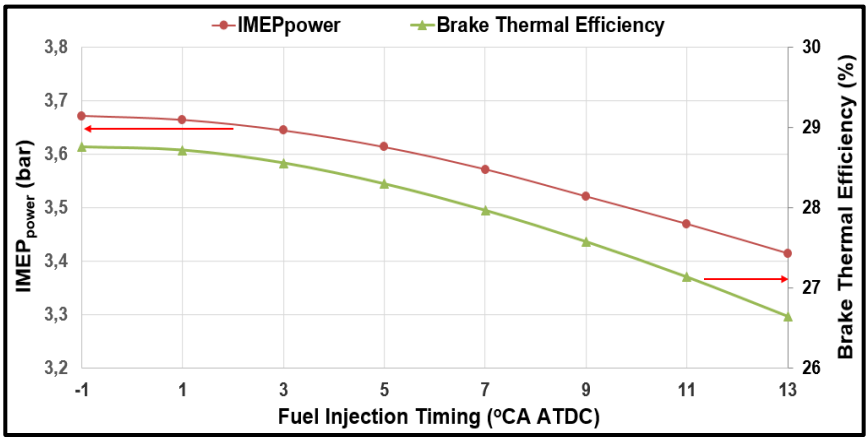

Figure 8: Impact of LFI on $IMEP_{power}$ and BTE

As Figure 9 is examined, it is understood why the system needs more fuel injection at retarded timings compared to nominal timing. Burning end timing of the 10% of the fuel (F%10) is very close to the TDC at nominal injection timing. However, as the injection timing is delayed, F%10 is completely combusted at positions almost up to 15°CA away from the TDC. This is valid for burning end timing of the 50% of the fuel (F%50) and the 90% of the fuel (F%90) as well. F%50 is completed almost 20°CA and F%90 is completed 35°CA away from the TDC. Overall, additional fuel usage in Figure 7 can be attributed to the retarded combustion completeness in Figure 9.

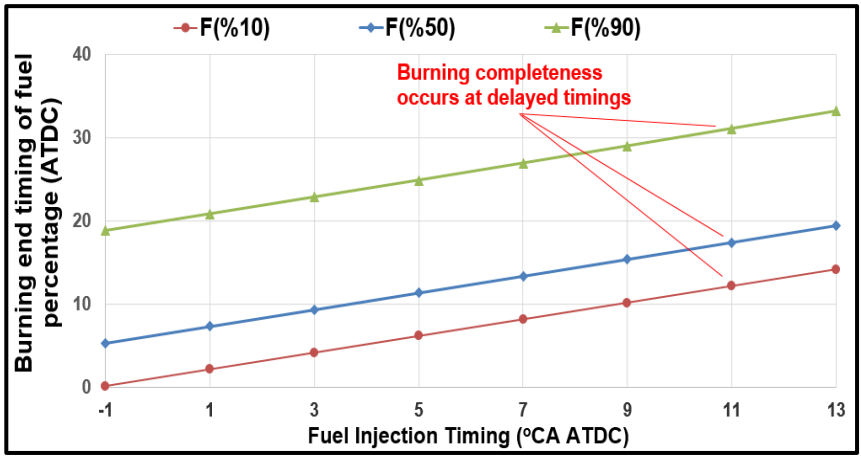

Figure 9: Impact of LFI on burning end timing of fuel percentages: F(%10), F(%50) and F(%90)

Those late burning end timings demonstrated in Figure 9 result in some dramatic change on in-cylinder pressure in Figure 10 below. There is a certain difference in the behavior of in-cylinder pressure between nominal and LFI-based modes, which needs to be further examined.

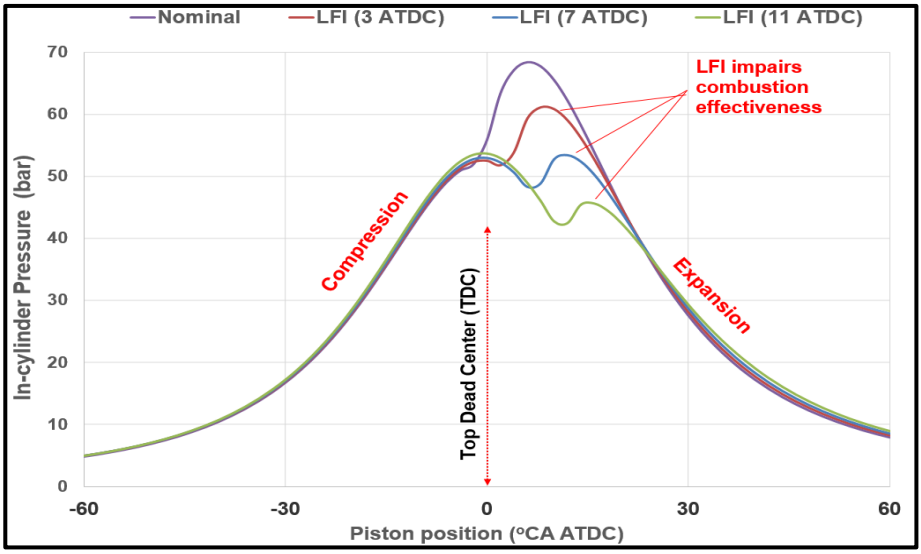

Figure 10: Impact of different LFI-based modes on in-cylinder pressure

In LFI-based modes on Figure 10, in-cylinder pressure in power stroke begins to rise at later timings compared to nominal mode. Therefore, the maximum in-cylinder pressure constantly decreases in the system. When injection timing is slightly delayed (3°CA ATDC), the reduction on maximum pressure is relatively low as the burning end timings shown on Figure 9 are relatively close to TDC. As the combustion occurs relatively close to TDC, a noticeable decrease in in-cylinder pressure is not expected. However, for moderately and extremely delayed injection timings (7°CA ATDC and 11°CA ATDC), burning end timings are far away from the TDC which causes combustion to start and finish at highly delayed timings compared to nominal mode. Combustion in those modes occurs at an environment where pressure is highly decreased. Therefore, combustion is ineffective at those cases compared to both nominal and slightly

delayed injection timing (3ºCA ATDC). In fact, this ineffective burning of fuel is the reason the system is faced with high fuel penalty in Figure 7 and the low BTE in Figure 8.

It is explicit from the results obtained in this section that the LFI method has a disadvantage – low BTE – when it is used to enhance exhaust temperatures at low loads. However, contrary to airflow reducing strategies, it can keep the volumetric efficiency at high levels which can be highly beneficial to improve the EAT heat-up process.

2.2. Effect of Combined RIVC+LFI on Engine System

It is found that LFI can elevate the engine-out temperature at a moderate level through injecting more fuel at retarded injection timings. The temperature rise is inadequate (approximately 30ºC) in order to keep EAT system above 250ºC. Therefore, in this section, it is combined with a different engine-base technique to further improve the temperature. Some combinations can raise the EAT inlet temperature sufficiently (such as simultaneous application of negative valve overlap and advanced exhaust valve opening), but they generally lead to undesirable high fuel inefficiency [Gosala et al. (2018), Sun et al. (2021)]. Thus, considering only the temperature rise on the exhaust unit is insufficient to evaluate the total EAT warm-up process. A combination should particularly assess the rise of fuel consumption in order to have a practical EAT thermal management in the system.

LFI is combined with RIVC to elevate turbine-exit exhaust temperature and thus, obtain improved EAT warm up in a diesel engine system. Steps in Table 2 are utilized on the model to yield the results. Effects of LFI-alone, RIVC-alone and RIVC+LFI combined methods on brake specific fuel consumption (BSFC) and exhaust temperature are shown in Figure 11.

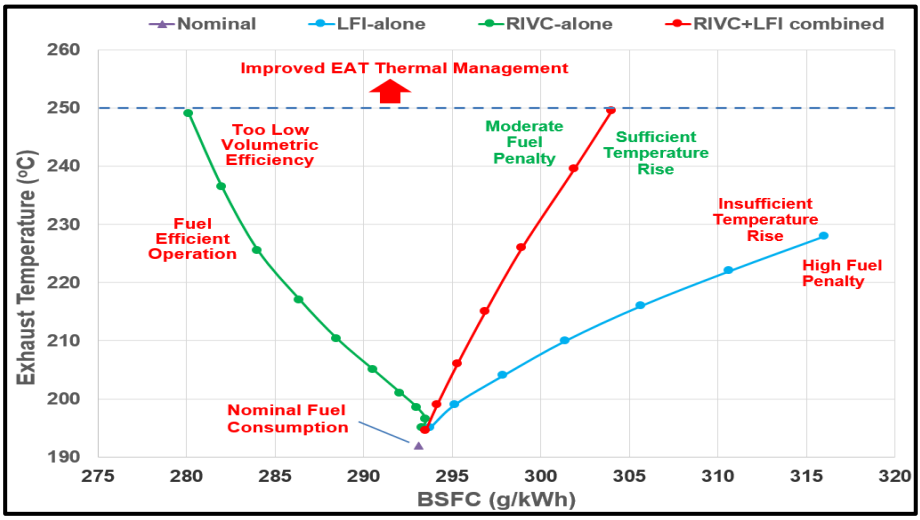

Figure 11: Comparison of LFI-alone, RIVC-alone and RIVC+LFI combined techniques on exhaust temperature and BSFC

The results for RIVC-alone in Figure 11 are taken from an early work where IVC is delayed up to 125°CA from the baseline [Basaran & Ozsoysal (2017)]. It is indicated in the figure that RIVC is considerably useful to yield high exhaust temperatures. It is also fuel-saving. However, the system is required to work with very low volumetric efficiency, which mostly decelerates EAT heat-up. Therefore, implementing RIVC-alone method is generally incapable of fast warm up of the EAT system. Moderate use of RIVC can be rather useful to achieve a high temperature with relatively high volumetric efficiency.

Unlike the positive effect of RIVC on BSFC, LFI-alone has a certain negative effect on fuel consumption in Figure 11. It is difficult to reach the threshold temperature (~250°C) via LFI. It can barely approach 230°C, which is unable to keep the EAT system in a well-performed manner. However, contrary to RIVC, LFI does not cause a significant decline on volumetric efficiency as mentioned previously in Figure 7. This positive effect on volumetric efficiency is useful as the potential on EAT warm up is considered. Therefore, LFI is combined with RIVC in Figure 11 as a third option to rise exhaust temperature.

The first aim for the combination of RIVC+LFI on the system is to reduce the high fuel penalty (BSFC > 315 g/kWh) seen in LFI-alone

mode. As RIVC+LFI is compared with other techniques in Figure 11, it still needs higher fuel consumption (BSFC ≅ 304 g/kWh) than RIVC-alone method. This can be predicted since RIVC is moderately used in the combination and the system is forced to consume more fuel owing to retarded injection of fuel. However, the temperature rise is better than LFI-alone method and very similar to RIVC-alone technique. The combined method has the capacity to maintain EAT temperature above 250^{o}C, which is certainly not likely with LFI-alone technique. Overall, it can be derived that the combined RIVC+LFI mode is appropriate for keeping BSFC at a moderate level and also keeping the exhaust temperature at a high level.

The second aim of the combination is to maintain the volumetric efficiency of the system at a relatively moderate level. Despite the high temperature improvement in Figure 11, RIVC-alone causes a significant decline on volumetric efficiency, which is not desired for rapid exhaust unit heat up [Basaran (2021)]. In order to have a quick EAT warm up, in-cylinder airflow and thus, exhaust flow rate should be controlled at a relatively high level. Therefore, the impact of each method on exhaust flow rate is demonstrated in Figure 12 below.

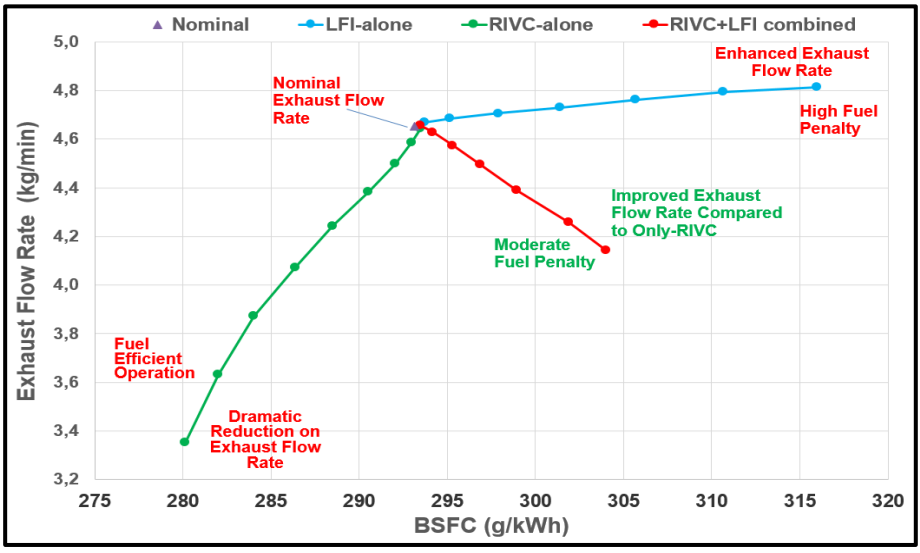

Figure 12: Comparison of LFI-alone, RIVC-alone and RIVC+LFI combined techniques on exhaust flow rate and BSFC

As Figure 12 is analyzed, it is seen that exhaust flow rate behaves differently in each mode. RIVC-alone owns the greatest exhaust flow reduction since its mechanism is designed to increase exhaust temperature via lowered in-cylinder airflow [Garg et al. (2016)]. LFI-alone causes a slight increase on exhaust flow rate, which is due mainly to the relatively constant volumetric efficiency and increased fuel injection rate seen formerly in Figure 7. Although it seems more beneficial at first compared to other methods in Figure 12, the high fuel penalty and the inadequate exhaust temperature rise obtained in Figure 11 do not allow LFI-alone strategy to be an attractive solution for enhanced EAT thermal management.

As the change of exhaust flow rate in RIVC+LFI combined mode is examined, similar to RIVC-alone method, it decreases steadily from the nominal condition. However, unlike RIVC-alone technique, BSFC goes up in this mode. The decline in exhaust flow rate is not as substantial as it is in RIVC-alone method, which is estimated since RIVC is not extremely used in the combined technique. Although exhaust mass flow rate is improved compared to fuel saving RIVC-alone mode, it is much lower compared to LFI-alone technique, which can be regarded as a disadvantage for EAT warm up. However, BSFC is reduced to about 304 g/kWh, which is a significant gain for the engine system.

2.3. Effect of Combined RIVC+LFI on EAT System

After calculating the results for exhaust temperature and exhaust flow rate, the potential of each method on EAT heat up can be compared in this section. Therefore, for the comparison, it is necessary to determine the total heat transfer rates from the exhaust-out flow to the EAT system in LFI-alone, RIVC-alone and RIVC+LFI combined modes, respectively. Considering the results in Figure 11 & 12, the comparison is made for the extreme use of each method – for operating points where RIVC-alone and combined RIVC+LFI can reach 250^{o}C and LFI-alone can achieve close to 230^{o}C exhaust temperature – in the system.
In order to obtain and compare the approximate heat transfer rates, the equation below is applied in the study [Incropera (2007)]:

$$\dot{Q} = C[\dot{m}_{exh}^{4/5}][T_{exhaust} - T_{EAT\ catalyst\ bed}] \quad (1)$$

The formulation (1) above considers both exhaust mass flowing ($\dot{m}_{exh}$) through the EAT system and the temperature difference between the exhaust unit ($T_{exhaust}$) and the EAT system (T_{EAT}). In the equation, C denotes a constant for the type of EAT chosen, which is the same for all techniques. In order to cancel C in the analysis, heat transfer rates (Q) are normalized through dividing all Q values in each method with the Q value calculated at 0°C T_{EAT} in nominal mode. The comparison of normalized Q values obtained in each mode is shown in Figure 13.

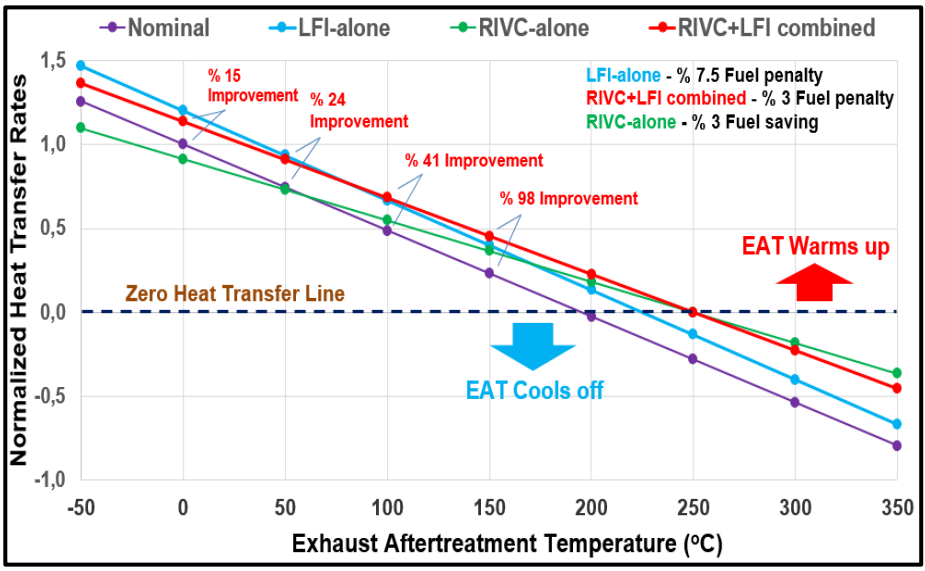

Figure 13: Comparison of LFI-alone, RIVC-alone and RIVC+LFI combined techniques on EAT heat-up

Nominal mode in Figure 13 has the worst heat transfer rates since it has the lowest $T_{exhaust}$. As seen, it can barely warm up the EAT unit only close to 200°C. It is also ineffective at improving EAT cool-off as it has high exhaust flow rate (Figure 12). Unlike nominal mode, RIVC-alone has the advantage of fuel efficiency (Figure 12). But its Q values in Figure 13 are even worse than the nominal mode until T_{EAT} exceeds 100°C, which certainly indicates that RIVC-alone is not a good

option for fast EAT warm up. It is rather effective at delaying EAT cool-off in Figure 13 due to its considerably reduced exhaust flow rate (Figure 12).

Unlike those ineffective techniques, LFI-alone and RIVC+LFI combined mode have a significant potential to enhance EAT warm up. LFI-alone seems to be the most effective among all methods when T_{EAT} remains below 50ºC. This is due to its high $T_{exhaust}$ and high exhaust flow rate (Figure 11 & 12). The RIVC+LFI combined mode is more effective than the nominal mode (up to % 24 improvement) between -50ºC and 50ºC T_{EAT} as well. However, it is still worse than LFI-alone mode. As T_{EAT} exceeds 50ºC, RIVC+LFI mode improves EAT heat up more than LFI-alone mode since it has higher – close to 25ºC – $T_{exhaust}$ (Figure 11). While LFI-alone mode can warm up the EAT system only up to 225ºC, RIVC+LFI mode can heat it up to 250ºC. Not only does it enhance the heat transfer rates up to 98% which none of the techniques achieves in Figure 13, but also it requires a lower fuel consumption penalty (3% instead of 7.5%) compared to LFI-alone method. As long as fuel efficient and fast EAT warm up is considered, RIVC+LFI combined method should at least be utilized when T_{EAT} remains between 50ºC and 250ºC. For the case T_{EAT} > 250ºC, RIVC-alone can be rather preferred as it does not need any fuel penalty and has improved EAT cool-off performance compared to other modes in Figure 13.

CONCLUSION

This study focuses on the improvement of EAT thermal management via implementing different engine-based methods in a diesel engine model. RIVC-alone, LFI-alone and the combined RIVC+LFI techniques are examined on the same model.

RIVC-alone technique has the advantage of high exhaust temperature rise (up to 55ºC). However, it also has the disadvantage of considerably reduced exhaust flow rate which worsens the EAT warm up duration.

LFI-alone technique is moderately effective at increasing exhaust temperature (up to 30ºC). It does not decrease exhaust flow

rate. However, it noticeably rises fuel consumption penalty (up to 7.5%).

RIVC+LFI combined technique rises fuel consumption penalty only up to 3%. It decreases exhaust flow rate relatively lower compared to RIVC-alone method. Also, it rises exhaust temperature more (up to 55^{o}C) compared to LFI-alone method.

RIVC+LFI combined technique seems to be more effective at improving EAT warm up (up to 98% heat transfer rate improvement) compared to both RIVC-alone and LFI-alone methods. It can enhance the EAT heat up faster than other techniques and thus, can reduce emission rates in heavy-duty highway and marine vehicles at low loads.

ACKNOWLEDGMENT

I would like to thank Lotus Engine Simulation Company for letting me utilize Lotus Engine Simulation (LES) Software in this study.

REFERENCES

Ardebili, S. M. S., Solmaz, H., Calam, A., & İpci, D. (2021). Modelling of performance, emission and combustion of an HCCI engine fueled with fusel oil-diethylether fuel blends as a renewable fuel. Fuel, Vol. 290, p. 120017.

Basaran, H. U. & Ozsoysal, O. A. (2017). Effects of application of variable valve timing on the exhaust gas temperature improvement in a low-loaded diesel engine. Applied Thermal Engineering, Vol. 122, pp. 758-767.

Basaran, H. U. (2019). Improving exhaust temperature management at low-loaded diesel engine operations via internal exhaust gas recirculation. Dokuz Eylül Üniversitesi Mühendislik Fakültesi Fen ve Mühendislik Dergisi, Vol. 21(61), pp. 125-135.

Basaran, H. U. (2020). Utilizing exhaust valve opening modulation for fast warm-up of exhaust after-treatment systems on highway diesel vehicles. International Journal of Automotive Science and Technology, Vol. 4, No. 1, pp. 10-22.

Basaran, H. U. (2021). Effects of Intake Valve Lift Form Modulation on Exhaust Temperature and Fuel Economy of a Low-loaded Automotive Diesel Engine. International Journal of Automotive Science and Technology, Vol. 5, No. 2, pp. 85-98.

Chaichan, M. T. (2014). Combustion and Emissions Characteristics for DI Diesel Engine Run by Partially-Premixed (PPCI) Low Temperature Combustion (LTC). International Journal of Mechanical Engineering (IIJME), Vol. 2, No. 10, pp. 7-16.

Chen, S., Tian, J., Li, J., Li, W. & Zhang, Z. (2021). Investigation of the Performance and Emission Characteristics of a Diesel Engine with Different Diesel-Methanol Dual-Fuel Ratios. Processes, Vol. 9, No. 11, p. 1944.

Cunacan, C., Tran, M. K., Lee, Y., Kwok, S., Leung, V. & Fowler, M. (2021). A Review of Heavy-Duty Vehicle Powertrain Technologies: Diesel Engine Vehicles, Battery Electric Vehicles, and Hydrogen Fuel Cell Electric Vehicles. Clean Technologies, Vol. 3, No. 2, pp. 474-489.

Dieselnet, standards. http://www.dieselnet.com/standards/eu/ld.php#stds (Retrieved: 22.08.2022)

Dieselnet, technology guide. https://dieselnet.com/tech/engine_fi.php. (Retrieved: 22.08.2022)

EPA. https://nepis.epa.gov/Exe/ZyPDF.cgi?Dockey=P100O9ZZ.pdf (Retrieved: 22.08.2022)

Epping, K., Aceves, S., Bechtold, R. & Dec, J. E. (2002). The potential of HCCI combustion for high efficiency and low emissions. SAE Technical Paper, No. 2002-01-1923.

Gaiser, G. & Seethaler, C. (2007). Zero-Delay Light-Off-A New Cold-Start Concept with a Latent Heat Storage Integrated into a Catalyst Substrate. SAE Technical Paper No. 2007-01-1074.

Gao, J., Tian, G. & Sorniotti, A. (2019). On the emission reduction through the application of an electrically heated catalyst to a diesel vehicle. Energy Science & Engineering, Vol. 7(6), pp. 2383-2397.

Garg, A. et al. (2016). Fuel-efficient exhaust thermal management using cylinder throttling via intake valve closing timing modulation. Proceedings of the Institution of Mechanical Engineers, Part D: Journal of Automobile Engineering, Vol. 230(4), pp. 470-478.

Girard, J., Cavataio, G., Snow, R. & Lambert, C. (2009). Combined Fe-Cu SCR systems with optimized ammonia to NOx ratio for diesel NOx control. SAE International Journal of Fuels and Lubricants, Vol. 1(1), pp. 603-610.

Gosala, D. B. et al. (2018). Diesel engine aftertreatment warm-up through early exhaust valve opening and internal exhaust gas recirculation during idle operation. International Journal of Engine Research, Vol. 19(7), pp. 758-773.

Guan, B., Zhan, R., Lin, H., Huang, Z. (2014). Review of state of the art technologies of selective catalytic reduction of NOx from diesel engine exhaust. Applied Thermal Engineering, Vol. 66(1-2), pp. 395-414.

Guan, B., Zhan, R., Lin, H., Huang, Z. (2015). Review of state-of-the-art of exhaust particulate filter technology in internal

combustion engines. Journal of Environmental Management, Vol. 154, pp. 225-258.

Hountalas, D. T., Mavropoulos, G. C. & Binder, K. B. (2008). Effect of exhaust gas recirculation (EGR) temperature for various EGR rates on heavy duty DI diesel engine performance and emissions. Energy, Vol. 33, No. 2, pp. 272-283.

Incropera, P., DeWitt, D., Bergman, T., & Lavine, A. (2007). Fundamentals of heat and mass transfer, John Wiley and Sons.

Joshi, A. (2022). A Review of Emissions Control Technologies for On-Road Vehicles. In *Engines and Fuels for Future Transport*, pp. 39-56. Springer, Singapore.

Jurchiş, B. M. et al. (2018). Particulate matter emission characteristics for a compression ignition engine fueled with a blend of biodiesel and diesel. In *IOP Conference Series: Materials Science and Engineering*, Vol. 444, No. 7, p. 072012. IOP Publishing.

Kessels, J. T. B. A., Foster, D. L. & Bleuanus, W. A. J. (2010). Fuel penalty comparison for (electrically) heated catalyst technology. Oil & Gas Science and Technology-Revue de l'Institut Français du Petrole, Vol. 65(1), pp. 47-54.

Kim, Y., Lim, O. & Kim, H. (2020). A Study on the Improvement of Diesel NOx Conversion Efficiency by Increasing the Ammonia Amount Adsorbed in a SCR Catalyst. Journal of ILASS-Korea, Vol. 25(4), pp. 196-203.

Koebel, M., Elsener, M. & Kleemann, M. (2000). Urea-SCR: a promising technique to reduce NOx emissions from automotive diesel engines. Catalysis today, Vol. 59(3-4), pp. 335-345.

Leach, F. et al. (2020). The scope for improving the efficiency and environmental impact of internal combustion engines. Transportation Engineering, Vol. 1, p. 100005.

Lotus Engineering. https://lotusproactive.files.wordpress.com/2013/08/getting-started-with-lotus-engine-simulation.pdf (Retrieved: 22/08/2022)

Lotus Engineering Software, Lotus Engine Simulation (LES) 2020 version. *Lotus Engineering*, Hethel, Norfolk.

Mallouppas, G., & Yfantis, E. A. (2021). Decarbonization in Shipping Industry: A Review of Research, Technology Development, and Innovation Proposals. Journal of Marine Science and Engineering, Vol. 9, No. 4, p. 415.

Martinovic, F., Castoldi, L. & Deorsola, F. A. (2021). Aftertreatment technologies for diesel engines: An overview of the combined systems. Catalysts, Vol. 11, No. 6, p. 653.

Munnannur, A., Ottinger, N. & Gerald Liu, Z. (2022). Thermal Management of Exhaust Aftertreatment for Diesel Engines. In *Handbook of Thermal Management of Engines*, pp. 29-90. Springer, Singapore.

Othman, M. F., Adam, A., Najafi, G. & Mamat, R. (2017). Green fuel as alternative for diesel engine: A review. Renewable and Sustainable Energy Reviews, Vol. 80, pp. 694-709.

Paule, M. et al. (2011). Development of the burner systems for EPA2010 medium duty diesel vehicles. Development, Vol. 1, p. 0295.

Reitz, R. D. & Duraisamy, G. (2015). Review of high efficiency and clean reactivity controlled compression ignition (RCCI) combustion in internal combustion engines. Progress in Energy and Combustion Science, Vol. 46, pp. 12-71.

Selleri, T. et al. (2021). An Overview of Lean Exhaust deNOx Aftertreatment Technologies and NOx Emission Regulations in the European Union. Catalysts, Vol. 11, No. 3, p. 404.

Shaver, G. M., Vos, K. & Joshi, M. (2022). Implementing variable valve actuation on a diesel engine at high-speed idle operation for improved aftertreatment warm-up. U. S. Patent No. 11,359,564, issued June 14, 2022.

Sun, K. et al. (2021). Experimental Study on the Thermal Management and Active Control of Diesel Engine Exhaust Products Based on Energy Saving and Environmental Protection Requirements. Fresenius Environmental Bulletin, Vol. 30(5), pp. 5244-5253.

Stanton, D. W. (2013). Systematic development of highly efficient and clean engines to meet future commercial vehicle greenhouse gas

regulations. SAE International Journal of Engines, Vol. 6(2013-01-2421), pp. 1395-1480.

Valera, H. & Agarwal, A. K. (2019). Methanol as an alternative fuel for diesel engines. In *Methanol and the alternate fuel economy*, pp. 9-33. Springer, Singapore.

Yao, M., Zhang, Q., Liu, H., Zheng, Z. Q., Zhang, P., Lin, Z., Lin, T. & Shen, J. (2010). Diesel engine combustion control: medium or heavy EGR? SAE Technical Paper, No. 2010-01-1125.

Zheng, M., Reader, G. T. & Hawley, J. G. (2004). Diesel engine exhaust gas recirculation – a review on advanced and novel concepts, Energy Conversion and Management, Vol. 45, No. 6, pp. 883-900.

CHAPTER 3

REVIEWING OF PARAMETERS AFFECTING ENERGY CONSUMPTION IN BUILDINGS

Muhammed Enes UMCU
Dr. Öğr. Üyesi Yusuf FEDAİ[1]

[1] Osmaniye Korkut Ata University, Fen Bilimleri Enstitüsü, Osmaniye, Turkey, 2111709101@ogr.oku.edu.tr Orcid Number; https://orcid.org/0000-0003-4546-8830

INTRODUCTION

Investments in power plants are increasing for the increasing demand for energy in our country and the world. Fossil fuel power plants are preferred for the cheap and quick establishment of these investments. As a result of a 2019 study, 63.3% of global electricity generation is derived from fossil fuels(*Annual Energy Outlook 2014*, 2014). These power plants trigger Global Warming and increase the greenhouse gas effect on the Earth. Carbon-Neutral studies that will increase global warming to a minimum have been considered.

Buildings account for 30% of global energy consumption(ÖZCAN et al., 2018). In addition, residential buildings account for approximately 40% of total CO_2 emissions(TSE, 2008). CO_2 emission and primary energy input have increased by 49% and 43%, respectively(Recast, 2010). Non-residential buildings cover 19% of the total energy consumed (*Annual Energy Outlook 2014*, 2014). In Turkey, 34% of the total energy consumed is used by buildings, and 85% of this energy is used for Heating and Cooling (ÖZCAN et al., 2018). In this context, it is seen that improving energy consumption in residential and non-residential buildings will save a significant amount of energy when looking at global energy consumption. In this regard, solutions have been put forward to reduce carbon emissions in buildings and even reduce them to zero. In this respect, Turkish Government published the Building Energy Regulation and TS 825 Standard in 2008 and the necessary works were started to reduce energy consumption in buildings (TSE, 2008). The European Parliament published the nZEB directive in 2010 and they want it to be adopted by 2030 (Recast, 2010). nZEB is Nearly-Zero-Energy-Building. nZEb sets that upper limit for building energy consumption. To adapt nZEB, every EU country needs to study localization. After these studies, every EU country is going to publish its requirements. nZEB requirement is mandatory for buildings after 2020 for every EU country (Hughes, 2022). In addition, the EU published these directives for building energy regulation: Energy Labeling Directive (1992/75/EWG) and its recast (2010/30/EU), Eco design Directive (2005/32/EC) and its recast (2009/125/EC), Energy Efficiency

Directive (EED, 2012/27/EU), Energy Service Directive (ESD, 2006/32/EC), Renewable Energy Directive (RED, 2009/28/EC) (*European Union NZEB Programs*).

DOE (Department of Energy) published ANSI/ASHRAE/IES STANDARD 90.1-2019. These requirements contain Commercial and Residential buildings. DOE proves about this requirement, these savings 4.7% site energy, 4.3 source energy, 4.3 energy cost, and 4.2 carbon emissions (DOE, 2021). The USGBC (U.S. Green Building Council) published the first LEED (Leadership in Energy and Environmental Design) certification in 1993. USGBC has been developing LEED to present (*Mission and vision*, 2022). LEED has four types of certification, these certificates: Certified (40-49 points), Silver (50-59 points), Gold (60-79 points), and Platinum (80+ points) certification. To achieve these certificates building must earn points. Buildings can earn points for these requirements, indoor environmental quality, waste management, carbon emissions, energy, and materials (*How LEED works*, 2022). Building points are collected, results are reviewed, and the building is certified.

To reduce the energy consumption of buildings and increase their efficiency, it is necessary to consider the items that affect energy consumption and adjust those items. To organize consumption items, it is necessary to understand the behavior of these parameters and make the necessary adjustments by moving forward in that plane. It is not always possible to see the effect of these parameters on each other and the annual energy consumption of buildings. In this context, energy simulations can meet this need of people. As a result, buildings play an important role in global climate change (Cao et al., 2016).

Making sense of the energy needed in buildings and showing it to users are systemic requirements that require high technology (Li et al., 2016). Energy simulations are tools that can solve complex and complex problems very easily (Morbitzer, 2003). The use of energy simulations is increasing and becoming more widespread. With increased use and improvements, problems are solved faster and more safely. Building energy simulations are a useful tool for showing the interactions these parameters have with each other (Hobbs et al., 2003).

Since energy simulations can also be used in the building design phase, improvements can be made to consumption by providing feedback to designers even at the design stage (Krygiel & Nies, 2008).

To operate energy simulations properly, it is necessary to create a virtual copy of the building on the computer and proceed through it. A definition of the building's building knowledge has been on the rise in recent years. This definition is BIM (Building Information Modeling). Autodesk BIM-based structure, which is a software services provider with an important place in the sector, is used (Studio, 2008). The green building XML (gbXLM) file format, which is the file format created by IFC (International Finance Corporation), is used for the virtual building created outside BIM (Roth, 2014). It is a necessity that energy simulations are user-friendly and easy to learn. For this purpose, the researchers and the US Department of Energy (DOE) produced EnergyPlus software, which is easy to use and understandable (Bazjanac & Maile, 2004).

With the increase of software such as EnergyPlus, the work on building energy efficiency has increased and has been a source of inspiration for future studies. A report published in the United States shows that non-residential buildings account for 18% of global energy consumption (EIA, 2021). In this context, it is seen that reducing the energy consumption values of non-residential buildings will have a serious impact on global energy consumption.

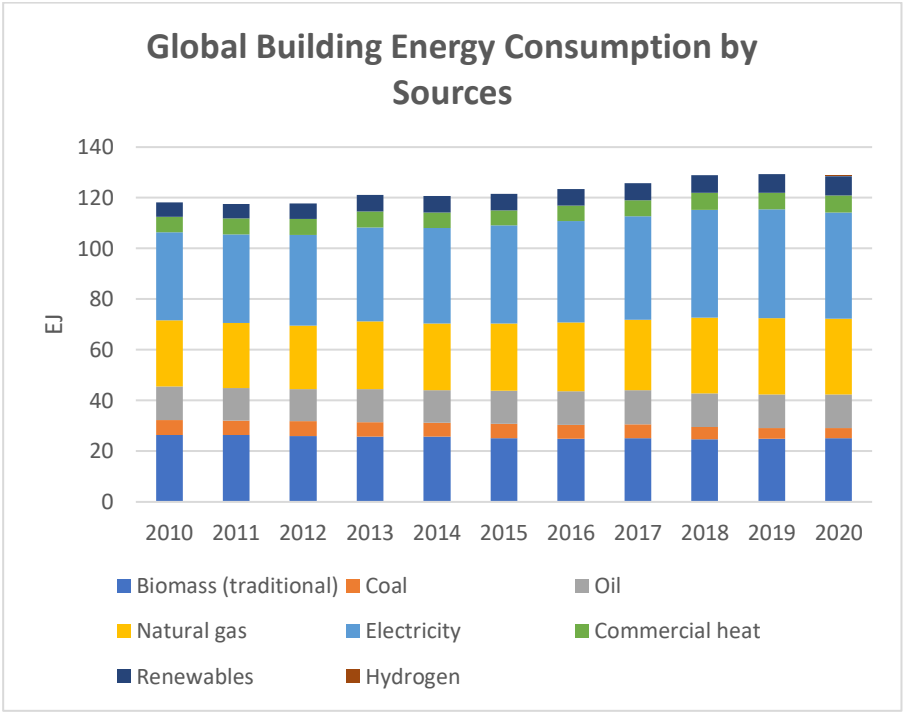

Figure 1 Global Building Energy Consumption by Sources (IEA, 2021a)

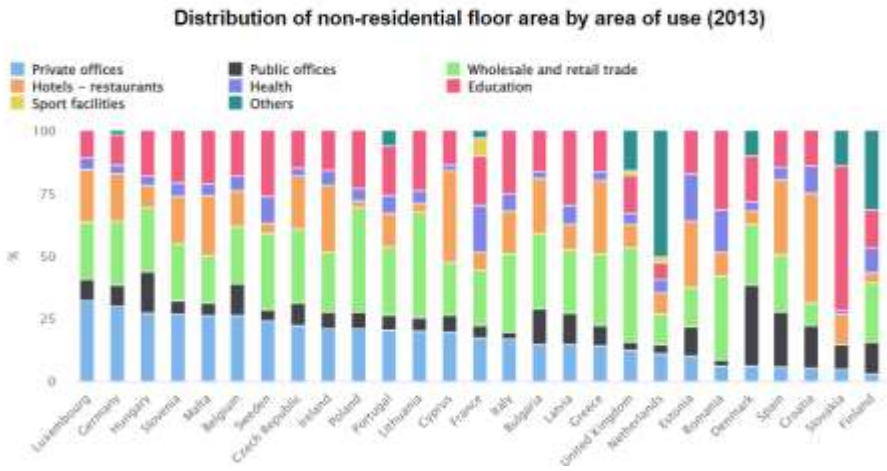

Figure 2 Distribution of non-residential floor area by the area of use in EU (2013) (Commission, 2015)

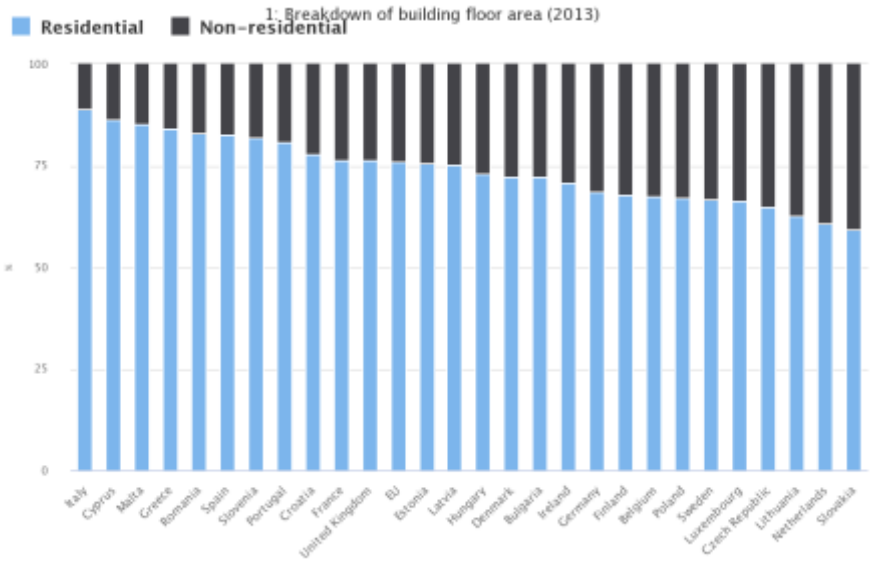

Figure 3 Breakdown of building floor area in EU (2013)(Commission, 2015)

Material and Method

When research is conducted for building energy simulations, multiple simulation tools and sources stand out. The most common are EnergyPlus (DOE, 2022), eQuest (Hirsch, 2009), Transys (*Transysy*, 2022), and IES Virtual Environment (Ltd.). In this research, articles created around the DesignBuilder software, which is considered user-friendly and good at reporting results, were examined. Design Builder is preferred because it is software that uses the EnergyPlus infrastructure and is constantly being developed. In the research, the parameters investigated for nonresidential buildings, adjusted temperature, air permeability rate, window ratio, and type, wind, insulation, lighting internal gain parameters were emphasized. The analysis will be done by examining the effect of these parameters on heating and cooling loads within the building. The extracted analyses will finally be evaluated and published in the conclusion section.

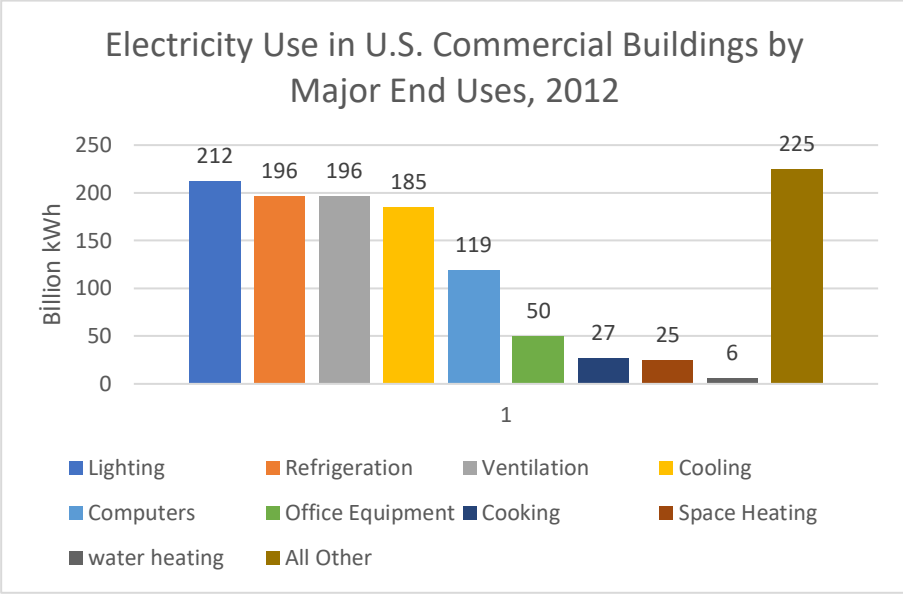

Figure 4 Electricity use in the U.S. Commercial Buildings by Major End Uses, 2012 (Administration, 2016)

Table 1 Non-Residential Building category according to GBP(D'Agostino et al., 2017)

Building Type	**Definition**
Education	Highschool, University, College, and Kindergarten etc.
Healthcare	Medical Centers, Hospitals, Nursing Homes
Hotel & Restaurant	Hotel, Boarding or Guest House, Restaurant, etc.
Institutional	Museums, Public Halls, Libraries, Art Galleries, Exhibition Halls
Industry	Manufacturing Buildings, Workshops, etc.
Logistic	Airports, railway stations, etc.
Office	Office Buildings
Sport	Gym Center, Tennis Courts, etc.
Wholesale & Retail	Retail Stores, Shopping Centers, Shops
Special Purpose	Amusement Parks, Bowling Alleys, Parking Lots, Stadiums, Theaters, Zoos Etc.

Table 2 Parameters Definitions

Parameter	Definition
Set and Set Back Temperature	The set temperature is the temperature that the thermostat should maintain. Set Temperatures is the temperature that the thermostat ought to maintain. The term "set back" refers to lowering the temperature on a thermostat for an amount once the house won't be inhabited or need the maximum amount of heating or cooling. (*What do "set point" and "set back" mean?*, 2012)
Infiltration	Infiltration is the inadvertent entry of outside air into a structure..(*Infiltration (Also Called Air Leakage) – Defined*, 2014)
Insulation	Building insulation refers to any object in a building that is used as insulation for thermal management.(Qin et al., 2021)
Window to Wall Ratio and Window Type	The Window Wall Ratio (WWR) is the proportion of fenestrated above-grade wall area computed as the ratio of wall fenestration area to gross above-grade wall area...(*Window-to-Wall Ratio*, 2019)
Equipment, Lighting Internal Heat Gain, and Energy Load	The electricity used for other equipment, such as computers and appliances, is referred to as equipment loads. (*Equipment and Lighting Loads*, 2018)
Building Geometry	Building geometry is the strategic planning of a building's shape and size. (Grosskopf, 2018)
Building Orientation Angle	Orientation is how construction is located in terms of the sun's paths in distinctive seasons, in addition to winning wind patterns. (Caitlin McGee, 2020)
Climate	Buildings are continuously situation by numerous climatic and environmental factors. Buildings have interaction with

the one-of-a-kind factors in their surrounding climate. (*What Climate Factors are Important Considerations for Building Projects?*)

Parameters

There are too many parameters to estimate for building energy demand or consumption (Lam et al., 2010). Parameters affecting building energy consumption, respectively; Examinations and analyses were carried out on the parameters of Set and Set Back Temperature, Infiltration, Insulation, Window Ratio, and Type, Equipment and Lighting Internal Wet Gain, Building Geometry, Air Conditioning System, Central Hot Water Source, Climate Conditions, and Control Strategies.

1.1 Set and Set Back Temperatures

People who live in the building and actively use the building want to keep themselves within the Thermal Comfort zone. This comfort zone was determined by trials as a result of a result in which the temperature and humidity of the psychometric chart were taken as input and the level of thermal comfort emerged as a result (VentureWell). The temperature in the building for Heating and Cooling has a considerable impact on the building's energy usage (Li et al., 2016). The American Society of Heating's report found that HVAC systems cover between 30% and 50% of total building energy consumption (Albieri et al., 2009). In Menberg K.'s old study, he created a standard building model to find out how much the Adjusted Temperature value affected the total energy result consumed, and within this model, he created four hundred samples by changing the Adjusted Temperature value from 18°C to 22°C. Bu aims to find the effectiveness of the parameter in terms of total consumption. As a result of this research, the average correlation of the Set and Set Back Temperature parameter was (Menberg et al., 2016). The adjusted cooling temperature creates a significant energy consumption within the cooling load (Guo et al., 2019). The research by Hoyt T. increased the temperature set for cooling from 22°C to 24°C, reducing the

cooling load by 29%, and reducing the temperature set for heating from 21.1°C to 20°C, reducing the heating load by 34% (Hoyt et al., 2015). According to Mechri H.E. research, Set and Set Back Temperatures have a considerable effect on building energy demand (Mechri et al., 2010). Simanic B. research on school buildings and as a result of this research set temperatures are significant parameters for school and non-residential buildings (Simanic et al., 2020). Attia S. researched different comfort models in the hot climate zone. Attia inspected the effect of ISO 7730(Standardization, 2005), EN 15251(EN15251, 2007), and ASHRAE 55 (Refrigerating et al., 2004) standards on energy savings in buildings. This research shows that these standards can save up to %16, %21, and %24.7 respectively (Attia & Carlucci, 2015).

2.2 Infiltration

Unintended air leaks and leaks within the building are called infiltration. This ratio is a serious factor in building energy consumption (Woods, 1992). Unwanted air leaks account for approximately 25% of the heating load and roughly 3% of the cooling load (Kalamees, 2007). This ratio can be calculated using building energy simulations. To calculate this rate, it must have AFN (Air Flow Network) or CFD (Computational Fluid Mechanics) modules within the simulation program. This ratio can be calculated with simulation software using factors such as press, temperature, year of construction of the Building, Insulation (Djunaedy et al., 2003). According to his research, Steven J. Emmerich found that the value of building energy demand is 13% to 33% for non-residential buildings (Emmerich, 2022). According to Jokisalu and Kurnitski's research, raising the air change rate from 1 L/s to 10 L/s increases the heating load by 4% to 21% (Jokisalu & Kurnitski, 2002). According to research by the Código Técnico de la Edificación, the effect of air permeability on annual energy consumption is 2 to 5 kWh/m2/year (HE, 2009). Han G. researched the relations between Infiltration and annual energy demand. This research shows that infiltration is responsible for %12 of annual energy consumption (Han et al., 2015). Jurelionis A. researched the impact of Infiltration on building energy consumption. This

research shows that infiltration can be responsible for up to %41 of building heat losses (Jurelionis & Bouris, 2016). Improvement in Infiltration, potential energy saves heating load 26% and cooling load 15% (Emmerich & Persily, 1995). There are some Infiltration models LEAKS, SWIFB, LBL, and RMS (Tian et al., 2019). These models can assist engineers in modeling infiltration. There are two standards for infiltration modeling: a static infiltration model (DIN 1946-6) and a dynamic infiltration model (EN 16798-7) for EU (Happle et al., 2017). It has been observed that even reducing this ratio alone will save a significant amount of energy.

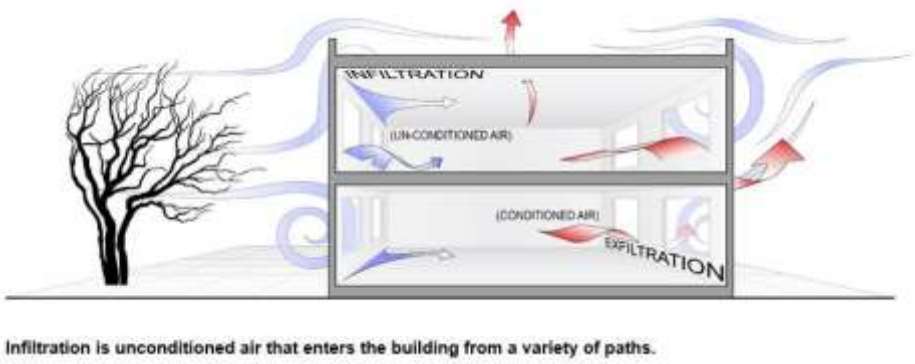

Figure 5 Illustration of Infiltration(Muscolino)

2.3 Insulation

The amount of insulation, variety, and quality of application in buildings all have a meaningful impact on building energy consumption. In general, it has been observed that the insulation situation of buildings is bad and that serious improvements can be made in buildings in this regard (Guo et al., 2015). As a result of Biswas K.'s research, insulation was observed (Heating, 2019). ASHRAE 90.1 (Lam et al., 2010) described a reduction in the demand for building energy for non-residential buildings by approximately 20% to 23% compared to non-insulated buildings (Biswas et al., 2016). Insulation should not be considered only for walls. It should also be considered that the insulation is the roof and floor foot. It is seen that a

single-layered roof consumes much more energy than an insulated roof (Zhao et al., 2019). Friess W. A.'s study shows that insulation on the exterior walls of the building alone saves between 40% and 47% of Energy (Friess et al., 2012). In E. Zilberberg's study, it was observed that the heat mass of the building where he was made would also increase, reducing the energy consumed for the total heating of the building by 3% (Zilberberg et al., 2021). The study by Ruan F. shows that the total energy consumed is reduced by up to 45%, including 20.5% in the cooling load and 48.2% in the heating load of the insulation of the building insulation (Ruan et al., 2015). According to the type of insulation and building, usage carried out by Eleftheriadis G., the effect on the energy consumption of the building for 20 years is seen to save between 18.4% and 47.1% (Eleftheriadis & Hamdy, 2018). The Masoso and Grobler study found that the insulation of the outer wall alone saved up to 30% of the total energy consumption of the building energy consumption (Masoso & Grobler, 2008). The study by Morozov M. used advanced insulation and found that these insulations saved energy between 35.67% and 36.52% (Morozov & Strizhak, 2016).

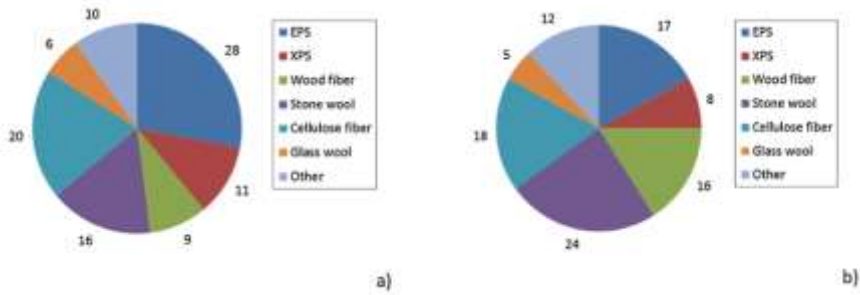

Figure 6 Envelope insulating materials averages: a) walls, b) roofs.in EU (D'Agostino et al., 2017)

2.4 Window to Wall Ratio and Type

The window/wall ratio (WWR) in buildings directly affects the solar radiation that enters the building and therefore the demand for heating and cooling. WWR is the most pre-embalm parameter for non-residential buildings in energy consumption based on the effects around

the building (Granadeiro et al., 2013). Windows account for 10% to 25% of total heat loss in a building (Kamal et al., 2000). Therefore, WWR is an easy-to-change parameter in building designs, since changing the WWR is easier than changing the thickness of ratio(Attia & Carlucci, 2015). A proper adjustment in WWR would result in a decrease in annual lighting and HVAC-based energy consumption of between 10% and 40% depending on climatic conditions (Ander, 2005). Window parameters can significantly change the annual energy demand for buildings (Ihm et al., 2012). When designing the building, the climate that the building will meet during the year and the extent of WWR on which front should be considered should be noted. Research by Goia F. found that WWR and incorrect choices would increase annual energy consumption by up to 25% (Goia, 2016). According to research conducted by Yildiz Y., it has been observed that the window/wall ratio of the building and the increases in the facades facing the window have a significant impact on the demand for building energy. An increase in the southern front reduces the demand for heating and increases the demand for cooling. In this context, multiple facades were discussed, and it was revealed that the most efficient was the Low-E type window. Maximum efficiency was found with Low-E coating and a 60% window/wall ratio on the eastern façade to reduce the total energy needed in the building (Yildiz et al., 2011). Climate is one of the most crucial factors for WWR's energy saving. Feng G.'s research found that in severely cold climates, the WWR increases in the West between 10% and 15%, and the WWR increase in the South save between 10% and 22.5% (Feng et al., 2017). Harmati N. research found that improvement of WWR according to Building façade and simulation results, annual heating demand can reduce by up to %83 (Harmati & Magyar, 2015). When choosing the facade for WWR, the increase on the Southern front for cold climates reduces the heating load. In addition, the increase in WWR on the Southern front in warm climates increases the cooling load (Sayadi et al., 2021). Ciacci C research found that WWR can't be negligible parameters for non-residential buildings (Ciacci et al., 2019). Delgarm N. research on sensitivity analysis to the same building and different parameters. Some

of these parameters; building orientation, window size, glazing conductivity, wall conductivity, different climates, etc. As a result of this research window size most dominant parameter of total energy demand at Iran's climate (Delgarm et al., 2018). Jiang W. research that energy consumption parameters weight in severe climate. This research shows that most of the weight parameter is WWR at South (Jiang et al., 2021). DesignBuilder software can be used for the facade and WWR ratios of the building by performing simulation work.

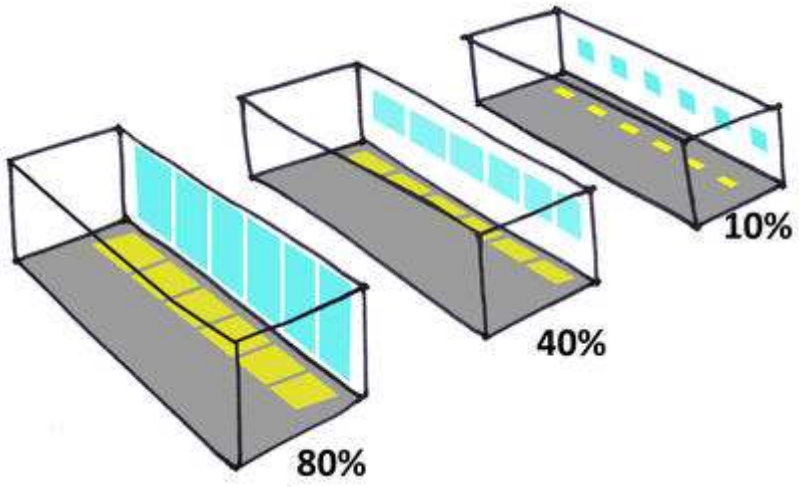

Figure 1 Lighting representation at different WWR values (Autodesk, 2018)

2.5 Equipment, Lighting Internal Heat Gain, and Energy Load

The equipment and lighting load for nonresidential buildings is an especially important item. According to the article published in Energy and Building, up to 50% of the total energy demand of buildings created for the office constitutes the electrical load from the outlet (Gandhi & Brager, 2016). Lighting is responsible for 30% to 40% of electricity consumption in non-residential buildings (Swisher et al., 1994). Therefore, it is responsible for one-third of the electricity bills (Busch et al., 1993). As a result of such an electrical load in the plug, the internal heat gain generated by electrically operated instruments is distributed within the building between 18 and 78

kWh/m2/year (Lapinskienė et al., 2017). Equipment and Lighting Internal Heat Gain reduces the heating load for non-residential buildings by approximately 56% while increasing the cooling load by up to 8-27 (Lapinskienė et al., 2017). Since the lighting requirement varies for residential and non-residential buildings, the electric load from lighting also varies according to this lighting requirement. For example, residential buildings need 150 Lumens per m2, while for office-type buildings, this number is 500 Lumen/m2 (*6.15 Lighting*). Replacing lamps used only for lighting in buildings reduces the consumption of lighting-induced electricity by between 13.9% and 64.9% according to lamp efficiency (Di Stefano, 2000).

2.6 Building Geometry

Different geometric ratios should be considered in buildings to increase the thermal gain of the sun in the buildings and to keep the heat inside. According to Hemsath and Bandhosseini's research, the aspect ratio of the building has a meaningful effect on the total amount of energy consumption (Hemsath & Bandhosseini, 2015). The research of Aksot and Inalli also revealed that square buildings in buildings in the cold climate zone of Turkey consume less energy than non-square buildings (Aksoy & Inalli, 2006). However, the study by Inanici and Demilbilek found that the aspect ratio is between 1.3 and 1.5 for binary in cold climates (Inanici & Demirbilek, 2000).

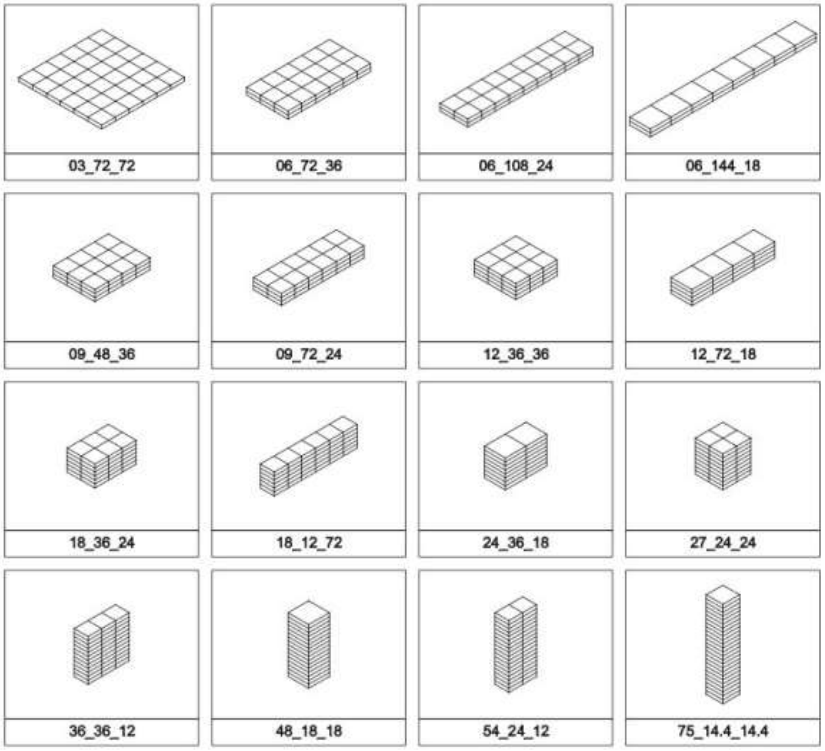

Figure 2 Geometric layouts that buildings can have (Ordoñez et al., 2014)

2.7 Building Orientation Angle

Building orientation angles have such a serious influence on the building's power demand. In the article published by the Chamber of Mechanical Engineers, the heating and cooling loads of a building in the Northern Hemisphere were calculated and evaluated according to different orientation angles (Duran & Oral).

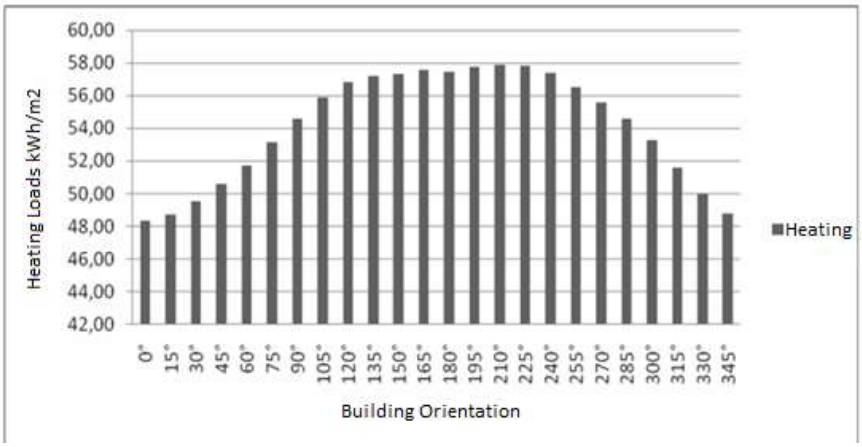

Figure 3 Annual heating loads according to Different Orientation Angles (Duran & Oral)

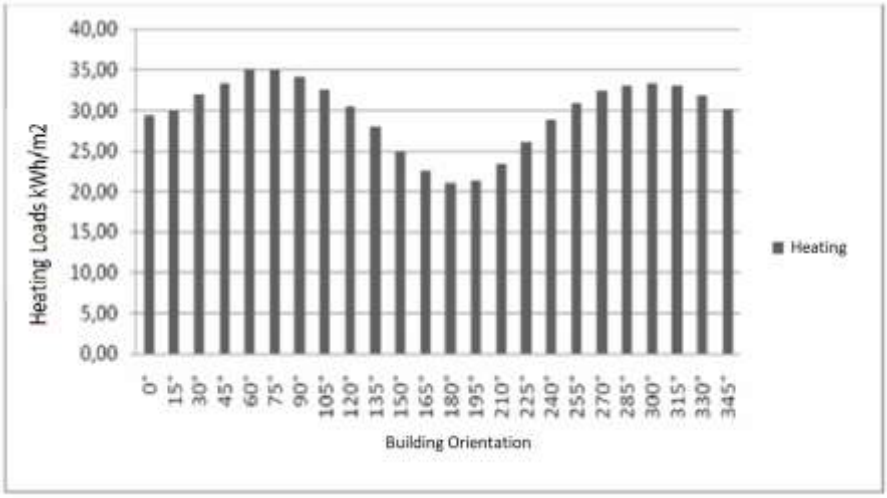

Figure 4 Annual cooling loads by Different Orientation Angles (Duran & Oral)

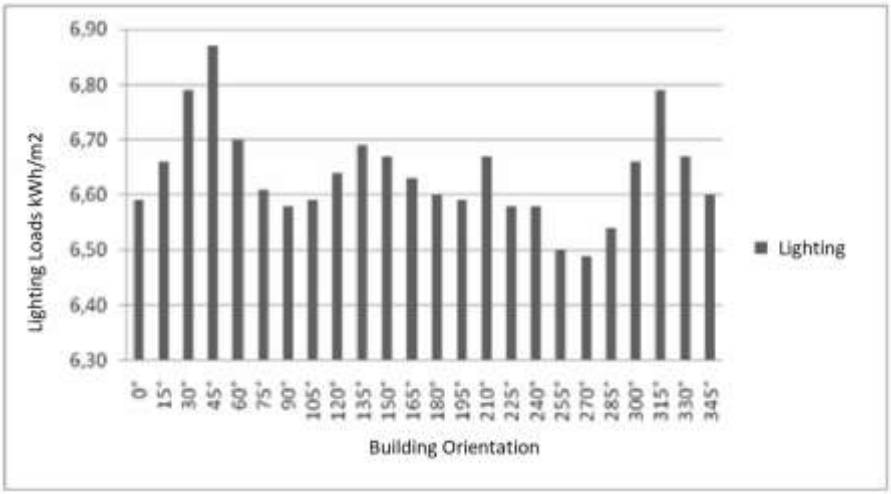

Figure 5 Annual Lighting Loads by Different Orientation Angles (Duran & Oral)

Research by (Vasov et al., 2018) on the impact of orientation on energy consumption. This research shows that by choosing the right orientation of the building, the heating energy demand % by 13.73 and the cooling energy demand % by up to 13.26 can be reduced.

2.8 Climate

Climate is the most important parameter affecting the energy consumption of the building (Pang et al., 2020). To understand the climate parameter influencing building energy demand, the Climates should be classified. One of the classification methods is the Heating Degree Days Method (HDD). HDD indicates how cold or hot the selected location (*Degree days*, 2021). For example, the International Energy Agency (IEA) suggests that the HDD Base Temperature is 18°C in Turkey (Laustsen, 2008; Pusat & Ekmekci, 2016). HDD calculation if the ambient temperature is lower than the reference temperature, the HDD for this day is equivalent to the change between the outdoor and base temperature changes (Pusat & Ekmekci, 2016; Tarım ve Orman Bakanlığı, 2019). Summated of like these situations along a year and can comment about the climate. HDD is useful for demand estimating and management of buildings (Layberry, 2008). Matzarakis A. research the relationships between the HDD and building heating demand. This research shows up there is significant

statistical relation between HDD and building heating demand (Matzarakis & Balafoutis, 2004).

Figure 9 An Example of HDD, Turkey Average Heating Degree Days Map 2018 (Tarım ve Orman Bakanlığı, 2019)

Bhandari M.'s study simulated the same building under different climatic conditions. As a result of these simulations, it was revealed that there were up to 90% differences between consumptions (Bhandari et al., 2012). Zhai Z. The study of J. worked for the future consumption of buildings because of climate change. As a result of these studies, it has been observed that buildings may increase by up to 27% from their current energy consumption if climate change occurs in the coming years (Zhai & Helman, 2019). As a result of the research conducted by Farah S. in Austria, it was found that as a result of climate change, the heating load decreased by between 21% and 22%, the cooling load increased by between 29% and 31%, and the total energy consumption increased by between 4% and 5% (Farah et al., 2019). Lam JC's simulation between 1976 and 1996 shows that the building's energy load increased by 14% (Lam, 1999). As a result of Zhao M.'s research, it is observed that the same building in the temperate climate region consumed 53% less energy than in the cold climate (Zhao et al., 2015). Altun A. F. research about the influence climate of on building energy demand. Altun Research in Turkey cities.

Istanbul, Ankara, Izmir, and Hakkari are among them. According to the findings of this study, climate patterns have a huge impact on yearly energy demand (Altun & Kılıç, 2019).

Result

The parameters that influence energy consumption in buildings and their effects are as described above. It is a visible fact how much impact the selected parameters have when building an energy-modeled building. It is recommended to select the parameters used as a result of the observations made and to use them from the ASHRAE 90.1 (Heating, 2019) standard if there is no possibility of observation. These effects help design a building according to different conditions. The study also found that improved climate conditions produce a higher Demand for Energy in buildings. Even without the Climate Effect, global Energy Demand in Buildings is increasing. Building Energy Use can be reduced to the levels of the twenty-first century. This gives a great incentive to go for energy-efficient buildings. The study also offers guidelines for increasing buildings' sustainability, including benchmarking and testing. It explains the opportunities for retrofitting existing buildings and systems.

Climate is the main component that impacts the heating and cooling load for non-residential buildings, according to study and experience. Climate change is an undeniable fact in today's world. The future energy demand of structures is determined by the climate. Climate Conditions impact Heating and Cooling Loads, not simply Heating Loads, contrary to popular belief. According to the research report, The weather has a massive effect on buildings. Even if the energy demands of buildings were to remain constant, climate conditions can change the load on building systems and contribute to the doubling of energy demand in buildings by 2050.

The study further finds that climate conditions have an impact on building energy use and efficiency. Improved climate conditions decrease building energy use by roughly 20%. The energy consumption in buildings in extreme environments has an even larger effect.

To make the most of climate change mitigation and adaptation, buildings need to be adapted to the climate to increase energy efficiency and comfort levels. Such building design changes to accommodate climate change could save buildings about $1.3 trillion and more than 100 million tons of CO_2 annually by 2050, according to the International Energy Agency (IEA, 2021b).

Recommendations

These recommendations are based on reviews of these parameters.

- The HDD method can help predict the energy demand of buildings in the future. This prediction shows how one can act according to conditions.
- WWR can be increased on the east side facade for Northern Hemisphere buildings. This improvement can be reduced building energy demand.
- Building insulation can be improved according to ASHRAE 90.1 or the energy standards of the located country.
- Buildings can be designed according to building energy simulation feedback.
- To improve the building, Infiltration can be applied Air impermeability materials on walls and roof.
- Daylights can be increased and building design can be changed as far as lightning standards and occupant's comfort.
- Set and Set Back temperatures can be reduced or increased to improve building energy efficiency.

REFERENCES

6.15 Lighting. https://www.gsa.gov/node/82715

Administration, U. S. E. I. (2016). *2012 Commercial Buildings Energy Consumption Survey*. https://www.eia.gov/energyexplained/use-of-energy/commercial-buildings-in-depth.php

Aksoy, U. T., & Inalli, M. (2006). Impacts of some building passive design parameters on heating demand for a cold region. *Building and Environment*, *41*(12), 1742-1754.

Albieri, M., Beghi, A., Bodo, C., & Cecchinato, L. (2009). Advanced control systems for single compressor chiller units. *International journal of refrigeration*, *32*(5), 1068-1076.

Altun, A. F., & Kılıç, M. (2019). Influence of window parameters on the thermal performance of office rooms in different climate zones of Turkey. *International Journal of Renewable Energy Research (IJRER)*, *9*(1), 226-243.

Ander, G. (2005). Windows and Glazing. Whole Building Design Guide. *Southern California*.

Annual Energy Outlook 2014. (2014). http://www.eia.gov/forecasts/aeo/

Attia, S., & Carlucci, S. (2015). Impact of different thermal comfort models on zero energy residential buildings in hot climate [Article]. *Energy and Buildings, 102*, 117-128. https://doi.org/10.1016/j.enbuild.2015.05.017

Autodesk. (2018). *Aperture Placement & Are*. https://knowledge.autodesk.com/support/revit/getting-started/caas/simplecontent/content/aperture-placement-area.html

Bazjanac, V., & Maile, T. (2004). *IFC HVAC interface to EnergyPlus-A case of expanded interoperability for energy simulation*.

Bhandari, M., Shrestha, S., & New, J. (2012). Evaluation of weather datasets for building energy simulation. *Energy and Buildings*, *49*, 109-118.

Biswas, K., Shrestha, S. S., Bhandari, M. S., & Desjarlais, A. O. (2016). Insulation materials for commercial buildings in North America: An assessment of lifetime energy and environmental

impacts. *Energy and Buildings*, *112*, 256-269. https://doi.org/10.1016/j.enbuild.2015.12.013

Busch, J. F., Du Pont, P., & Chirarattananon, S. (1993). Energy-efficient lighting in Thai commercial buildings. *Energy*, *18*(2), 197-210.

Caitlin McGee, C. R., Dick Clarke. (2020). Orientation. https://www.yourhome.gov.au/passive-design/orientation#:~:text=Orientation%20is%20how%20a%20building,be%20protected%20from%20their%20effects.

Cao, X., Dai, X., & Liu, J. (2016). Building energy-consumption status worldwide and the state-of-the-art technologies for zero-energy buildings during the past decade. *Energy and Buildings*, *128*, 198-213.

Ciacci, C., Bazzocchi, F., Di Naso, V., & Rocchetti, A. (2019). Influence of Window-Wall ratio on global energy consumption of Nzeb kindergartens in Italy. Proceedings of the 16th IBPSA International Conference and Exhibition, Building Simulation,

Commission, E. (2015). *Building stock characteristics*. https://ec.europa.eu/energy/eu-buildings-factsheets_en

D'Agostino, D., Cuniberti, B., & Bertoldi, P. (2017). Energy consumption and efficiency technology measures in European non-residential buildings. *Energy and Buildings*, *153*, 72-86.

Degree days. (2021). https://www.eia.gov/energyexplained/units-and-calculators/degree-days.php#:~:text=Heating%20degree%20days%20(HDD)%20are,for%20the%20two%2Dday%20period.

Delgarm, N., Sajadi, B., Azarbad, K., & Delgarm, S. (2018). Sensitivity analysis of building energy performance: A simulation-based approach using OFAT and variance-based sensitivity analysis methods. *Journal of Building Engineering*, *15*, 181-193.

Di Stefano, J. (2000). Energy efficiency and the environment: the potential for energy efficient lighting to save energy and reduce carbon dioxide emissions at Melbourne University, Australia. *Energy*, *25*(9), 823-839.

Djunaedy, E., Hensen, J., & Loomans, M. (2003). Development of a guideline for selecting a simulation tool for airflow prediction. Eighth International IBPSA Conference, Eindhovan, Netherlands,

DOE. (2021). *Building Energy Codes Program*. https://www.energy codes.gov/determinations

DOE. (2022). *EnergyPlus*. https://energyplus.net/

Duran, Ö., & Oral, G. K. KONUT YERLEŞMELERİNDE TASARIM PARAMETRELERİNİN ENERJİ YÜKLERİ AÇISINDAN DEĞERLENDİRİLMESİ.

EIA, U. (2021). Energy consumption by sector. *Monthly Energy Review; July*.

Eleftheriadis, G., & Hamdy, M. (2018). The impact of insulation and HVAC degradation on overall building energy performance: a case study. *Buildings*, *8*(2), 23.

Emmerich, S. a. P., Andrew and Mcdowell, Timothy. (2022). Impact of Infiltration on Heating and Cooling Loads in U.S. Office Buildings. *Building and Fire Research Laboratory*.

Emmerich, S. J., & Persily, A. K. (1995). A workplan to analyze the energy impacts of envelope airtightness in office buildings.

EN15251, C. S. (2007). Indoor environmental input parameters for design and assessment of energy performance of buildings addressing indoor air quality, thermal environment, lighting and acoustics. *Thermal Environment, Lighting and Acoustics*.

Equipment and Lighting Loads. (2018). https://knowledge.autodesk. com/support/revit/getting-started/caas/simplecontent/content/equipment-and-lighting-loads.html

European Union NZEB Programs. https://nzeb.in/definitions-policies/ international-roadmaps/european-union-eu/

Farah, S., Whaley, D., Saman, W., & Boland, J. (2019). Integrating climate change into meteorological weather data for building energy simulation. *Energy and Buildings*, *183*, 749-760.

Feng, G., Chi, D., Xu, X., Dou, B., Sun, Y., & Fu, Y. (2017). Study on the influence of window-wall ratio on the energy consumption

of nearly zero energy buildings. *Procedia Engineering*, *205*, 730-737.

Friess, W. A., Rakhshan, K., Hendawi, T. A., & Tajerzadeh, S. (2012). Wall insulation measures for residential villas in Dubai: A case study in energy efficiency. *Energy and Buildings*, *44*, 26-32.

Gandhi, P., & Brager, G. S. (2016). Commercial office plug load energy consumption trends and the role of occupant behavior. *Energy and Buildings*, *125*, 1-8.

Goia, F. (2016). Search for the optimal window-to-wall ratio in office buildings in different European climates and the implications on total energy saving potential. *Solar Energy*, *132*, 467-492.

Granadeiro, V., Duarte, J. P., Correia, J. R., & Leal, V. M. (2013). Building envelope shape design in early stages of the design process: Integrating architectural design systems and energy simulation. *Automation in construction*, *32*, 196-209.

Grosskopf, M. (2018). GEOMETRY OF BUILDINGS. https://www.tuvsud.com/en/resource-centre/stories/geometry-of-buildings

Guo, S., Yan, D., Peng, C., Cui, Y., Zhou, X., & Hu, S. (2015). Investigation and analyses of residential heating in the HSCW climate zone of China: Status quo and key features. *Building and Environment*, *94*, 532-542.

Guo, S., Yang, H., Li, Y., Zhang, Y., & Long, E. (2019). Energy saving effect and mechanism of cooling setting temperature increased by 1 C for residential buildings in different cities. *Energy and Buildings*, *202*, 109335.

Han, G., Srebric, J., & Enache-Pommer, E. (2015). Different modeling strategies of infiltration rates for an office building to improve accuracy of building energy simulations. *Energy and Buildings*, *86*, 288-295.

Happle, G., Fonseca, J. A., & Schlueter, A. (2017). Effects of air infiltration modeling approaches in urban building energy demand forecasts. *Energy Procedia*, *122*, 283-288.

Harmati, N., & Magyar, Z. (2015). Influence of WWR, WG and glazing properties on the annual heating and cooling energy demand in buildings. *Energy Procedia*, *78*, 2458-2463.

HE, C. (2009). Código Técnico de la edificación. *Documento Básico de Ahorro de Energía (Spanish Energy Saving Code)*.

Heating, A. S. o. (2019). ANSI/ASHRAE/IES Standard 90.1-2019 -- Energy Standard for Buildings Except Low-Rise Residential Buildings. In: Refrigerating and Air-Conditioning Engineers.

Hemsath, T. L., & Bandhosseini, K. A. (2015). Sensitivity analysis evaluating basic building geometry's effect on energy use. *Renewable Energy*, *76*, 526-538.

Hirsch, J. (2009). *eQuest*. https://www.doe2.com/equest/

Hobbs, D., Morbitzer, C., Spires, B., Strachan, P., & Webster, J. (2003). Experience of using building simulation within the design process of an architectural practice.

How LEED works. (2022). https://www.usgbc.org/leed

Hoyt, T., Arens, E., & Zhang, H. (2015). Extending air temperature setpoints: Simulated energy savings and design considerations for new and retrofit buildings. *Building and Environment*, *88*, 89-96.

Hughes, C. (2022). *CT1 NEW NEARLY ZERO ENERGY BUILDINGS*. https://epbd-ca.eu/topics-teams/topics/ct1-new-nearly-zero-energy-buildings

IEA, I. E. (2021a). *Global building energy use and floor area growth in the Net Zero Scenario, 2010-2030*. https://www.iea.org/data-and-statistics/charts/global-building-energy-use-and-floor-area-growth-in-the-net-zero-scenario-2010-2030

IEA, I. E. (2021b). *Global CO2 emissions from building operations in the Net Zero Scenario, 2010-2030*. IEA. https://www.iea.org/data-and-statistics/charts/global-co2-emissions-from-building-operations-in-the-net-zero-scenario-2010-2030

Ihm, P., Park, L., Krarti, M., & Seo, D. (2012). Impact of window selection on the energy performance of residential buildings in South Korea. *Energy policy*, *44*, 1-9.

Inanici, M. N., & Demirbilek, F. N. (2000). Thermal performance optimization of building aspect ratio and south window size in five cities having different climatic characteristics of Turkey. *Building and Environment*, *35*(1), 41-52.

Infiltration (Also Called Air Leakage) – Defined. (2014). https://energy.ces.ncsu.edu/infiltration-also-called-air-leakage-defined/#:~:text=Air%20leakage%20is%20sometimes%20called,air%20into%20the%20building.

Jiang, W., Liu, B., Li, Q., Li, D., & Ma, L. Y. (2021). Weight of energy consumption parameters of rural residences in severe cold area [Article]. *Case Studies in Thermal Engineering*, *26*, 14, Article 101131. https://doi.org/10.1016/j.csite.2021.101131

Jokisalu, J., & Kurnitski, J. (2002). Simulation of energy consumption in typical Finnish detached house. *Helsinki University of Technology, HVAC Laboratory, report B*, *74*, 2002.

Jurelionis, A., & Bouris, D. G. (2016). Impact of Urban Morphology on Infiltration-Induced Building Energy Consumption. *Energies*, *9*(3), 177. https://www.mdpi.com/1996-1073/9/3/177

Kalamees, T. (2007). Air tightness and air leakages of new lightweight single-family detached houses in Estonia. *Building and Environment*, *42*(6), 2369-2377.

Kamal, M. A., Greig, N. H., Alhomida, A. S., & Al-Jafari, A. A. (2000). Kinetics of human acetylcholinesterase inhibition by the novel experimental Alzheimer therapeutic agent, tolserine. *Biochemical pharmacology*, *60*(4), 561-570.

Krygiel, E., & Nies, B. (2008). *Green BIM: successful sustainable design with building information modeling*. John Wiley & Sons.

Lam, J. C. (1999). Climatic influences on the energy performance of air-conditioned buildings. *Energy Conversion and management*, *40*(1), 39-49.

Lam, J. C., Wan, K. K., Lam, T. N., & Wong, S. (2010). An analysis of future building energy use in subtropical Hong Kong. *Energy*, *35*(3), 1482-1490.

Lapinskienė, V., Motuzienė, V., Džiugaitė-Tumėnienė, R., & Mikučionienė, R. (2017). *Impact of Internal Heat Gains on Building's Energy Performance* Proccedings of 10th International Conference "Environmental Engineering",

Laustsen, J. (2008). Energy efficiency requirements in building codes, energy efficiency policies for new buildings. IEA Information Paper.

Layberry, R. (2008). Degree days for building energy management — presentation of a new data set. *Building Services Engineering Research and Technology*, *29*(3), 273-282. https://doi.org/10.1177/0143624408093886

Li, H. X., Gül, M., Yu, H., Awad, H., & Al-Hussein, M. (2016). An energy performance monitoring, analysis and modelling framework for NetZero Energy Homes (NZEHs). *Energy and Buildings*, *126*, 353-364.

Ltd., I. E. S. *IES Virtual Environment*. http://www.iesve.com/

Masoso, O., & Grobler, L. (2008). A new and innovative look at anti-insulation behaviour in building energy consumption. *Energy and Buildings*, *40*(10), 1889-1894.

Matzarakis, A., & Balafoutis, C. (2004). Heating degree-days over Greece as an index of energy consumption. *International Journal of Climatology*, *24*(14), 1817-1828. https://doi.org/ https://doi.org/10.1002/joc.1107

Mechri, H. E., Capozzoli, A., & Corrado, V. (2010). USE of the ANOVA approach for sensitive building energy design. *Applied Energy*, *87*(10), 3073-3083.

Menberg, K., Heo, Y., & Choudhary, R. (2016). Sensitivity analysis methods for building energy models: Comparing computational costs and extractable information. *Energy and Buildings*, *133*, 433-445. https://doi.org/10.1016/j.enbuild.2016.10.005

Mission and vision. (2022). https://www.usgbc.org/about/mission-vision

Morbitzer, C. A. (2003). *Towards the integration of simulation into the building design process* University of Strathclyde].

Morozov, M., & Strizhak, P. A. (2016). Researches of advanced thermal insulating materials for improving the building energy efficiency. Key Engineering Materials,

Muscolino, N. *Infiltration*. https://www.aerobuild.com/2019/04/01/ infiltration/

Ordoñez, A., Carreras, J., Korolija, I., Zhang, Y., & Coronas, A. (2014). Impact of building geometry on its energy performance depending on climate zones. Proceedings of the BSO14: Second Building Simulation and Optimization Conference, London, UK,

ÖZCAN, N. Y., Kuzgunkaya, E., & Akkurt, G. G. (2018). Isıl konfor sıcaklıklarına bağlı olarak bir konutun enerji performansının değerlendirmesi: İzmir örneği. *Sakarya University Journal of Science*, *22*(2), 784-798.

Pang, Z., O'Neill, Z., Li, Y., & Niu, F. (2020). The role of sensitivity analysis in the building performance analysis: A critical review. *Energy and Buildings*, *209*, 109659.

Pusat, S., & Ekmekci, I. (2016). A study on degree-day regions of Turkey. *Energy Efficiency*, *9*(2), 525-532.

Qin, Z., Li, M., Flohn, J., & Hu, Y. (2021). Thermal management materials for energy-efficient and sustainable future buildings. *Chemical Communications*, *57*(92), 12236-12253.

Recast, E. (2010). Directive 2010/31/EU of the European Parliament and of the Council of 19 May 2010 on the energy performance of buildings (recast). *Official Journal of the European Union*, *18*(06), 2010.

Refrigerating, Engineers, A.-C., & Institute, A. N. S. (2004). *Thermal environmental conditions for human occupancy* (Vol. 55). American Society of Heating, Refrigerating and Air-Conditioning Engineers.

Roth, S. (2014). Open green building XML schema: A building information modeling solution for our green world. *URL http://gbxml. org/–Überprüfungsdatum*, 08-25.

Ruan, F., Qian, X. Q., Zhu, Y. T., Wu, M. L., Qian, K. L., & Feng, M. P. (2015). Wall insulation effect on building energy efficiency with the intermittent and compartmental energy consuming method. Applied Mechanics and Materials,

Sayadi, S., Hayati, A., & Salmanzadeh, M. (2021). Optimization of window-to-wall ratio for buildings located in different climates:

An IDA-indoor climate and energy simulation study. *Energies*, *14*(7), 1974.

Simanic, B., Nordquist, B., Bagge, H., & Johansson, D. (2020). Influence of User-Related Parameters on Calculated Energy Use in Low-Energy School Buildings. *Energies*, *13*(11), 2985. https://www.mdpi.com/1996-1073/13/11/2985

Standardization, I. O. f. (2005). Ergonomics of the thermal environment — Analytical determination and interpretation of thermal comfort using calculation of the PMV and PPD indices and local thermal comfort criteria. In.

Studio, G. B. (2008). Autodesk Green Building Studio. In.

Swisher, J., Christiansson, L., & Hedenström, C. (1994). Dynamics of energy efficient lighting. *Energy policy*, *22*(7), 581-594.

Tarım ve Orman Bakanlığı, M. G. M. (2019). *4.8-Isıtma ve Soğutma Gün-Dereceleri*. https://cevreselgostergeler.csb.gov.tr/isitma-ve-sogutma-gun-dereceleri-i-100365#:~:text=T%C3%BCrkiye'de%20%C4%B1s%C4%B1tma%20ve%20so%C4%9Futma,%2DDereceleri%201725%20G%C3%BCn%2DDerecedir.

Tian, Z., Yang, J., Lei, Y., & Yang, L. (2019). Sensitivity analysis of infiltration rates impact on office building energy performance. IOP Conference Series: Earth and Environmental Science,

Transysy. (2022). https://www.trnsys.com/

TSE. (2008). BİNALARDA ISI YALITIM KURALLARI. In. https://intweb.tse.org.tr/.

Vasov, M. S., Stevanović, J. N., Bogdanović, V. B., Ignjatović, M. G., & Ranđelović, D. J. (2018). Impact of orientation and building envelope characteristics on energy consumption case study of office building in city of Nis. *Thermal Science*, *22*(Suppl. 5), 1499-1509.

VentureWell. *Psychrometric Charts*. https://sustainabilityworkshop.venturewell.org/node/1195.html

What Climate Factors are Important Considerations for Building Projects? https://www.build-review.com/what-climate-factors-are-important-considerations-for-building-projects/

What do "set point" and "set back" mean? (2012). https://selveyheating.wordpress.com/2012/08/02/what-do-set-point-and-set-back-mean/#:~:text=Set%20Point%20is%20the%20temperature,for%20winter%20is%2068%20degrees.

Window-to-Wall Ratio. (2019). https://help.buildingenergyscore.com/support/solutions/articles/8000026042-window-to-wall-ratio#:~:text=The%20Window%2Dto%2DWall%20Ratio,gross%20above%20grade%20wall%20area.

Woods, T., A. Parekh, A. (1992). Assessment and Potential Control of Air-Leakage in High-Rise Buildings. *Proceedings of Sixth Conference on Building Science and Technology*(Identification), 68-82.

Yildiz, Y., Özbalta, T. G., & Arsan, Z. D. (2011). Farklı Cam Türleri ve Yönlere Göre Pencere/Duvar Alanı Oranının Bina Enerji Performansına Etkisi: Eğitim Binası, İzmir. *Megaron*, *6*(1).

Zhai, Z. J., & Helman, J. M. (2019). Implications of climate changes to building energy and design. *Sustainable Cities and Society*, *44*, 511-519.

Zhao, D., Aili, A., Yin, X., Tan, G., & Yang, R. (2019). Roof-integrated radiative air-cooling system to achieve cooler attic for building energy saving. *Energy and Buildings*, *203*, 109453.

Zhao, M., Künzel, H. M., & Antretter, F. (2015). Parameters influencing the energy performance of residential buildings in different Chinese climate zones. *Energy and Buildings*, *96*, 64-75.

Zilberberg, E., Trapper, P., Meir, I., & Isaac, S. (2021). The impact of thermal mass and insulation of building structure on energy efficiency. *Energy and Buildings*, *241*, 110954.

CHAPTER 4

A COMPARATIVE ASSESSMENT OF THE SEISMIC VULNERABILITY EVALUATION METHODOLOGIES FOR REINFORCED CONCRETE BUILDINGS

Assist. Prof. Dr. Ayşe Elif ÖZSOY ÖZBAY[1]

Assoc. Prof. Dr. Işıl SANRI KARAPINAR[2]

[1] Maltepe University, Faculty of Engineering and Natural Sciences, Department of Civil Engineering, İstanbul, Turkey.
E-mail: ayseelifozsoyozbay@maltepe.edu.tr. ORCID: /0000-0001-5397-398X.
[2] Maltepe University, Faculty of Engineering and Natural Sciences, Department of Civil Engineering, İstanbul, Turkey.
E-mail: isilkarapinar@maltepe.edu.tr. ORCID: 0000-0002-3695-5867.

INTRODUCTION

Due to the consequences of unpredictable seismic hazards, there are significant concerns about the seismic vulnerability of existing buildings. Therefore, the researchers have made many attempts aimed at developing different methodologies to mitigate the catastrophic effects of earthquakes. For the classification of the large building stocks with respect to their seismic vulnerabilities, there is a demand for easy, fast and reliable methods of screening the building stocks. Instead of using detailed analysis, by the help of the proposed rapid methodologies, prioritization of the buildings having high seismic risk becomes more practical and time-saving for the decision-makers. As put forward, especially by the seismic-prone countries, applying these methodologies to the existing building stocks has a major role in the pre and post-earthquake strategies.

The rapid visual screening (RVS) method is an evaluation process of seismic assessment of existing buildings relating the screened building data with the building's potential damage grade to classify the buildings for the prioritization of retrofitting or deciding on other major seismic management strategies. The vulnerability assessment procedure of the structures by RVS was first documented by the Federal Emergency Management Agency (FEMA) and revised several times. The procedure presented in FEMA P-154 was also adopted by many countries (FEMA 2015a, 2015b). While the application of the RVS methodologies adopted by many countries is similar in outline, minor differences occur in the scoring process due to different local construction materials, country-specific design procedures and construction techniques (NRC/IRC 1992, NZSEE 2006). Also, a similar methodology has been developed in Turkey named "Specifications for Determination of Seismically Vulnerable Buildings" (SDSVB-2019) presenting a screening procedure for the seismic risk evaluation of the buildings on a regional scale. With the implementation of this approach, case studies have been performed to rank the seismic vulnerability of buildings with different typologies in Turkey (Sanrı Karapınar, Özbay, & Ünen, 2021; Özsoy Özbay, Sanrı Karapınar, & Ünen, 2020).

This review targets to present a comparative evaluation of the methods in FEMA P-154 and SDSVB-2019 and to put forward the advantages and disadvantages of both in the seismic assessment of reinforced concrete buildings. In this concept, the theoretical basis and the conceptual framework of the methodologies are compared and discussed. The differences between the implementations of these evaluation methods are given in detail for the seismic risk prioritization of the existing buildings.

RVS METHOD IN FEMA P-154

FEMA P-154 provides an RVS method mainly applicable to reinforced concrete, masonry and steel buildings as well as precast concrete frame structures and the tilt-up buildings. Concerning the types of buildings defined in FEMA P-154, the reinforced concrete structures are categorized in three main groups as moment-resisting frames, shear wall systems and the framed structures with unreinforced masonry infill walls named as C1, C2 and C3, respectively.

The assessment procedure in FEMA P-154 requires the data form selection depending on the site-specific seismicity level. Thus, the preliminary stage of the assessment is to estimate the seismicity of the survey region for the building location. The level of seismicity is identified utilizing the spectral acceleration response values calculated with the use of the U.S. Geological Survey online tool (USGS, 2022). As given in Table 1, the seismicity of the region is categorized into five levels ranging from *low* to *very high* depending on the short and long period spectral accelerations, S_s and S_1 which are determined for the geographical coordinates of the building.

Table 1. Levels of seismicity in FEMA P-154 (FEMA, 2015a)

Seismic region	**S_s**	**S_1**
Low	<0.25g	$S_1 < 0.10g$
Moderate	$0.25g \leq S_s < 0.50g$	$0.10g \leq S_1 < 0.20g$
Moderately high	$0.50g \leq S_s < 1.00g$	$0.20g \leq S_1 < 0.40g$
High	$1.00g \leq S_s < 1.50g$	$0.40g \leq S_1 < 0.60g$
Very high	$S_s \geq 1.50g$	$S_1 \geq 0.60g$

The information about the soil conditions is also required for the scoring of the building. FEMA P-154 utilizes the soil classification provided by ASCE/SEI 7-10 (ASCE, 2010) in which site classes are ranged from *rock* to *poor soil* having the abbreviations from A to F. As the worst local site condition, the soil types having liquefaction potential, highly-sensitive clays or clays with a very high level of plasticity are categorized as site class F. Since these types of soils are highly vulnerable to geologic hazards under a potential seismic action, further structural and geotechnical evaluations are recommended for the building. Therefore, FEMA P-154 procedure is not applicable for the given soil class.

The building score is calculated depending on the building-specific parameters which are the basic score and the score modifiers having negative or positive values depending on their effects on the structural behavior for Level 1 assessment as presented in Table 2. Hereafter, the basic score and the score modifiers are added to obtain the resulting score of the building. As can be seen in Table 2, the final score is mainly based on the score modifiers concerning the existence of vertical and plan irregularities besides the soil conditions and the seismic code that the building was subject to during the construction period. Since base scores were determined by considering the site classes as C and D, the effect of different site classes is taken into account by the score modifiers in the screening procedure.

Table 2. Basic scores and score modifiers for reinforced concrete buildings in Level 1 assessment procedure (FEMA, 2015a)

Seismicity	**Low**			**Moderate**			**Mod. high**			**High**			**Very high**		
Type of the structure	**C 1**	**C 2**	**C 3**	**C 1**	**C 2**	**C 3**	**C 1**	**C 2**	**C 3**	**C 1**	**C 2**	**C 3**	**C 1**	**C 2**	**C 3**
Basic Score	3.3	4.2	3.5	2.1	2.5	2	1.7	2.1	1.4	1.5	2	1.2	1	1.2	0.9
Severe vertical irregularity	-1.3	-1.2	-1.1	-1.1	-1.2	-1	-1	-1.1	-0.8	-0.9	-1	-0.7	-0.7	-0.8	-0.6
Mod. vertical irregularity	-0.7	-0.7	-0.6	-0.7	-0.7	- 0.6	-0.6	-0.6	-0.5	-0.5	-0.6	-0.4	-0.4	-0.4	-0.3
Plan irregularity	-1	-1	-0.9	-0.8	-1	-0.8	-0.7	-0.9	-0.6	-0.6	-0.8	-0.5	-0.4	-0.5	-0.3
Pre-Code	-	-	-	-0.3	-0.4	-0.3	-0.4	-0.7	-0.1	-0.4	-0.7	-0.1	-0.1	-0.2	0
Post-benchmark	2.3	2.2	-	2	2.3	-	1.9	2.1	-	1.9	2.1	-	1.4	1.7	-
Soil type A and B	0.9	1.2	1.2	1.1	1.5	1.3	0.6	0.8	0.7	0.4	0.5	0.3	0.2	0.3	0.1
Soil type E: Low rise	-1.4	-2	-1.6	-0.7	-1	-0.7	-0.2	-0.2	-0.4	0	0	-0.2	-0.1	-0.2	0
Soil type E: Mid/High rise	-1.3	-1.9	-1.6	-0.8	-1	-0.8	-0.6	-0.8	-0.4	-0.5	-0.7	-0.3	-0.1	-0.3	-0.1
Min. score	0.5	0.6	0.5	0.3	0.3	0.3	0.3	0.3	0.3	0.3	0.3	0.3	0.3	0.3	0.3

As the second stage of the RVS procedure, FEMA P-154 provides a more detailed evaluation method by the use of data collection forms prepared for Level 2 assessment. In Level 2 assessment of reinforced concrete buildings, inspection for vertical irregularities involve additional characteristics including the existence of topographic effects, weak and soft story, short columns and discontinuities of the floor levels. In addition, the irregularities in the plan are subcategorized into torsional irregularity, non-parallel lateral system, the existence of openings in the floor diaphragm and out-of-plane offset of the beams. Moreover, the effect of pounding on adjacent buildings and the degree of redundancy are also taken into consideration in the risk decision of the inspected building.

RVS METHOD IN SDSVB-2019

The RVS procedure proposed by SDSVB-2019 provides a simple methodology to be applied for the regional scale vulnerability estimation of masonry and reinforced concrete buildings. Implementation of the RVS method requires pre-field assessment of the seismic hazard level and the soil type of the region in the former stage of the RVS process; and identification of the building characteristics through visual inspections.

The hazard zone is estimated using the soil class and site-specific response parameters calculated at the site location of the building by the online tool available from AFAD (2022). Table 3 represents the hazard zones corresponding to the estimated short-period spectral acceleration coefficient, S_{DS} values, and the site classes (ZA-ZE) as described in the Turkish Seismic Code (2018).

Table 3. Identification of the hazard zones in SDSVB-2019

Hazard zone	S_{DS}	Site class
I	$S_{DS} \geq 1.0$	ZC, ZD, ZE
II	$S_{DS} \geq 1.0$	ZA, ZB
	$0.75 \leq S_{DS} \leq 1.0$	ZC, ZD, ZE
III	$0.75 \leq S_{DS} \leq 1.0$	ZA, ZB
	$0.50 \leq S_{DS} \leq 0.75$	ZC, ZD, ZE
IV	$0.50 \leq S_{DS} \leq 0.75$	ZA, ZB
	$S_{DS} \leq 0.50$	All site classes

Conforming to the procedure, the performance score (PS) of the inspected building is determined as:

$$PS = BS + SSS + \sum[VSMxVS] \quad (1)$$

where BS and SSS are the base score and structural system score, respectively as given in Table 4.

Table 4. Base scores and the structural system scores in SDSVB-2019

No. of stories	Base scores (BS) for seismic hazard zones				Structural system score (SSS)	
	I	II	III	IV	Moment resisting frames	Moment resisting frames with shear walls
1-2	90	120	160	195	0	100
3	80	100	140	170	0	85
4	70	90	130	160	0	75
5	60	80	110	135	0	65
6-7	50	65	90	110	0	55

VS and VSM correspond to the vulnerability score and the vulnerability score modifier in Eq. (1), respectively. The vulnerability scores, VS regarding the structural parameters to be determined during the inspections include the construction quality and the existence of structural irregularities, pounding effect, short column, soft story, heavy overhang and topographic effects as listed in Table 5. For each vulnerability parameter, the vulnerability score modifier, VSM in Eq. (1) is regarded as 0 or 1 depending on whether the inspected parameter "exists" or "does not exist" in the surveyed building. For construction quality score modifier, VSM is taken as 0, 1 and 2 according to the inspected quality as *good*, *moderate* and *poor*, respectively.

Table 5. Vulnerability scores in SDSVB-2019

Number of stories	Vulnerability Scores (VS)										
	Soft story	Const. quality	Heavy overhang	Pounding effect aligned-mid	Pounding effect aligned-corner	Pounding effect not aligned-mid	Pounding effect not aligned-corner	Vert. irregularity	Plan irregularity	Short column	Topog. Effects
1-2	-10	-10	-10	0	-10	-5	-15	-5	-5	-5	-3
3	-20	-10	-20	0	-10	-5	-15	-10	-10	-5	-3
4	-30	-15	-30	0	-10	-5	-15	-15	-10	-5	-3
5	-30	-25	-30	0	-10	-5	-15	-15	-10	-5	-3
6-7	-30	-30	-30	0	-10	-5	-15	-15	-10	-5	-3

COMPARISON OF THE SEISMIC ASSESSMENT METHODOLOGIES

As the primary concern of RVS methodologies in literature, implementation of the procedures in FEMA P-154 and SDSVB-2019 serve for the physical vulnerability evaluation of the building stocks supporting the seismic risk prioritization activities. FEMA P-154 method has been developed using the capacity spectrum-based method in which the seismic vulnerability is determined by the use of fragility curves derived from the structural analysis of the buildings exposed to a certain level of the seismic event. On the other hand, the theoretical framework of the screening approach in SDSVB-2019 mainly depends on the statistical determination of the damage data of the buildings derived from post-earthquake inspections.

In the calculation of the performance score in SDSVB-2019, the number of stories is a major parameter that significantly affects the base score, the structural system score and the vulnerability scores involved in the assessment procedure. Regarding the vulnerability parameters defined in SDSVB-2019, the vertical irregularity is described as the existence of discontinuities in columns or shear walls along the building height. Also, in the screening procedure, unfavorable layouts in the plan of the structural system triggering torsional effects are considered as the plan irregularities affecting the overall performance of the building under potential earthquakes.

FEMA P-154 also takes into account the structural irregularities that exist in plan and elevation in terms of the score modifiers related to the vulnerability parameters. Unlike the vulnerability parameters in SDSVB-2019, the parameters concerning the existence of weak/soft story, short column, out-of-plane setbacks resulting in heavy overhangs, and the sloping site causing a full story height difference between the sides of the building are considered as the vertical irregularities in FEMA P-154. On the other hand, the potential damage to the building due to the presence of short column, soft story, heavy overhang, and sloped topography of the site are introduced as different vulnerability parameters to be inspected in addition to the vertical irregularities in SDSVB-2019.

It is also noteworthy that both methodologies, FEMA P-154 and SDSVB-2019 take into account the pounding potential of the adjacent buildings as a vulnerability parameter to be identified during the visual inspections. Based on the damage observations and the detailed analysis of the buildings through structural modeling, the position of the inspected building along the row of buildings and the vertical alignment of the story levels are indicated as the critical aspects to assess the pounding effect. Hence, in both of the methodologies, a building located at the edge of the building block is penalized with a lower score compared to a building between two others in the scoring system. Moreover, the story levels that do not align in elevation are considered as an unfavorable condition for the assessment procedures in FEMA P-154 and SDSVB-2019 as well.

By the completion of the screening activities and scoring calculations for a specific survey region according to the methodology given SDSVB-2019, the assessed buildings are ranked with respect to their performance scores from the lowest to the highest representing the priority level for detailed intervention. On the other hand, in FEMA P-154, the building's final score is associated with the collapse probability of the building subjected to the specified seismic action, hence the results below a threshold score represent the set of buildings that require immediate intervention for detailed assessment. Therefore, having performed the methods in FEMA P-154 or SDSVB-2019, seismic risk distribution of the buildings can be determined for the study region while identifying the threshold score level of the buildings having the highest priority among the entire building stock depends on the decision-makers.

CONCLUSION

The objective of this study is to overview the RVS methodologies introduced by FEMA P-154 and SDSVB-2019 and reveal the differences in the implementation of these methods being used for the thorough strategy for the RVS activities. The advantages of using these methodologies in the seismic evaluation of buildings for the pre- and post-earthquake management are underlined. The vulnerability

ranking procedure presented in both of the methods is compared in terms of the theoretical basis and the conceptual framework. In detail, the seismicity regions are interpreted and the vulnerability parameters to be considered in both procedures are analyzed comparatively. Also, this study reveals how to prioritize the most vulnerable buildings by the seismic risk distributions using both of the procedures.

Both of the screening approaches provide reliable evaluation schemes aiming to determine the regional seismic risk distribution of large numbers of buildings, supporting the earthquake risk mitigation activities. The RVS methodology defined in SDSVB-2019 has a significant efficiency to assess the seismic vulnerability of existing buildings, while FEMA P-154 provides a more comprehensive approach that allows the evaluation of different building typologies.

The comparison of these two methodologies within this study has highlighted the significance of the application of rapid visual screening procedures and the conclusions have added to a growing body of literature on the seismic assessment methodologies.

REFERENCES

AFAD (2022). Türkiye deprem haritaları interaktif web uygulaması. Accessed May 11, 2022. https://tdth.afad.gov.tr/

NRC/IRC (1992). Manual for Screening of Buildings for Seismic Investigation. *National Research Council of Canada*, Institute for Research in Construction, Ottawa.

NZSEE (2006). Assessment and improvement of the structural performance of buildings in earthquakes, *New Zealand Society for Earthquake Engineering*, Wellington, New Zealand.

FEMA (2015a). FEMA P-154 Rapid visual screening of buildings for potential seismic hazard: A handbook.

FEMA (2015b). FEMA P-155 Rapid Visual Screening of Buildings for Potential Seismic Hazards: Supporting Documentation.

Özsoy Özbay, A. E., Sanrı Karapınar, I., & Ünen, H. C. (2020). Visualization of seismic vulnerability of buildings with the use of a mobile data transmission and an automated GIS-based tool. *Structures*, 24(January), 50–58. https://doi.org/10.1016/j.istruc.2020.01.004

Sanrı Karapınar, I., Özbay, A. E. Ö., & Ünen, H. C. (2021). GIS-Based Assessment of Seismic Vulnerability Information of Old Masonry Buildings Using a Mobile Data Validation System. *Journal of Performance of Constructed Facilities*, 35(3), 04021009. https://doi.org/10.1061/(asce)cf.1943-5509.0001574

SDSVB (2019). Riskli Yapıların Tespit Edilmesine İlişkin Esaslar. *Çevre ve Şehircilik Bakanlığı*.

Türkiye Bina Deprem Yönetmeliği. (2018). İçişleri Bakanlığı Afet ve Acil Durum Yönetimi Başkanlığı. Resmi Gazete, 30364(1).

ASCE (2010). Minimum Design Loads for Buildings and Other Structures ASCE/SEI 7-10. *American Society of Civil Engineers*, Reston, Virginia.

USGS (2022). Seismic Design Maps Web Services. Accessed May 10, 2022. https://earthquake.usgs.gov/hazards/designmaps/.

CHAPTER 5

INVESTIGATION AND MITIGATION STUDIES OF TRANSPORTATION BASED GREENHOUSE GAS EMISSIONS IN ADANA CITY

Dr. Çağrı ÜN[1]

[1] Foreign Relations Department Manager, Adana Metropolitan Municipality, Adana, Türkiye, cagri.un@adana.bel.tr. Orcid: 0000-0002-7925-5000

INTRODUCTION

In October 2018, the Intergovernmental Panel on Climate Change (IPCC) issued a warning that the world needs to reduce global greenhouse gas (GHG) emissions by 45% by around 2030 and to reach netzero emissions by 2050 to prevent the negative impacts of climate change (IPCC, 2019).

At this point; The Global Covenant of Mayors is the first and most ambitious initiative launched by the European Commission, aimed at local authorities and citizens as direct leadership in tackling global climate change. Since 2008, the Covenant of Mayors aims to increase its work on sustainable energy and climate change. By joining this convention, municipalities voluntarily commit to reducing greenhouse gas emissions and improving climate resilience through the implementation of the Sustainable Energy and Climate Action Plan. The commitments made for the parties are linked to the climate and energy policy of the European Union. These include the European Union's 2030 climate and energy framework and the EU Climate Change Adaptation Strategy for parties that will join after 2015. Local authorities are committed to reducing CO_2 emissions (and possible other greenhouse gases) by at least 40%, increasing resilience to the effects of climate change, and ensuring safe access to sustainable and affordable energy by 2030. Cities which parties to the GcoM, have identified the following common visions for 2050;

- Strengthening the capacity to adapt for the unavoidable climate change impacts
- To ensure for citizens safely, sustainable and affordable energy

Parties also make their political commitments to practical measures and projects. They commit to submit the Sustainable Energy and Climate Action Plan (SECAP), a strategy and policy document outlining the key actions which they plan to take, within two years of the local council's decision to transform it.

Greenhouse gas emissions in the SECAP method is expressed

under three main sectors as waste, stationary energy and transportation;

- **Stationary Energy:** All greenhouse gas emissions arising from fuel burned in fixed sources in the city and energy consumption from the grid, are expressed separately under residential buildings, commercial buildings & facilities, institutional buildings & facilities, industry, forestry and aquaculture activities. Loss/illegal emissions arising from electrical energy consumption within the city limits are included in the greenhouse gas emission inventory. Emissions arising from lost and illegal electrical energy are allocated to each of them in line with the electricity consumption of fixed sources on a category basis.
- **Transportation:** The amount of fuel consumed during transportation, transportation activities and associated greenhouse gases are expressed on the basis of fuel and transportation categories. Emissions within the operations of the municipality are expressed according to the type of fleet used by local governments within the framework of transportation activities.
- **Waste:** All greenhouse gas emissions arising from the management of solid wastes and treatment of waste water within the city limits in the base year.

The methodology followed in Adana's GHG inventory for 2020 and the GHG reporting framework are based on the Global Protocol on Community Scale GHG Emissions Inventories used by the GCoM and the Emissions Inventory Guidelines used by the European Convention of Mayors.

1. BASIC INFORMATIONS ABOUT ADANA CITY

Adana; with an area of 13,844 km², which is 1.77% of Turkey's, and it is Turkey's 6th most populous city with a population of 2,258,718 according to 2020 TUIK data. Between 2007 and 2020, 49.9% of Adana's population, which increased annually by an average of 0.91%, is female and 50.1% is male. At the same time, Adana

province ranks 12th in Turkey in terms of population density (number of people per km²) with 161.65 persons/km².

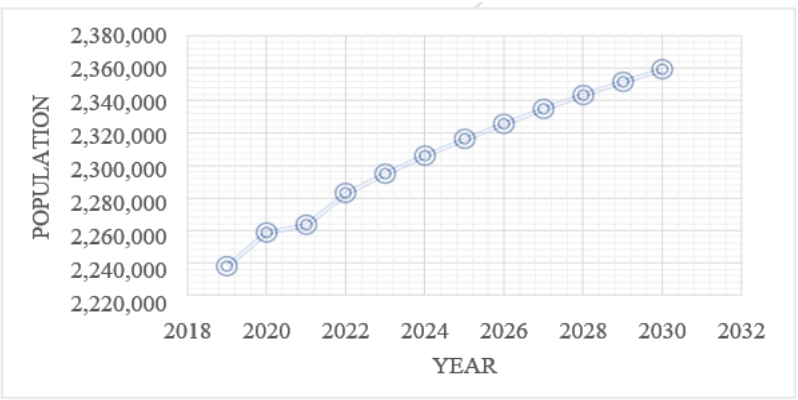

Figure 1: Adana City 2030 Population Projection

Table 1: Adana City Technical Informations

Area	13.844 km^2
Population density (The year of 2020)	161,65 per/km^2
Average sunshine duration (hours) Measurement Period (1929 - 2021)	7,5 hour
Population (The year of 2020)	2.258.718
Average monthly precipitation amount (mm) Measurement Period (1929 - 2021)	668,7 mm
Total greenhouse gas emission (The year of 2020)	9,7 $MtCO_2e$
Greenhouse gas per capita release (The year of 2020)	4,3 tCO_2e/person
Average temperature (°C) Measurement Period (1929 - 2021)	19,2 °C

In the figures below; Adana city average monthly rainfall (Fig.2), Adana city for the years 1955-2017 average temperature (Fig.3) and Adana city for the years 1928-2017 average day & night temperatures (Fig.4) precipitation amount and temperatures are given. In these figures; it is seen that Adana province is affected by the temprerature in the summer months and the precipitation decreases especially in the summer period.

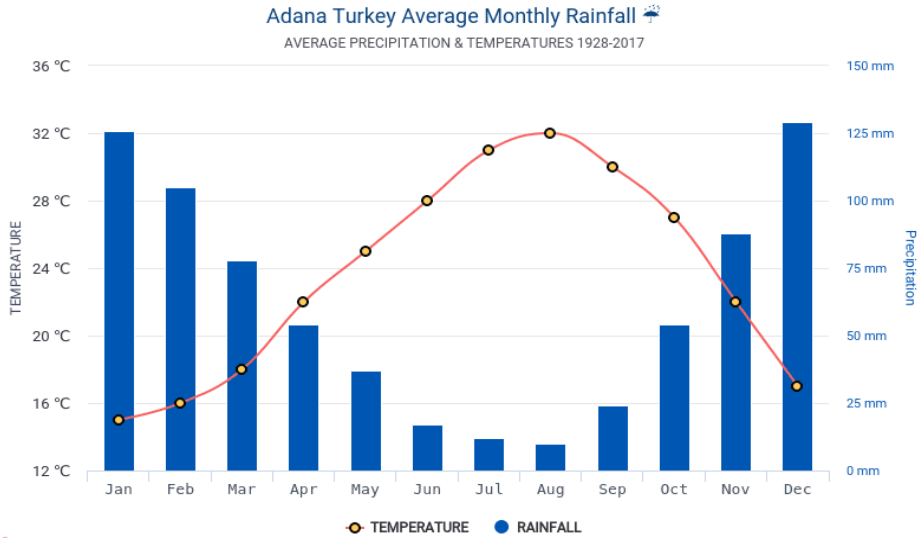

Figure 2: Adana City Average Monthly Rainfall (URL-1)

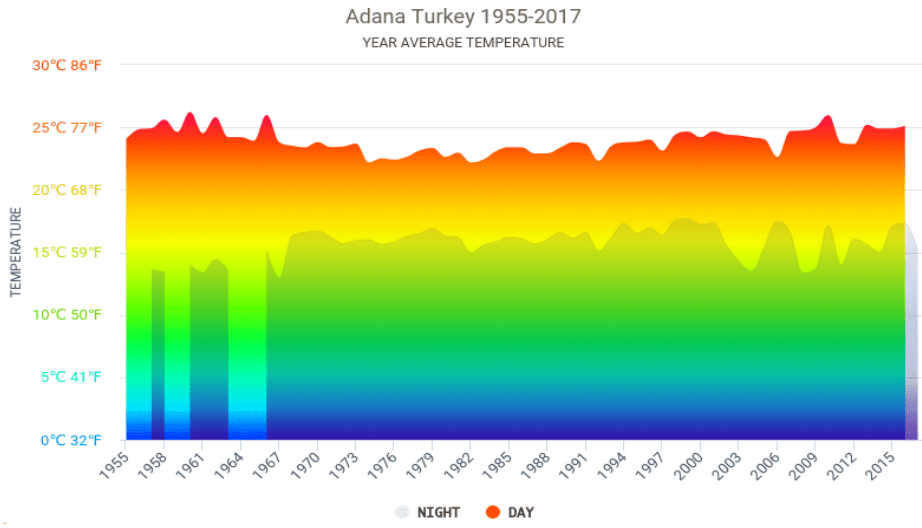

Figure 3: Adana City 1955-2017 Average Temperature (URL-1)

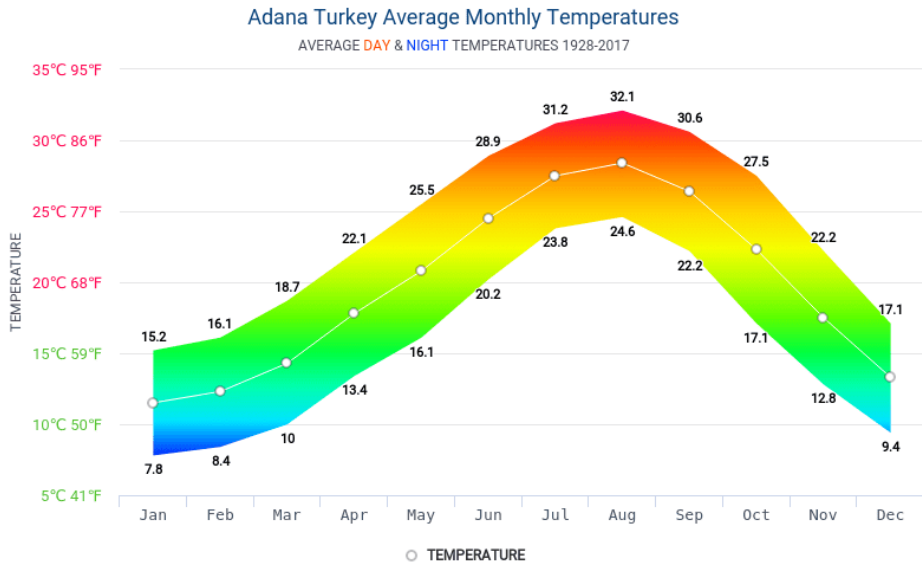

Figure 4: Adana City 1928-2017 Average Day & Night Temperatures (URL-1)

2. SECAP STUDIES IN ADANA

The IPCC Climate Change 2021: The Physical Science Basis Report says that, The Mediterranean Region, where the city of Adana is located, is one of the regions in Europe that is expected to be most affected by climate change. Negative effects due to climate change such as increasing temperatures, droughts, water scarcity and more frequent extreme weather events have begun to be felt in Adana, as in many other provinces today (IPCC, 2021).

Adana Metropolitan Municipality, which has always clearly shown its determination to fight against the climate crisis with its current strategic plans, local policies and projects, declared its determination in this fight at the international level as a party to the Global Covenant of Mayors (GCoM) in 2021. With this commitment, by 2030, compared to the base year 2020, aims to reduce emissions by 40%. In this context, Adana Metropolitan Municipality prepared the Sustainable Energy and Climate Action Plan (SECAP) together with the relevant stakeholder organizations in the 10-month period between September 2021 and June 2022. On the way to this goal, Adana Metropolitan Municipality (AMM) has developed an overview of GHG emissions and determined appropriate strategies to achieve the reduction target it has committed. In addition, with the Risk and Vulnerability Analysis study prepared specifically for the city, the climate hazards and vulnerabilities that affect/may affect the city were identified, an adaptation strategy was developed for the city and adaptation actions were determined against these risks.

The visions of the city of Adana; to be a low-carbon-intensive city that integrates the actions that will achieve the reduction target with its existing projects and plans, to have high energy efficiency, to access sustainable and reliable energy sources which are regionally resistant to the negative effects it will be affected by the climate crisis.

When the effects of climate change in Adana are examined, heat waves with increasing duration and severity, drought and excessive precipitation, the floods and forest fires are considered as priority issues. In addition, issues such as expanding carbon sink areas, investments in waste, transportation and renewable energy for a

sustainable environment, rainwater harvesting and improving wastewater recovery are also great importance. In this process, AMM aims to mobilize investments in low-carbon green urban development based on an integrated urban planning approach by promoting innovation, participatory planning and partnerships between various public and private sector organisations (SECAP, 2022).

In the fight against climate change, the analysis of strengths and weaknesses, which are internal factors, opportunities and threats, which are external factors, in particular for Adana province. With these analyses, the current situation of the city of Adana is clearly defined in all its aspects. This analysis also helped define priorities when designing and selecting SECAP actions and measures. The results of this analysis are summarized in the table below (SECAP, 2022).

Table 2: SECAP SWOT Analysis Table for Adana City

STRENGTHS	• Presence of companies and educated workforce that can use up-to-date technology and make quality production in the building sector throughout the city. • Widespread use of conventional renewable energy systems such as solar water heating • A significant part of the heating and cooling in the city is done with air-sourced air conditioners. • The fact that the city is in a very rich region in terms of various renewable energy sources • With transportation services management, which is one of the strategic objectives; the goal of providing economical, safe and comfortable service to every point of the city • The Transportation Master Plan study currently underway • Expansion of the rail system network • Bicycle path project that will cover the whole city in a way to encourage active transportation • Presence of smart transportation systems • Road and infrastructure maintenance and renovation works covering the whole city • The city's size is appropriate in terms of population and built-up area, enabling the use of economies of scale. • Presence of important natural areas and values in and around the city • Finding opportunities to renew and improve the city through urban transformation projects. • Obtaining biogas during the disposal of wastewater sludge and thus generating electricity • The fact that the sanitary landfill site meets an important need for both treatment (recycling processes) and safe disposal of solid wastes generated in Adana • There is no methane leakage in the landfill and the methane gas obtained is converted into electricity and converted into added value. • Having a vision for the dissemination of some good practice opportunities in the district municipalities to Adana in general, before the metropolitan municipality.

WEAKNESSES	• A significant portion of the existing building stock is of low quality in terms of energy efficiency. • The efficiency of commonly used air conditioners is quite low. • Rooftop (or urban) PV systems have not yet become widespread • A significant portion of the power plants established around Adana are thermal power plants using fossil fuels. • Different modes of transportation are not integrated with each other. • The city is designed to bring motor vehicles to the fore. • Low awareness of active transportation • Inadequate traffic control • Presence of neighborhoods in the city where social segments with high vulnerability to natural hazards and risks are concentrated • Presence of sub-regions and neighborhoods in the city that have completed their economic and physical life and contain low-quality buildings • The city does not have a multimodal and widespread public transportation system. The new urban development areas are located in the northern part of the city with poor public transportation connection, and this area is close to nature protection areas. • Inability to access important urban uses such as universities and hospitals by rail. Insufficient social reinforcement areas, especially urban green areas, due to dense and unplanned construction in the city. • Insufficient administrative and financial resources required for urban transformation applications. • High rate of water loss and leakage. Difficulty of doing infrastructure work due to narrow roads in the center • Not treating all of the wastewater • The planning in the existing infrastructures has been made without considering the changes in the climate. • A standard/advanced approach has not yet been established for collecting, analyzing, reporting and monitoring data on solid waste at city scale. • Low public awareness of waste reduction and separation at source (households) • The wastes are contaminated with organic materials due to the inability to separate the wastes efficiently at their source (households), and due to this situation, the waste separation processes in the disposal facility cannot be carried out with the desired efficiency. • The existence of unregulated landfills and the unavoidable illegal waste dumping in some periods, especially in districts far from the center. • Insufficient level of activities (prevention of waste, repair campaigns, promotion of recycling, etc.) aimed at reducing different waste groups at their source, especially organic wastes.

OPPORTUNITIES	• Opportunity to benefit from solar energy for electricity and heat generation with very high insolation levels throughout the year. • A suitable ground structure and high ground water level for ground source heat pumps and district heating cooling in the city center, which was established on the riverside and on an alluvial plain • Significant interest in the establishment of renewable energy facilities in the region • Opportunity to implement projects that will encourage the transition to public transportation • Reduction potential of private car use with mobility management and road network optimization • Opportunity to provide additional income with various pricing applications • Opportunity to switch to electric vehicles • Opportunity to provide stakeholder participation in the planning, implementation and monitoring processes of transportation projects • The city's topography allows the use of bicycles. • Presence of plateaus and transhumance culture that provide a temporary settlement environment in summer • Presence of natural and artificial water channels in the city • Affordability of internal consumption of renewable energy projects and treatment plants • It is a must to fulfill some of the obligations brought by the regulations • The fact that legal regulations are being developed day by day with factors that encourage the reduction and separation of wastes at the source. • The increase in the socioeconomic level contributes to the awareness of the public about waste reduction and segregation at the source. • The high potential of using the financial resources (eg EU financing) transferred to Turkey as a developing country to be used in environmental management in waste management • Due to the climate of the Adana region, it has an advantageous position in the biological decomposition of organic wastes (eg airless digestion, composting). • Changes in consumption habits and consumer preferences cause an increase in the waste composition of materials that are difficult to recycle for certain product groups.

The first greenhouse gas inventory prepared in accordance with SECAP standards for Adana belongs to 2020. Therefore, the year 2020 is expressed as the base year. Greenhouse gases evaluated within the scope of the inventory are carbon dioxide (CO_2), methane (CH_4) and nitrogen oxides (N_2O). These gases are major greenhouse gases in terms of emissions from energy use within city limits and emissions from activities other than energy use. In other words, emissions are largely CO_2, CH_4 and nitrogen originate from N_2O. The carbon dioxide equivalent (tCO_2e) of emissions from CH_4 and N_2O has been included in the inventory using the global warming potentials specified in the IPCC 5th Assessment Report (AR5) (SECAP, 2022).

For Adana, greenhouse gas emission projections for 2030 were calculated by using the greenhouse gas emission inventory calculations for the calendar year 2020 as the base year data.

In the process of determining the targets, for each of the emission reduction strategies, the internal stakeholders of Adana Metropolitan Municipality (AMM) were worked altogether. Organizing regular focus group meetings and trainings has contributed a lot of for this process. For these important steps; clear and detailed targets have been established that have been intensively studied with the relevant units and affiliates of the Municipality. Many divisions of AMM have responsibilities in the goal of reducing greenhouse gas emissions. The support of academia, NGOs, private sector, citizens, central government and other public institutions is essential for Adana to achieve its climate goals.

At this stage, mitigation actions were presented to external stakeholders in a workshop, opinions of external stakeholders were taken for the selected actions and reflected in the study results.

3. TRANSPORTATION BASED GREENHOUSE GAS EMISSIONS

Transportation is a central feature of our life. Globalization has steadily increased the movement of goods and people. So transportation is one of the largest energy use sectors. Pre-pandemic, transport made up 29% of global primary energy use and around 25%

of global energy-related carbon dioxide (CO_2) emissions (Kaya et. al., 2019).

The transportation sector is expected to be a crucial part of the solution. A sector that can help reduce greenhouse gas (GHG) emissions, including carbon dioxide (CO_2) and non-CO_2 gases such as methane (CH_4), nitrous oxide (N_2O), partially fluorinated hydrocarbons (HFC), perfluorinated hydrocarbons (PFC), sulfur hexafluoride (SF_6) and nitrogen trifluoride (NF_3). To a greater or lesser extent, these gases are harmful to the environment as they trap heat in the atmosphere, causing global warming (Bruhwiler et. al., 2021).

Greenhouse gas; hydrofluorocarbon (HFC), perfluorocarbon (PFC), sulfurhexafluoride (SF6), which occur in the industrial production process with water vapor (H_2O), carbon dioxide (CO_2), methane (CH_4), nitrogen oxide (N_2O), ozone (O_3) gases present in different amounts in the atmosphere consists of fluorinated compounds. CO_2 gas constitutes approximately 80% of the total greenhouse gas and is the most important of the anthropogenic greenhouse gases. (Oral ve Uğuz, 2020).

Greene (1997) stated that, among the main reasons for the increase in greenhouse gases; the impact of the transportation sector, which ranks second after the industrial sector with CO_2 emissions, is quite large. The negative effects of the transportation sector on the environment, especially due to greenhouse gas emissions, need to be resolved or at least improved for sustainable transportation. It is known that the environmental impacts and problems arising from the transportation sector are caused by excessive fossil fuel use (Greene, 1997).

3.1. Transportation Based Greenhouse Gas Emissions in Adana

According to the greenhouse gas inventory occured for Adana province within the scope of SECAP, the share of the transportation sector in total greenhouse gas emissions is quite high. In this context, it is clearly seen that one of the sectors that needs to be handled carefully

in order to reach the 40% total greenhouse gas reduction target in the 2030 target year, is the transportation sector. While determining the proposed mitigation actions for Adana province in order to achieve the desired target; the short, medium and long term actions prepared. Shortlisted actions includes interventions such as;

- ❖ Transition to alternative fuel-based and to use more efficient vehicles
- ❖ Dissemination of electric vehicles
- ❖ Promoting the transition to public transport and active transport
- ❖ Parking restrictions and road pricing

While calculating the reduction amounts to be provided by the actions, primary data obtained from AMM and secondary data obtained from national and international sources were used and various assumptions were also made. As a result of the steps followed in this context, it is foreseen that the reduction actions in the short list will contribute to more sustainable transportation in the 2030 target year compared to the current situation. While determining the adaptation actions for Adana city, the current situation of the city, educational outputs, relevant reference documents and best practice examples were taken into consideration, as in determining the mitigation actions. In addition, attention has been paid to the fact that the proposed adaptation actions are aimed at combating the effects of extreme weather conditions/events caused by the climate crisis. Identified compliance actions; includes policy measures such as reducing the heat island effect, protecting the transportation infrastructure against environmental impacts and ensuring behavioral change in transportation preferences. In addition to the fact that the said actions can be implemented mostly in the short term, it is aimed to minimize the short-term and long-term service interruptions that can be seen after the disaster through these actions.

In the analyzes made within the scope of SECAP, it was observed that according to the temperature and precipitation analyzes, which are the main climate parameters of Adana province and its surroundings until 2100, as well as the values in extreme climate parameters; temperature projections indicate that towards the end of the century, monthly average temperatures in Adana will increase between 1°C and 4°C compared to the present (1910-2010 average). The pessimistic scenario shows that monthly average temperatures will rise up to 4°C until 2100 (SECAP, 2022).

The results of the Adana greenhouse gas transportation emission inventory for the base year 2020 are given in the tables below. The percentage of the transportation sector in the total greenhouse gas urban inventory is 27%. When the distribution of emissions in the transportation sector for Adana province is analyzed, it is understood that the biggest emission source is fuel consumption in private passenger cars and commercial vehicles (98%). The projection calculations in question are IPCC etc. It was prepared using the "Kaya Identity" methodology.

The current situation in the transportation topic and the steps to be taken in the reduction target of greenhouse gas emissions are given in the tables below. In Table 3; it has been observed that, in transportation emmissions, originated from private passenger and commercial vehicles have 98% emission source. It is understood that the biggest emission source is fuel consumption in private passenger cars and commercial vehicles (98%). In addition, the emission increase was calculated in the projections until 2030 (Table 4). With the high emission values in vehicles; promoting and disseminating the use of electric private cars by establishing charging stations in central regions topic seems an important target (Table 5).

Table 3. Detailed Emission Values in Transportation Title for Adana City

2020 Base Year Adana City Inventory (tCO_2e) – Transportation Title		Originating from the sub-sectors of the transport emissions (%)	Percentage of emissions from the transport in total emissions (%)
Sourced from Municipal Vehicles (Light and Heavy Commercial Vehicles, Construction Machinery)	24.003	%0,9	%0,2
Public Transportation Which Aimed to Municipality	19.500	%0,7	%0,2
Originated from Private Passenger and Commercial Vehicles	2.596.602	%98	%27
Total	2.640.105	-	%27

Table 4. Adana Province 2020-2030 Greenhouse Gas Emission Projections (tCO2e) – Transportation (SECAP, 2022)

Year	**2020**	**2021**	**2022**	**2023**	**2024**	**2025**	**2026**	**2027**	**2028**	**2029**	**2030**
Sourced from Municipal Vehicles (Light and Heavy Commercial Vehicles, Construction Machinery)	24.003	24.332	24.826	25.247	25.663	26.075	26.487	26.899	27.311	27.724	28.137

Public Transportation Which Aimed to Municipality	19.500	19.767	20.169	20.511	20.849	21.184	21.518	21.853	22.187	22.523	22.859
Originated from Private Passenger and Commercial Vehicles	2.596.602	2.632.156	2.685.608	2.731.141	2.776.180	2.820.766	2.865.299	2.909.850	2.954.439	2.999.083	3.043.802
Total	2.640.105	2.676.255	2.730.603	2.776.898	2.822.691	2.868.025	2.913.304	2.958.601	3.003.937	3.049.330	3.094.798

Table 5. Adana Province Greenhouse Gas Emission Reduction Actions - Transportation

Reduction	Mitigation Action Details	Reduction Rate	Duration
Transition to alternative fuel-based and more efficient vehicles	Conversion of the existing fleet used in urban passenger mobility to electric buses	%0,3	Short and Medium term
Transition to alternative fuel-based and more efficient vehicles	The existing fleet, which is used in passenger mobility between the central district and the outer districts, is based on electric buses. converting	%0,02	Short and Medium term
Electric vehicles (including infrastructure)	Promoting and disseminating the use of electric private cars by establishing charging stations in central regions	%7	Long term
Transition to public transport	Increasing the efficiency of the existing rail system line, constructing the new light rail line and encouraging the citizens to use the rail system	%2	Medium term
Transition to public transport	The modernization of the railway line, which connects the central district and the outer districts, and encouraging the citizens to use railway transportation thanks to the number of trips to be increased.	%0,1	Medium term
Transition to public transport	Ensuring that citizens are encouraged to use public transportation by improving the level of service thanks to the number of routes and frequency of services to be increased by	%1	Short and Medium term

	expanding the existing bus fleet		
Transition to public transport	Accelerating public transport journeys across the city compared to private car journeys by creating bus lanes on the city's central axes	%0,1	Short term

Reduction	**Mitigation Action Details**	**Reduction Rate**	**Duration**
Transition to active transport	Increasing the share of bicycle use in urban transportation, which is a non-motorized mode of transportation, should be integrated with public transportation for this purpose. To occur and dissemination of bicycle routes	%1	Short and Medium term
Road network optimization	Reducing the share of individual transportation in urban transportation, increasing parking restrictions and/or costs in the city for this purpose	%2	Medium and long term
Road network optimization	Reducing the motorized transportation demand of employees through working from home and flexible working practices, reducing car use	%2	Short term
Road network optimization	In order to restrict the use of private cars in certain time periods and/or certain regions/corridors, entrances to the relevant region/corridor remuneration	%0,2	Long term
Road network optimization	The entry of private vehicles that do not meet certain emission conditions to the low emission zone to be determined in the city center restrictions or charges for entry	%1	Long term

4. THE EFFECTS OF ALTERNATIVE FUELS ON TRANSPORTATION EMISSIONS

In its most general definition, alternative fuels are the fuels that other than conventionally used gasoline and diesel that are used to generate energy or power. The emission effect and energy output provided by alternative fuels vary depending on the fuel source. Examples of alternative fuels are biodiesel, ethanol, electricity, propane, compressed natural gas and hydrogen.

Alternative fuels used in transportation sector are briefly explained below (URL-3).

- **Biodiesel** is a clean-burning, renewable alternative fuel that

can be produced from a wide variety of vegetable and animal oils. Biodiesel does not contain petroleum, but can be mixed at any level with a petroleum type to do a biodiesel blend. It can be used in compression ignition (diesel) engines with little or no modification.

- **Ethanol** is a renewable alternative type of biofuel made from various plant materials. Ethanol can be mixed with gasoline in varying amounts. Most spark-ignition gasoline engines work well with 10 percent ethanol (E10) blends. E85, a mixture of 85 percent ethanol and 15 percent unleaded gasoline, is an alternative fuel for use in FFVs.
- **Electricity** used to power vehicles is provided by the electricity grid and stored in the vehicle's batteries. Vehicles that run on electricity have no tailpipe emissions.
- **Propane** also known as liquefied petroleum gas, is a by-product of natural gas processing and crude oil refining. Propane is less toxic than other fuels. It has a high octane rating and excellent properties for spark-ignited internal combustion engines. Currently, less than 2 percent of U.S. propane consumption is used for transportation; however, interest is growing due to its domestic availability, high energy density, and clean-burning qualities.
- **Compressed Natural Gas (CNG)** is a natural gas that is extracted from wells and compressed. Natural gas is a fossil fuel comprised mostly of methane and is cleaner burning than gasoline or diesel fuel. Natural gas vehicles have been found to produce less greenhouse gas emissions than gasoline vehicles, but very little natural gas consumption is currently used for transportation fuel.
- **Hydrogen (H_2)** is a renewable alternative fuel that can be used to generate electricity. The chemical reaction between oxygen and hydrogen generates electrical power, and the only source of emission is water vapor. Depending on the energy source causing the chemical reaction, hydrogen is known as an emission-free transportation fuel. (URL-3).

Petroleum-based fuels currently compose over 90 percent of the fuel used for transportation and spread high amounts of GHG's. Alternative fuels – any fuel that is not petroleum based – are looked at as a potential solution for reducing greenhouse gas emissions.

Examples of alternative fuels include electricity from renewable sources, ethanol, biodiesel, propane and hydrogen. The use of alternative fuels has the potential to reduce emissions of carbon dioxide and other greenhouse gases released by trucks and vehicles, which account for the largest share of greenhouse gas emissions in the US at 28 percent (URL-2).

Extreme rainfall caused by climate change can deploy infrastructure that provides alternative fuels. Floods and droughts are likely to impress lake and river water levels, which can damage infrastructure for the distribution, generation and transmission of alternative fuels. Extreme temperatures may cause stoppages in the power system. It also has the potential to reduce the capacity of power transmission lines. Power stoppages caused by intense weather can also pose a threat to electricity used to power trucks and cars (URL-2).

There are 312.7 million vehicles in the European Union roads, powered by gasoline (54 %) and diesel (42%). Light duty vehicles were responsible for 52% of transport emissions in 2018 (light-duty trucks 8% and cars 44%). The rest including Electric Vehicles (EVs) and gaseous fuels account for approximately 4% (Hybrid Electric Vehicles 0.7%, BEV 0.3%, NG + LPG 2.8%) The average energy share of renewables (including hydrogen, green electricity, liquid biofuels, biomethane and etc.) used in transport increased from 1.5% in 2004 to 8.3% in 2018 (Panoutsou et. al., 2021).

Advanced biofuels are necessary for the transition to zero carbon as planned by the European Green Deal and United Nation Sustainable

Development Goals. Their use can decrease emissions and depend on imported fossil fuels while biomass supply can also establish employment in rural areas. Their production costs however are higher than their fossil similars and they still require significant innovation, technological development and scale up. Even though the Renewable Energy Directive II set clear targets both the industry and the scientific

community agree that additional interventions are needed with focus on the challenges these fuels face along the value chain. This will increase investor confidence and avoid risking the 2050 climate aims (Panoutsou et. al., 2021).

5. CONCLUSIONS

Within the framework of the greenhouse gas emission calculation and reduction proposals of the city of Adana, transportation reduction actions and proposals have been studied and determined.

The total greenhouse gas emission amount for the province of Adana in 2020 is 9.7 $MtCO_2e$ and the carbon footprint per capita is calculated as 4.3 tCO_2e. The percentage of the transportation sector in the total city inventory is 27%. Therefore, the SECAP study is more focused on the sector that causes the most emissions, such as transportation.

It is predicted that the greenhouse gas emission amount of Adana city in 2030 will be 7,047,098 tCO_2e, excluding emissions originating from the industry sector. However, if all the actions in the above table that make a numerical contribution to emission reduction can be carried out until 2030, the greenhouse gas emission amount for Adana in 2030 will be kept at the level of 3,450,466 tCO_2 equivalent (excluding emissions from industrial activities).

In the greenhouse gas emission reduction scenarios in the field of transportation for the city of Adana, the actions that come to the fore under the heading of transportation are as follows;

- Conversion of the existing fleet used in urban passenger mobility to electric buses
- Encouraging the citizens to use public transportation by improving the service level thanks to the number of routes and frequency of services to be increased by expanding the existing bus fleet
- Smart transportation applications by increasing the efficiency of the existing rail system line, constructing the new light rail system and encouraging the citizens to use the rail system

- Reducing the share of individual transportation in urban transportation, increasing the parking restrictions and/or costs in the city for this purpose
- Increasing the share of bicycle use, which is a non-motorized mode of transportation, in urban transportation, and for this purpose, creating and disseminating bicycle routes integrated with public transportation.
- Use of alternative fuels (biodiesel, ethanol, hydrogen, etc.) in urban transportation vehicles
- With the application of sustainable road construction technologies, it should be ensured that more environmentally friendly roads are built.

With SECAP, it is aimed to determine strategies that will reduce its emissions in 2030, to have high resistance for climate change, to have sustainable and accessible energy resources and reach the green development goals.

REFERENCES

Bruhwiler, L., Basu, S., Butler, J.H. et al. (2021). Observations of greenhouse gases as climate indicators, Climatic Change, 165:12.

Greene, D. L. (1997). Sustainable Transport. Journal of Transport Geography, 5(3), pp 177-190.

Intergovernmental Panel on Climate Change (IPCC)., (2019). Global Warming of 1.5°C Special Report.

Intergovernmental Panel on Climate Change (IPCC)., (2021). Climate Change 2021: The Physical Science Basis Report.

Kaya, Y., Yamaguchi, M. & Geden, O. (2019). Towards net zero CO_2 emissions without relying on massive carbon dioxide removal, Sustain Sci. Pp 14, 1739–1743

Oral, O., Uğuz, S. (2020). Türkiye'deki Farklı Sektörlere Ait Sera Gazı Emisyon Değerlerinin Çok Katmanlı Algılayıcılar ve Topluluk Öğrenmesi Yöntemleri ile Tahmin Edilmesi, Uluslararası Mühendislik Araştırma ve Geliştirme Dergisi, 12(2), pp 464- 478.

Panoutsou, C., Germer, S., Karka, P., Papadokostantakis, S., Kroyan, Y., Wojcieszyk, M., Maniatis, K., Marchand, P., Ingvar, L. (2021). Advanced biofuels to decarbonise European transport by 2030: Markets, challenges, and policies that impact their successful market uptake, Energy Strategy Reviews, 34, 100633.

Sustainable Energy and Climate Action Plan (SECAP) of Adana City., (2022). Republic of Türkiye, Ministry of Environment, Urbanization and Climate Change & Adana Metropolitan Municipality & World Bank & Sustainable Cities & ILBANK & EU & ARUP.

Williams, P. A. (1947). Creative Reading, The English Journal, Vol. 36, No. 9 (Nov, 1947), pp 454-459

URL-1: www.hikersbay.com/climate-conditions/turkey/adana/

URL-2: https://eri.iu.edu/erit/implications/alternative-fuels.html

URL-3: https://www.transportation.gov/sustainability/climate/fuels-and-vehicle-technology

CHAPTER 6

THEORETICAL AND EXPERIMENTAL COMPARISON OF MINIMUM FLUIDIZATION SPEED*

Aysun SENGUL[1], Assoc. Prof. Dr. Soner CELEN[2],

Prof. Dr. Aysen HAKSEVER[3]

[1] Asos Process Engineering, Tekirdağ, Turkey. Orcıd ID: 0000-0003-1502-6775 ozturkaysun93@gmail.com
[2] Namık Kemal University, Tekirdağ, Turkey. Orcıd ID: 0000-0001-5254-4411.scelen@nku.edu.tr
[3] Namık Kemal University, Tekirdağ, Turkey. Orcıd ID: 0000-0002-5380-1755.ahaksever@nku.edu.tr
* Yüksek Lisans Tezinden Üretilmiştir. Tez adı: Dikey Tip Akışkan Yataklı Kurutucuda Silis Kumun Kurutma Prosesinin İncelenmesi. 1.Danışman: Prof. Dr.Ayşen HAKSEVER, 2.Danışman: Doç. Dr. Soner ÇELEN

1. INTRODUCTION

In the fluidized bed dryer used for drying silica sand, the fluidized bed height, size, and fluidization rate are important, as well as the fluid temperature. Many literature studies have been conducted on this subject. These studies;

Nakamura et al, (1985) experimentally measured the minimum fluidization rates at temperatures up to 526,85 ºC for glass beads of equal size between 0.2 mm and 4 mm in beds with diameters ranging from 30 mm to 50 mm.

Lin et al, (2002) aimed to examine the effect of high temperature and particle size distribution on the minimum fluidization rate. In their work, they fluidized the four particle size distributions of silica with air at temperatures between 700 °C and 900 °C and at atmospheric pressure.

Goo et al, (2010) determined the minimum fluidization rates of silica sand in a fluid bed dryer measuring 0.078 m x 8.5 m in the temperature range from 25 °C to 800 °C. The effect of particle size on minimum fluidization and transport rates has been determined, and correlations have been proposed to estimate velocity at different temperatures.

Shao et al, (2013) investigated the fluidization properties of silica sands of different shapes, sizes, and densities in a 0.2 m x 0.2 m and 2 m high fluidized bed. In their study, pressure drop, flow pattern, minimum fluidization velocity, pressure difference, and fluidization images were investigated under different operating conditions and a fluidization rate correlation was developed.

Fotovat et al, (2015) studied the fluidization of sand particles in a fluidized bed dryer through experiments and numerical simulation. The experiments were fluidized in a 152 mm diameter bed with a static height of 228 mm and, using a pair of fiber optic sensors, the bubbling properties of these mixtures in the upper half of the dense bed were determined by surface gas varying from U=0.2 m/s to U=1.0 m/s. speeds were determined. Three-dimensional numerical simulations were performed using the Eulerian n-fluid approach using Neptune CFD software.

Farraji and Taofeeq (2020) studied and analyzed the effect of temperature and particle size on the minimum fluidization rate on a small pilot scale of a fluidized bed reactor. The experiments were carried out in the range of 300–425 μm, 425–500 μm, 500–600 μm and 600–710 μm of silica sand and at a temperature range of 20 °C–850 °C.

Drying is a fundamental process of enormous commercial importance in all industrial applications, from food to agriculture, mining, and even manufacturing (Jafari, 2017; Kepceoğlu et al., 2020). Drying is the process of removing water or other liquids from gases, liquids, and solids. However, the most common use of the concept of drying is the process of removing water or volatile substances from solid materials by thermal methods (Güngör and Özbalta, 2009).

When choosing a dryer, the typical features of dryers should be considered. Along with the dryer type, it is also important to choose the right operating conditions for optimum quality and cost of thermal dehumidification (Mujumdar, 2000).

Today, fluid bed dryers are replacing traditional drying methods with the advantages of high drying speed, high thermal efficiency, small flow area, low cost, and easy control. With these dryers, samples such as sand, coal, sawdust, foodstuffs, ceramics, health samples, agricultural chemicals, detergents, fertilizers, polymers, and resins can be dried. With these dryers, samples such as chemistry, sand, coal, sawdust, foodstuffs, ceramics, health samples, agricultural chemicals, detergents, fertilizers, polymers, and resins can be dried (Parlak, 2014; Mujumdar, 2006).

It is known that in fluid bed dryers, since the hot air is given from the bottom, the sample is suspended, so the drying times are short, and it has the ability to dry in a homogeneous temperature environment. Since each particle floats freely in hot air and behaves like a fluid, it increases the drying rate considerably (Gür, 2016).

The most important parameter in a fluidized bed is the minimum fluidization speed, which is defined as the speed at which fluidization begins in the bed (Bozkurt et al., 2020). A fluidized bed is operated at superficial gas velocities higher than the minimum fluidization rate. The minimum fluidization rate is typically derived from experiments. There are several ways to experimentally determine the minimum fluidization rate. It can also be estimated using various correlations. (Mujumdar, 2006).

In this study, the determination of the minimum fluidization rate in vertical fluidized bed drying was investigated experimentally and theoretically. In addition, the diameter of the silica sand selected as the sample was taken as 274±0.5 μm and its effect at 120 ^{o}C temperature and three different bed heights (50 mm, 100 mm and 150 mm) was investigated.

2. EXPERIMENTAL MATERIALS AND PARAMETERS

This study was carried out in the laboratory of Asos Process Engineering factory, with a moist silica sand sample obtained from a construction company (Figure 1a). During the experiments carried out, the sample temperature and sample moisture values at the end of the 3^{rd}, 6^{th}, 9^{th}, and 12^{th} minutes were measured. The sample temperature was measured with a thermometer during sampling. The moisture of the samples taken at the specified minutes was measured with a RADWAG brand moisture analyzer (Figure 1b). The drying air temperature used in the experiments was determined as 120 °C, and the experiments were carried out at this temperature. The drying experiments of silica sand used in the study were carried out at bed heights of 50 mm, 100 mm, and 150 mm (Table 1) (Şengül, 2022).

(a) (b)

Figure 1. a) Silica sand, b) Moisture measuring device

In order to measure the initial moisture values of the silica sand, which was supplied with a diameter of 274±0.5µm and kept in an airtight manner, separate samples were taken and three measurements were made in the moisture analyzer. According to the values obtained, the average initial moisture values of the samples were determined as 9.57%.

In this study, silica sand was dried with the vertical type fluidized bed dryer shown in Figure 2. According to the values in the experimental parameters determined for each experiment, the dryer was run empty for an average of 20–30 minutes, and the desired temperature was achieved. In this computer-controlled dryer system, the experimental parameters were set by entering information from the

computer screen. Experiments were carried out with 9.51 mm/s vibration to ensure fluidization of the sand. In order to see the boiling movement of the sample during drying, the chamber post of the dryer is made of glass. In the sample chamber of the dryer, there is a perforated stainless steel sheet with 2 mm diameter holes that allows the passage of hot air to the sample. In this drying system, the hot air to be used for drying is given to the dryer from the air heater by means of a fan. A dust bag filter is used in the upper part of the dryer to prevent sample loss during drying.

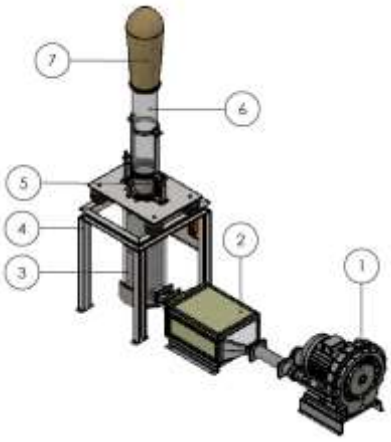

Figure 2. Experiment system, 1: Fan, 2: Resistance Heater, 3: Hot Air Supply Line, 4: Chassis, 5: Sample Container, 6: Inspection Glass Column, 7: Cloth Filter

The parameters used in the experiments are given in Table 1.

Table 1. Experimental parameters

Number of Experiments	Experiment Variables		
	Particle Size (µm)	**Bed Height (mm)**	**Temperature ºC**
Experiment-1	274±0.5	50	120
Experiment-2	274±0.5	100	120
Experiment-3	274±0.5	150	120

2.1. Minimum Fluidization Rate

One of the most important factors affecting the dynamic conditions of fluidized beds is the minimum fluidization rate (Coltters and Rivas, 2004). In this study, the determination of the minimum fluidization rate was made both theoretically and experimentally.

The minimum fluidization rate (U_{mf}) was calculated by the viscosity of the air (μ_f), the density of the air (ρ_f), Reynolds numbers (Re_{mf}), particle diameter (d_p), Temperature (T), the density of the particle (ρ_p), gravitational acceleration (g) and the Archimedean number (Ar) (Equation 1-4).

$$U_{mf} = \frac{Re_{mf} \cdot \mu_f}{\rho_f \cdot d_p} \quad (1)$$

$$\rho_f = 1{,}2 \cdot \left(\frac{293}{T}\right) \quad (2)$$

$$\mu_f = 1{,}46x10^{-6} \cdot \frac{T^{1{,}504}}{(T+120)} \quad (3)$$

$$Ar = \frac{\rho_p \cdot d_p^3 \cdot (\rho_p - \rho_f) \cdot g}{\mu_f 2} \quad (4)$$

2.2. Correlation Equations in the Literature

There are some correlations in Table 2 for the minimum fluidization speed of some researchers in the literature. Comparisons were made with experimental values using these correlations.

Table 2. Correlation equations

Model Name	**Correlation equations**
Wen and Yu (Wen and Yu, 1966)	$Re_{mf} = (33{,}7^2 + 0{,}0408Ar)^{0,5} - 33{,}7$
Bourgeis and Grenier (Bourgeis and Grenier, 1968)	$Re_{mf} = (25{,}46^2 + 0{,}0382Ar)^{0,5} - 25{,}46$
Saxena and Vogel (Saxena and Vogel, 1977)	$Re_{mf} = (25{,}28^2 + 0{,}0571Ar)^{0,5} - 25{,}28$
Babu, Shah and Talwalker (Babu et al., 1978)	$Re_{mf} = (25{,}25^2 + 0{,}0651Ar)^{0,5} - 25{,}25$
Vaid and Sen Gupta (Vaid and Sen Gupta, 1978)	$Re_{mf} = (24^2 + 0{,}0546Ar)^{0,5} - 24$

3. RESEARCH FINDINGS

In Experiment 1-3, which is given in Table 3-5, silica sand with an initial humidity of 9.57%, a bed height of 50 mm, and a wet weight of 836 g was subjected to drying at 120 °C air temperature for 12 minutes. The experiments were carried out with vibration to provide fluidization to the sand. The product temperature of the sample was measured at 36.50 °C in the 3rd minute, the product humidity was 1.898%, the product temperature was 72.90 °C, and the product humidity in the 6th minute was 0.138%, the product temperature was 80.80 °C, and the product moisture in the 9th minute was 0.131%, and the product temperature in the 12th minute, 83.20 °C and product humidity were measured as 0.089% (Figure 3).

Table 3. Exp-1, dp_1= 0.000274±0.5 m, h= 50 mm, T= 120 °C drying table

Exp.No	PS (µm)	BH (mm)	T (°C)	IM %	t (min)	ST (◦C)	SM (%)
Exp-1	274±0.5	50	120	9.57	3	36.50	1.898
Exp-1	274±0.5	50	120	9.57	6	72.90	0.138
Exp-1	274±0.5	50	120	9.57	9	80.80	0.131
Exp-1	274±0.5	50	120	9.57	12	83.20	0.089

PS: Particle Size, BH: Bed Height, T: Temperature, IM: Initial Moisture, t: Time, ST: Sample Temperature, SM: Sample Moisture

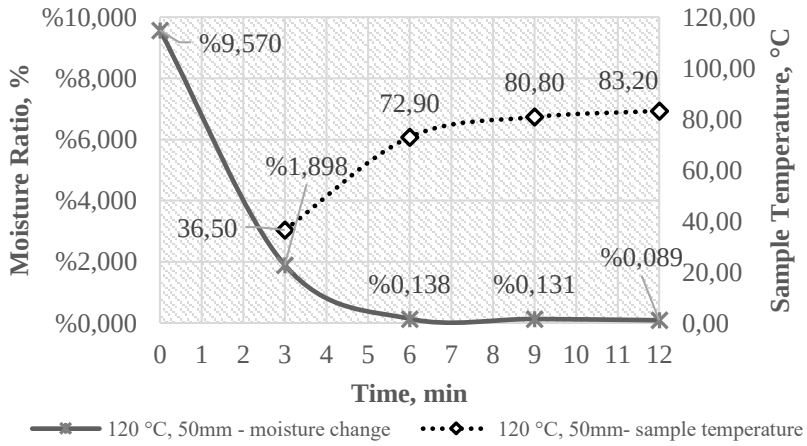

Figure 3. Experiment-1, dp_1= 0.000274±0.5 m, h= 50 mm, T= 120 °C sample moisture and temperature change

In Table 4, the sample temperature was measured at 29.50 °C at the 3rd minute, and the sample moisture was 3.937%, the sample temperature at the 6th minute was 57.50 °C and the sample moisture was 0.716%, the sample temperature at the 9th minute was 70.60 °C and the sample moisture was 0.126%, the sample temperature at the12th minute, was 79.00 °C and the sample moisture was 0.084% (Figure 4).

Table 4. Experiment-2, dp_1= 0.000274±0.5 m, h= 100 mm, T= 120 °C drying table

Exp.No	PS (µm)	BH (mm)	T (°C)	IM %	t (min)	ST (◦C)	SM (%)
Exp-2	274±0.5	100	120	9.57	3	29.50	3.937
Exp-2	274±0.5	100	120	9.57	6	57.50	0.716
Exp-2	274±0.5	100	120	9.57	9	70.60	0.126
Exp-2	274±0.5	100	120	9.57	12	79.00	0.084

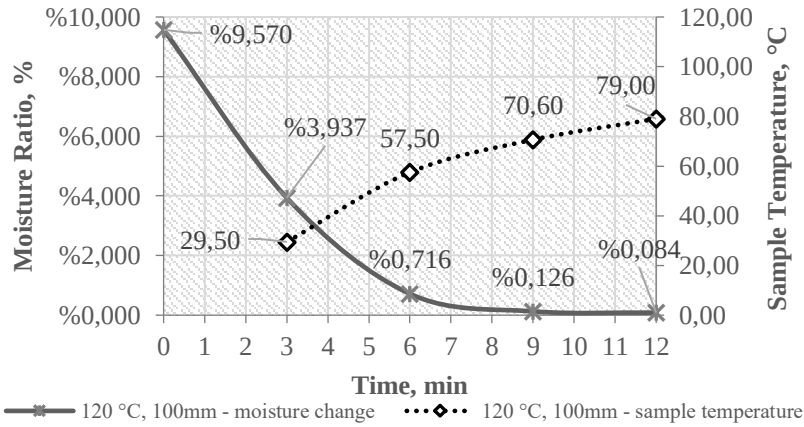

Figure 4. Experiment-2 dp_1= 0.000274 m, h= 100 mm, T= 120 °C sample moisture and temperature change

In Table 5, the sample temperature was measured at 31.60 °C in the 3rd minute and the sample moisture was 5.886%; the sample temperature at the 6th minute was 31.40 °C and the sample moisture was 3.276%; the sample temperature at the 9th minute was 39.20 °C and the sample moisture was 0.127%; and at the 12th minute, the sample temperature was 45.30 °C and the sample moisture was measured as 0.085 % (Figure 5).

Table 5. Experiment-3, dp_1= 0.000274±0.5 m, h= 150 mm, T= 120 °C drying table

Exp.No	PS (µm)	BH (mm)	T (°C)	IM %	t (min)	ST (◦C)	SM (%)
Exp-3	274±0.5	150	120	9.57	3	31.60	5.886
Exp-3	274±0.5	150	120	9.57	6	31.40	3.276
Exp-3	274±0.5	150	120	9.57	9	39.20	0.127
Exp-3	274±0.5	150	120	9.57	12	45.30	0.085

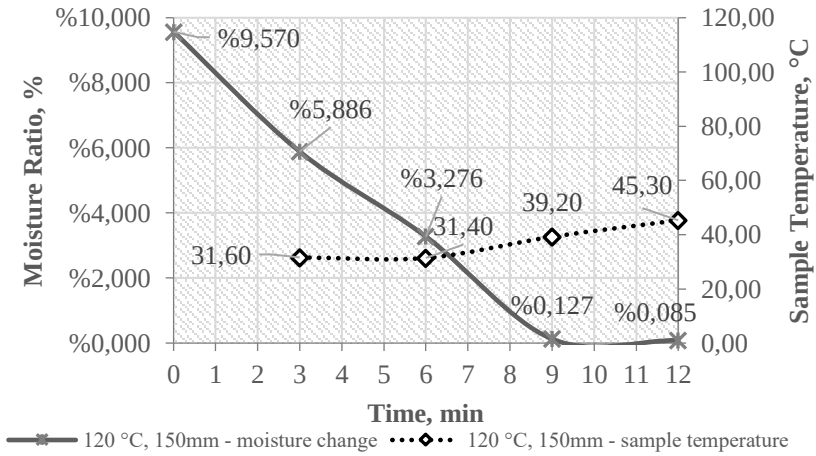

Figure 5. Experiment-3, dp_1= 0.000274±0.5 m, h= 150 mm, T= 120 °C sample moisture and temperature change

In Figure 6, it is seen that the moisture of silica sand dried at different bed heights decreases over time.

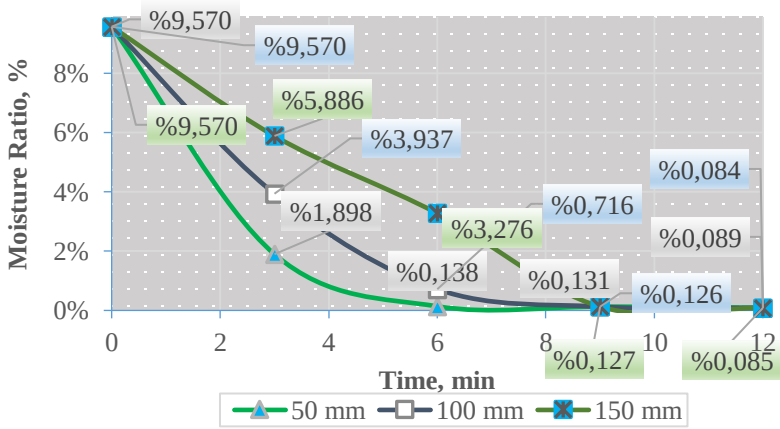

Figure 6. Change of moisture of silica sand dried at 120 ºC with time

In all analyses, the viscosity and density of the air were calculated, and the bed void value was taken as ε=0.42 and the sphericity value as φ=0.85. All parameters are given in Table 6.

Table 6. Ground State Parameters For Silica Sand Tests

Parameter	**Symbol**	**Value**
Bed Height -1 (50 mm)	h	0.05
Bed Height -2 (100 mm)	h	0.1
Bed Height -3 (150 mm)	h	0.15
Particle Density (kg/m$^{3)}$	ρ_p	2330
Air Density (kg/m^3)	ρ_f	0.8947
Viscosity of Air (kg/m.s)	μ	2.2709E-05
Bearing Space (dimensionless)	ε	0.42
Sphericity (dimensionless)	φ	0.85

Table 7. Minimum Fluidization Rate Table Obtained from the Experiments and Calculated According to the Correlation Equations in the Literature

Experiment Parameters		U_{mf} (m/s)	Theoretical Results (m/s)				
			Wen and Yu	Bourgeis and Grenier	Saxena and Vogel	Babu. Shah and Talwalker	Vaid and Sen Gupta
Exp-1	50 mm	0.1	0.0454	0.0557	0.0838	0.0954	0.0843
Exp-2	100 mm	0.1	0.0454	0.0557	0.0838	0.0954	0.0843
Exp-3	150 mm	0.1	0.0454	0.0557	0.0838	0.0954	0.0843

Table 8. Deviation Rates of Correlation Results with Experimental Data

Experiment Parameters		Mathematical Calculation Results Deviation Ratio				
		Wen and Yu	Bourgeis and Grenier	Saxena and Vogel	Babu, Shah and Talwalker	Vaid and Sen Gupta
Exp-1	50 mm	54.60%	44.29%	16.19%	4.57%	15,68%
Exp-2	100 mm	54.60%	44.29%	16.19%	4.57%	15,68%
Exp-3	150 mm	54.60%	44.29%	16.19%	4.57%	15,68%

As can be seen in Table 7-8, the deviations between the experimentally obtained minimum fluidization velocity and the values calculated from the theoretical models are between 4.57% and 54.60%. These deviations are thought to be caused by ambient conditions and experimental measurement errors in experimental studies.

CONCLUSION

Among the various factors affecting the dynamic conditions of fluidized beds, one of the most important is the initial velocity of fluidization, that is, the minimum fluidization rate. For the estimation of the minimum fluidization rate in the drying of silica sand, the test and the agreement of the correlations in question were compared and their deviations examined.

The initial moisture value of the silica sand used in the studies was determined as 9.57% with the moisture analyzer. Silica sand samples were screened and the particle size was determined as dp_1=0.000274 m. The experiments were carried out at drying air temperatures of 120 °C and bed heights of 50 mm, 100 mm and 150 mm. When the experiments were compared, it was seen that the moisture loss of the sample accelerated as the drying air temperature increased. According to the results, the fastest drying was achieved at 50 mm bed height.

The minimum fluidization rate theoretically varies between 0.054-0.0954 m/s. The Babu, Shah and Talwalker models were found to be the closest (0.0954 m/s) to the experimental result. It was measured as 0.1 m/s in this study. When the experimental results were examined, it was seen that the minimum fluidization rate did not change with the bed height.

ACKNOWLEDGEMENTS

The authors thank Asos Process Engineering for making use of its laboratory.

REFERENCES

Babu, S.P., Shah, P. and Talwalker, A. (1978). Fluidization correlations for coal gasification materials-minimum fluidization velocity and fluidized bed expansion ratio, Chem.Eng. Prog. Symp. Ser. Vol. 74, pp 176–186.

Bourgeis, P. and Grenier, P. (1968). Ratio of terminal velocity to minimum fluidization velocity for spherical particles, Can. J. Chem. Eng. Vol. 46.

Bozkurt, S., Altay, Ö., Koç, M. and Kaymak Ertekin, F. (2020). Fluidized Bed Applications in Powder Food Processes, Turkish Journal of Agriculture - Food Science and Technology, Vol. 8, No. 4, pp 818-825.

Coltters, R., and Rivas, A. L. (2004). Minimum fluidation velocity correlations in particulate systems. Powder Technology, Vol. 147, pp 34-48.

Farraji, A., and Taofeeq, H. (2020). Effect of elevated temperature and silica sand particle size on minimum fluidization velocity in an atmospheric bubbling fluidized bed. Chinese Journal of Chemical Engineering, Vol. 28, pp 2985-2992.

Fotovat, F., Ansart, R., Hemati, M. and Simonin, O. (2015). Sand-assisted fluidization of large cylindrical and spherical biomass particles: Experiments and simulation. Chemical Engineering Science, Vol. 126, pp 543-559.

Goo, J. H., Seo, M. W., Kim, S. D. and Song, B. H. (2010). Effects of temperature and partıcle sıze on mınımum fluıdızatıon and transport velocıtıes ın a dual fluıdızed bed. proceedings of the 20th International Conference on Fluidized Bed Combustion, pp 305-310.

Güngör, A. and Özbalta, N. (2009). Kurutmanın Temelleri ve Endüstriyel Kurutucular Kurs Notları. IX. Ulusal Tesisat Mühendisliği Kongresi. İzmir.

Gür, M. (2016). Balkabağının Akışkan Yataklı Kurutucuda Kurutulmasının Deneysel Ve Teorik İncelenmesi, Uludağ

Üniversitesi Mühendislik Fakültesi Dergisi, Vol. 21, No. 2, pp 145-158.

Jafari, H., Farahbod, F., 2017. The experimental survey on the rotary dryer performance: drying of wetted salt from effluent bio wastewater, Journal of Applied Biotechnology & Bioengineering, Vol. 4, No. 3, pp 567-570.

Kepceoğlu, S., Moralar, A. and Çelen, S. (2020). Determination Of The Ideal Flow Rate In Drying Of Table Salt, Theory and Research in Engineering II, Chapter 3, Gece Publishing.

Lin, C.-L., Wey, M.-Y. and You, S.D. (2002). The effect of particle size distribution on minimum fluidization velocity at high temperature. Powder Technology, Vol. 126, pp 297-301.

Mujumdar, A. S. (2000). Mujumdar's practical guide to ındustrial drying. Edited by Sakamon, 187 pages.

Mujumdar, A.S. (Ed.)., 2006. Handbook of Industrial Drying (3rd ed.). CRC Press.

Nakamura, M., Hamada, Y. and Toyama, S. (1985). An experimental investigation of‘ minimum fluidization velocity at elevated temperatures and pressures. The Canadian Journal Of Chemical Engıneerıng, Vol. 63, pp 8-13.

Parlak, N. (2014). Akışkan Yataklı Kurutucuda Zencefilin Kuruma Kinetiğinin İncelenmesi, Journal of the Faculty of Engineering and Architecture of Gazi University, Vol. 29, No. 2, pp 261-269.

Saxena, S.C. and Vogel, G.J. (1977). The measurement of incipient fluidization velocities in a bed of course dolomite at temperature and pressure, Trans. Inst. Chem. Eng. Vol. 55, pp 184–189.

Shao, Y., Li, Z., Zhong, W., Bian, Z. and Yu, A. (2020). Minimum fluidization velocity of particles with different size distributions at elevated pressures and temperatures. Chemical Engineering Science, Vol. 216, 115555.

Şengül, A. (2022). Dikey Tip Akışkan Yataklı Kurutucuda Silis Kumun Kurutma Prosesinin İncelenmesi, TNKÜ, Fen Bilimleri Enstitüsü, Yüksek Lisans Tezi, Tekirdağ.

Vaid, R.P. and Sen Gupta, P. (1978). Minimum fluidization velocities in beds of mixtures, Can. J. Chem. Eng. Vol. 56, pp 292–296.

Wen, C.Y. and Yu, Y.H. (1966). A generalized method for predicting the minimum fluidization velocity, AICHE J. 12.

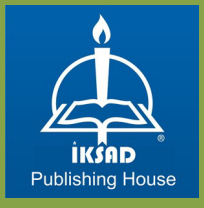

ISBN: 978-625-8213-08-9